UNIVERSITÀ DEGLI STUDI DI PADOVA

# UNIVERSITÀ DEGLI STUDI DI PADOVA

Sede Amministrativa: Università degli Studi di Padova

Dipartimento di
Ingegneria Industriale - DII

CORSO DI DOTTORATO DI RICERCA IN: INGEGNERIA INDUSTRIALE
CURRICOLO: INGEGNERIA CHIMICA, DEI MATERIALI E MECCANICA
CICLO XXIX

## TRIBOLOGICAL BEHAVIOUR OF HIGH THERMAL CONDUCTIVITY TOOL STEELS FOR HOT STAMPING

**Direttore della scuola:** Ch.mo Prof. Paolo Colombo
**Coordinatore:** Ch.mo Prof. Giovanni Meneghetti
**Supervisore**: Ch.mo Prof. Andrea Ghiotti

**Dottorand**o: Francesco Medea

# ACKNOWLEDGEMENTS

Padova, 15/12/16

In completing this Thesis, many people have earned my thanks.

I firstly would like to thank the Prof. Andrea Ghiotti and Stefania Bruschi for their guidance, support and help in my research work.

I am grateful to my colleagues at the Precision Manufacturing Engineering Group and to my friends for making an enjoyable atmosphere to work in; Simonetto (l'eroe), Stefano (Furia), Novella (Novellino), Marco (Bellin), Michieletto (Checco), Bordin (l'artista), Francesco (Sgara) and all thesis students.

Finally and most profoundly, I would like to thank my gorgeous Family for believing in me and for its encouragement. This goal could not have been reached without them.

A special thanks, a little bit "cicciottino", goes to my lovely girlfriend Nicol for filling my heart with love, for making me smile and always supported.

Francesco Medea

# Table of Contents

# Abstract

In the last years, the use of High Strength Steels (HSS) as structural parts in car manufacturing, has rapidly increased thanks mainly to their favourable strength to weight ratios and stiffness, which allow a reduction of the fuel consumption to accommodate the new restricted regulations for CO2 emissions control, but still preserving or even enhancing the passengers' safety. However, the formability at room temperature of HSS is poor, and for this reason, complex-shaped HSS components are produced applying the plastic deformation of the sheet metal at high temperature. The use of hot stamping technology, which was developed during the 70's in Sweden, has become increasingly used for the production of HSS for the car body-in-white. By using this technology, several improvements have been made, if compared with the forming at room temperature, such as the reduction of spring back and the forming forces, the production of more complex shapes, a more accurate microstructure control of the final piece and the achievement of components with high mechanical properties. The hot stamping process of HSS parts consists mainly in heating a metal sheet up to austenitization temperature and then a simultaneous forming and hardening phase in closed dies, water-cooled, to obtain a fully martensitic microstructure on the final components; in this way, ultimate tensile strength passes from 600 MPa up to 1500-1600 MPa.

Anyway, several tribological issues arise when the die and metal sheet interact during the forming process at elevated temperatures; the absence of any types of lubricant due to elevate process temperature and in order to preserve the quality of the part for the later stages of the process chain, leads to high friction forces at interface; moreover, and the severe wear mechanisms together with surface damage of forming dies, can alter the quality of the component and can also have an high impact on the process economy due to frequent windows-maintenance or reground of tools. Furthermore, considering that the thermal conductivity of the die material influences the cooling performance, obtained during the quenching phase, and being the quenching time the predominant part of the cycle time, the productivity of the process is influenced too. On this base tool steels play a capital role in this process, as they strongly influence the properties of the obtained final product and have a strong impact to investment and maintenance costs.

The survey of the technical and scientific literature shows a large interest in the development of different coatings for the blanks from the traditional Al-Si up to new Zn-based coating and on the analysis of hard PVD, CVD coatings and plasma nitriding, applied on dies. By contrast, fewer investigations have been focused on the development and test of new tools steels grades capable to improve the wear resistance and the thermal properties that are required for the in-die quenching during forming. The research works reported are focused on conventional testing configurations, which are able to achieve fundamental knowledge on friction behaviour, wear mechanisms and heat transfer evaluation, with both a high accuracy for the process parameters and less information about situations that replicate the thermal-mechanical conditions to which the forming dies are subject during the industrial process.

Alternatively, the tribological performance have been studied through costly and time-consuming industrial trials but with a lower control on process parameters.

Starting from this point of view, the main goal of this PhD thesis is to analyse the tribological performance in terms of wear, friction and heat transfer of two new steel grades for dies, developed for high-temperature applications, characterized by a High Thermal Conductivity with the purpose to decrease the quenching time during the hot stamping process chain and overcome the limits in terms of process speed. Their performances are compared with a common die steel grade for hot stamping applications.

To this aim, a novel simulative testing apparatus, based on a pin on disk test, specifically designed to replicate the thermo-mechanical cycles of the hot stamping dies, was used to evaluate the influence of different process parameters on the friction coefficient, wear mechanisms and heat transfer at interface die-metal sheet. Unlike other research works reported in the literature, which individually analyse the friction, the wear mechanisms and thermal aspects, by means of the methodology used in this thesis, the tribological characterization as a whole is obtained by means of a single approach, in order to analyse the simultaneous global evolution of the tribological system.

# Sommario

Negli ultimi anni, l'utilizzo degli acciai alto resistenziali per sviluppare parti strutturali nell'industria automobilistica è aumentato notevolmente, grazie soprattutto al loro favorevole rapporti resistenza-peso e rigidezza, consentendo una riduzione del consumo del carburante per assecondare le nuove restrizioni in termini di emissioni di CO2 e conservando nel frattempo, la sicurezza dei passeggeri. Tuttavia, la formabilità a temperatura ambiente degli acciai alto resistenziali è scarsa e per questo motivo, i componenti con geometrie complesse sono prodotti applicando la deformazione plastica ad elevata temperatura. L'uso della tecnologia dello stampaggio a caldo, che è stata sviluppata durante gli anni '70 in Svezia, è diventata sempre più popolare per la produzione di parti che costituiscono il telaio delle automobili. Utilizzando tale tecnologia, si sono ottenuti notevoli miglioramenti - se confrontata con la formatura a freddo - come la riduzione del ritorno elastico e delle forze di stampaggio, la possibilità di ottenere geometrie più complesse, un accurato controllo della microstruttura del componente e l'ottenimento di pezzi con elevate proprietà meccaniche. Il processo di stampaggio a caldo di parti in acciaio alto resistenziale consiste principalmente nel riscaldamento di una lamiera fino alla temperatura di austenitizzazione e poi nell'applicazione simultanea della fase di formatura e tempra in stampi chiusi per ottenere una microstruttura martensitica sui componenti finali; in questo modo, il carico di rottura passa da 600 MPa a 1500-1.600 MPa.

Tuttavia, diversi problemi tribologici sorgono quando lo stampo e lamiera interagiscono durante il processo di formatura a temperature elevate; l'assenza di qualsiasi tipo di lubrificante a causa delle elevate temperature di processo e per preservare la qualità del pezzo per le successive fasi di lavorazione porta ad elevate forze di attrito all'interfaccia stampo-lamiera e i severi meccanismi di usura insieme ai danni superficiali degli stampi di formatura possono alterare la qualità del prodotto finale e possono anche avere un impatto negativo sull'economia del processo a causa della frequente manutenzione o sostituzione degli stampi. Inoltre, considerando che la conducibilità termica del materiale dello stampo influenza le performance di raffreddamento che possono essere ottenute durante la fase di tempra in stampo e quindi, la produttività del processo, essendo il tempo di tempra la parte predominante del tempo ciclo, gli acciai per stampi ricoprono un ruolo importante in questo processo; influenzano fortemente le proprietà finali del pezzo ed hanno un forte contributo sugli investimenti e costi di manutenzione.

Un'analisi della letteratura tecnico-scientifica mostra un grande interesse per lo sviluppo di diversi rivestimenti per le lamiere alto resistenziali, dal tradizionale Al-Si fino al nuovo rivestimento base Zn e sull'analisi di rivestimenti PVD , CVD e nitrurazione plasma da applicare sugli stampi, mentre molte meno indagini sono state focalizzate sullo sviluppo e test di nuovi gradi di acciai per stampi, capaci di migliorare la resistenza all'usura e le proprietà termiche che sono necessari per la tempra in stampo durante la formatura. I lavori di ricerca riportati sono concentrati su configurazioni di test convenzionali, che sono in grado di

raggiungere la conoscenza fondamentale sul comportamento dell'attrito, dei meccanismi di usura e della valutazione del trasferimento di calore, con una elevata precisione per quanto riguarda i parametri di processo, ma non riescono a replicare le condizioni termo-meccaniche a cui gli stampi di formatura sono soggetti ciclicamente durante il processo industriale. In alternativa, le prestazioni tribologiche sono studiate attraverso costose prove industriali in termini di tempo e denaro, ma con un basso controllo sui parametri di processo.

Partendo da questo punto di vista, l'obiettivo principale di questa tesi è quello di analizzare le prestazioni tribologiche in termini di usura, attrito e di trasferimento di calore di acciai per stampi, sviluppati per applicazioni ad alta temperatura, caratterizzati da una elevata conducibilità termica al fine di diminuire il tempo di tempra durante le fasi dello stampaggio a caldo e superare gli odierni limiti in termini di velocità di processo. Le loro prestazioni sono confrontate con un comune acciaio per stampi utilizzato nella formatura a caldo.

A questo scopo, un nuovo apparecchio di prova, basato su un pin on disk test, specificamente progettato per replicare sugli stampi i cicli termo-meccanici del processo della stampa a caldo, è stato utilizzato per valutare l'influenza dei diversi parametri di processo sul coefficiente di attrito, meccanismi di usura e trasferimento di calore all'interfaccia stampo-lamiera. A differenza di altri lavori di ricerca riportati in letteratura, i quali analizzano singolarmente l'attrito, i meccanismi di usura e gli aspetti termici, mediante la metodologia utilizzata in questa tesi, la caratterizzazione tribologica nel suo complesso è ottenuta mediante un unico approccio, al fine analizzare l'evoluzione globale simultanea del sistema tribologico nel suo complesso.

# Chapter 1

# **Introduction**

## 1.1. The industrial problem

The increasing demand for fuel-efficient vehicles, improved safety, and crashworthiness [1][2], has led automotive industry to introduce new alloys in car manufacturing, characterized by a high stiffness and strength-to-weight ratio. To meet the need to form these new materials, hot stamping has been widely applied in the automotive industry [3][4][5] to produce components of the car body-in-white characterized by a high strength-to-weight ratio, which allow a reduction of the fuel consumption [6], but still preserving the passengers' safety.

The introduction of sheet metal–forming operations conducted at elevated temperatures and, in particular, of the hot stamping of High Strength Steel (HSS) sheets allows (i) enhancing the material formability limits thanks to the material ductility increase at increasing temperatures [7] and (ii) obtaining high mechanical-properties component thanks to its quenching phase into the water-cooled dies just after the plastic deformation.

Hot stamping is the sheet metal–forming process that combines the forming and the heat treatment stages in order to improve the mechanical properties of the metal sheet respect to those of the initial blank. Hot stamping was developed and first patented in 1977, but only in 1984 Saab Automobile AB [8] adopted the technology based on hardened boron steels to manufacture components for automobiles [9].

During the hot stamping process of HSS sheets, which has a ferritic-pearlitic microstructure in the as-delivery condition, the thermal and mechanical cycles allows obtaining a fully martensitic structure and strength values that are almost triple than the initial ones [8], which guarantees its elevate mechanical properties.

The typical temperature versus time diagram of a hot-stamping cycle of HSS is illustrated in Fig. 1.1. The blank material, which has a ferritic-pearlitic microstructure in the as-delivery condition [9] and low mechanical properties at room temperature, is heated in a furnace above the austenitization temperature.

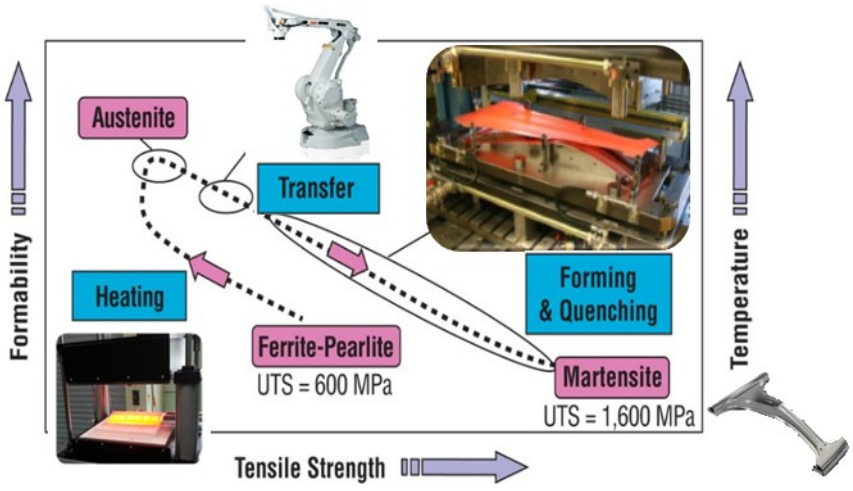


Fig. 1.1 Typical Formability versus Tensile Strength diagram of a hot-stamping cycle of HSS. Adapted from [10].

After an appropriate soaking time, long enough to obtain a homogeneous austenitic microstructure [11], the blank is transferred as fast as possible to the forming press, where it is simultaneously formed and quenched in closed die. At the end of the process cycle, the

formed piece presents a fully martensitic microstructure, with strength levels above 1500-1600 MPa [12][13][14] but nevertheless an acceptable ductility [15].

Two variants of the hot stamping process are actually used in industry environment, with regard to the forming phase: direct and indirect hot stamping (see Fig. 1.2). The direct hot stamping (Fig. 1.2a) involves heating the metal sheet and the simultaneous forming and quenching phase. In the indirect hot stamping (Fig. 1.2b) the metal sheet undergoes a longer process chain, in which the blank is first pre-formed at room temperature, then heated up to the steel austenitization temperature, and only subsequently moved to a press where the quenching and calibration phases are simultaneously carried out using conditioned dies [16].

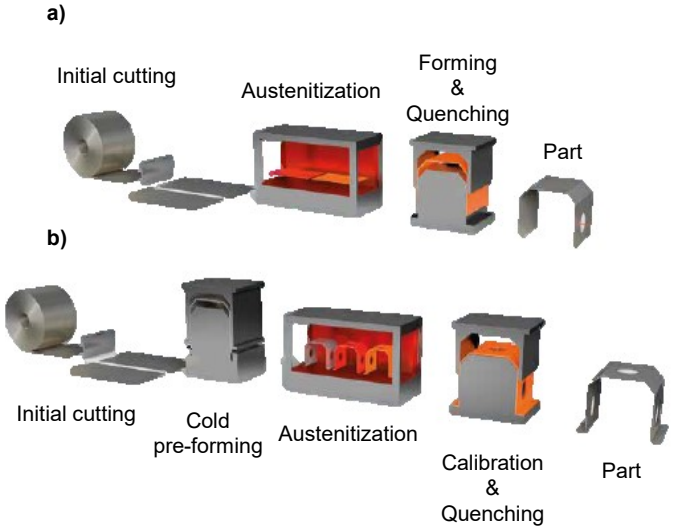


Fig. 1.2 Hot stamping process variants: (a) direct hot stamping and (b) indirect hot stamping.

Usually, the direct process is used for components characterized by a relatively low degree of forming and a small drawing depth, while the indirect method is used where a complex geometry of the workpiece is required [17]. Tools lubrication is generally avoided due to the elevated temperature and to preserve the surface quality of the final component, with particular regards to the paintability and weldability [18].

Currently, process of hot stamping of High Strength Steels is mainly utilized in the automotive industry for the production of components of the car body in white, such as B pillars, A pillars, bumpers, roof rails etc. [19][20], Fig. 1.3.

Despite the advantages that the hot stamping leads in terms of (i) the shorter process chain, especially in the case of direct hot stamping, (ii) the increase of mechanical properties just after the deformation process and without the need of additional heat treatments, (iii) the reduction of the total weight of the vehicles thanks to thinner components maintaining the frame stiffness, (iv) a high shape precision [21], (v) the absence of lubricants that are often hazardous for the environment and require expensive cleaning operations [22], due to the elevated temperatures and pressures at the interface die-metal sheet, friction and wear become particularly critical for the sheet sliding in the dies cavities and their service life [23] and the heating phase, with the subsequent inevitable contact with air during transport and forming, cause the oxidation and decarburization of the metal sheets [13] [14].

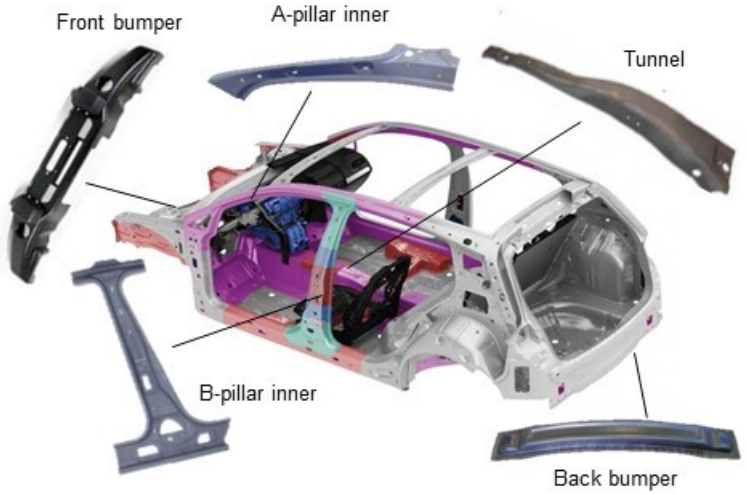


Fig. 1.3 Typical hot-stamped components of the car body-in-white.

For these reasons, the 22MnB5 steel sheets that are used in hot stamping are commonly coated to avoid the oxidation and decarburation during the heating stage [26]: Al-Si coating is the most common used but recently a new Zn based coating was developed [27]. In detail, Al-Si coating is used for direct hot stamping process because during coated blank heating the steel diffusion process from the coating–substrate interface area to the coating surface is thermally activated. The resulting intermetallic Al-Fe phase has a higher melting point [28][26] compared to the Al-Si coating in the initial state and allows a high barrier against oxidation. Nevertheless, due to the lower forming limits of the Al–Si layer compared to the base material in the initial state at room temperature, the sheets with hot-dip Al-Si coating cannot be used for the indirect process and they are not suitable for cold forming.

To solve the problem of having a cathodic protection during indirect hot stamping process, the Zn-based coating is used; the hot-dip galvanized zinc layer reacts with the base material to form intermetallic zinc–iron-phases during heating and hot stamping phases.

## 1.2. The scientific relevance

Nowadays, coatings partially solve problems of oxidation and decarburation of the sheets during the process chain and are helpful in the reduction of friction at elevated temperatures but despite this, the severe wear mechanisms at the interfaces between the dies and the blanks, the evolution of thermo-mechanical stress applied on die sliding surfaces and the influence of the process parameters on friction forces may represent critical points for the feasibility of the process. Another critical point, being hot stamping a quite slow process (2, max 3 shots per minute)[29], it is to shorten quenching phase, since that long quenching phases are not attractive from the point of view of production cycle; consequently improvements are necessary as far as the strategy for quenching in the die, making the process more productive. Moreover, although traditionally, hot formed parts are designed to have a fully martensitic microstructure in order to present the maximum strength performance, some structural parts, may benefit from zones of reduced strength and greater ductility for improved energy absorption and fracture resistance [30], Fig. 1.4. This type of hot stamped components, which

possess different zones with different mechanical properties, are identified with the name of *tailored component* and in the existed literature, operation as tailored welded blanks [30], die with different temperature [31][32], blank of different initial temperature [33] and subsequent heat treatment [34] were investigated to achieve components with the desired characteristics.

In order to obtain a decrease of the quenching time with the aim of making the process more competitive in terms of manufacturability, new tool materials with an elevate thermal conductivity are being developed; at the same time, a die for hot stamping applications can be realized with zones of different steel grades that have several thermal conductivity properties. In this way, where high strength is required, and therefore a fully martensitic structure (~1500-1.600 MPa UTS), die materials with a High Thermal Conductivity are used, while in the zones where components are to have tailored properties (~800 MPa UTS), tool steels with a lower thermal conductivity can be used [35]. In addition to a high conductivity, these steels should offer a high hardness and good wear resistance to withstand tribological impact during service life and also to present a sufficient toughness to avoid cracking due to thermal and mechanical stresses.

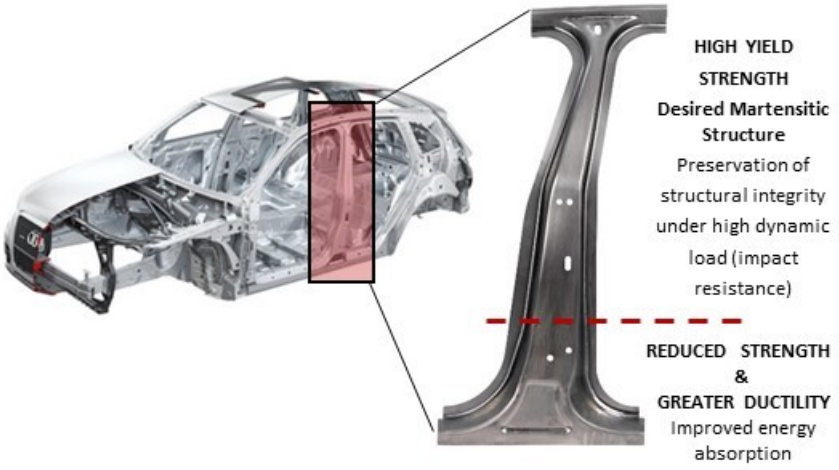


Fig. 1.4 Schematic of a B-pillar with tailored properties. Adapted from [35].

These phenomena have not been investigated in depth until now, and they have therefore in need of new methodologies, new approaches to replicate in a laboratory environment the hot stamping conditions, keeping under control friction, thermal aspects, wear mechanisms and tool damage that are established by varying the main parameters of process, with the purpose to improve the productivity and feasibility in hot stamping of High Strength Steel parts.

## 1.3. Objective and work organisation

The research work has a twofold objective in terms to propose and assess approaches and methodologies (i) to analyse friction and wear phenomena present during hot stamping of HSS sheet, in order to reproduce in a laboratory environment the thermal and mechanical cycles to which the dies are subjected during the high temperature forming phase and, on this base, (ii) investigate on field of new die steel grades, with the aim of improving the common materials performances actually used to manufacture dies and tools to overcome the limits in

terms of processes speed and feasibility. Despite the fast cooling rate typical of hot stamping, which must be at least equal to 27 °C/s, the total time required to perform the quenching stage still represent the largest part of the total process cycle time. So, to overcome the low productivity of hot stamping lines [36], significant developments are necessary to improve the cooling performance of the quenching phase and new die materials with high thermal conductivity are strongly required [37].

The tribological investigations will be developed by using a comprehensive approach, including the simulation of the tribological phenomena at the interfaces between the dies and the blank during the process, the product surface quality analysis, control of thermal and mechanical cycles and the tool wear. The results of experiments will be correlated with the process characteristics, in order to provide the optimal window of process parameters that assures the required product performances. The reference industrial process is the direct hot stamping of quenchable HSS sheets coated.

In order to fulfil the proposed objectives, the following targets have been outlined:

- ✓ Analysis of the reference industrial case in order to identify the most relevant process parameters influencing friction, wear phenomena and thermal aspects;
- ✓ Analysis of the state-of-the-art with a particular emphasis on the tribology at elevated temperatures, with particular reference to the testing methodologies and the latest improvements for such applications;
- ✓ Analysis of friction, wear and thermal parameters in a laboratory environment, during the stamping of the HSS metal sheets coated, by varying the main process parameters for the evaluation of new steel grades for dies.

This thesis is divided into six chapters. The first one contains a brief description of the hot stamping process and the main tribological issues related to it, a short introduction of the research activity and the work organisation. The second chapter describes the literature review; a short description of tribology in terms of friction, wear and lubrication is carried out and its importance at elevated temperatures and then, particular emphasis is given to present existing studies of characterization regarding friction, wear and heat transfer of hot stamping of HSS. The third chapter describes the aim of the work and the approach used. The fourth chapter is devoted to a detailed description of the new procedures developed and instruments used. The results are presented in the fifth chapter in terms of friction, wear and thermal aspects of new steel grades for dies for hot stamping application against High Strength Steel sheets coated and the performances evaluation of the new simulative procedure. The final chapter, six, briefly presents conclusions.

# Chapter 2

# **Literature review**

The Chapter introduces initially the word tribology, the fundamental concepts of friction and contact mechanics, wear phenomena and lubrication, even providing simplified analytical reports, useful for quantitative evaluations. Then, a section presents the most relevant methodologies to investigate the tribological aspects connected to hot stamping, focusing on the testing approaches used in laboratories and industry. The second paragraph presents a survey of the existing studies concerning tribological investigation of coated and uncoated HSS sheets in hot stamping process and new developments in the field of steel grades for dies specifically developed for hot stamping applications. Finally the most relevant output and the existing research gap are resumed.

# 2.1. Introduction to tribology

The word tribology was first reported in a landmark report by Jost (1966) and it is derived from the Greek word tribos meaning rubbing, so the literal translation would be "the science of rubbing" [38].

Tribology is the science and technology of interaction surfaces in relative motion and of related subjects and practices. During these interactions that take place at the interface, forces are transmitted, mechanical energy is converted, physical and the chemical nature, including surface topography, of the interacting materials are altered [39][40]. Tribology includes mechanical engineering, materials science, chemical engineering and more; for this reason it is defined an interdisciplinary field. This wide variety of skills is required due to many different physical phenomena occurring at a sliding interface; moreover, there are also many different areas of focus within the tribology field. Generally, there are three major areas of interest within tribology: friction, wear and lubrication. Each of these is described in more detail below.

## 2.1.1 Friction

Friction is defined as the resistance to relative motion exhibited by the contact surfaces of two bodies under the application of a normal load. The relative motion can be either sliding, rolling or flowing over another body with which it is in contact. Friction is an energy-dissipating process, in which the kinetic energy of the moving body is transformed into heat, with consequent temperature variation of the contact surfaces [41].

### a. Types of friction

The following main type of friction can be distinguished:

- ✓ *Static friction* regards two bodies in contact that do not present relative motion under the influence of a resultant force. It is determined by the interlocking of the irregularities of two surfaces that prevent any relative motion up until some limit where motion occurs.

- ✓ *Kinetic friction* is defined as the force that resists to motion when two surfaces are moving with a relative velocity; it is, therefore, equal and opposite to the force required to maintain the relative sliding of the surfaces.
- ✓ *Rolling friction* is the force resisting the motion when a body (such as a ball, wheel, roll) rolls on a surface. At micro-scale it is caused by the interference of small indentations formed as one surface rolls over another. The phenomena that affect rolling friction are mainly due to non-elastic effects that involve both hysteresis losses and plastic deformation of the contact surfaces.
- ✓ *Flowing friction* determines an energy loss when a liquid flow in a cavity due to viscous effects generated by the surfaces that are in contact with the liquid.

Friction has a significant impact in many metalforming processes, influencing the material flow in the dies cavities and consequently the deformation and the forces required in the processes. Furthermore, it may generate large amount of heat at the interface between dies and the component, with relevant impact on the tools wear phenomena and the microstructure of the formed components. Moreover, most mechanical components have one or more moving parts. In some components, such as bearings and gears, the aim is to minimize the resistance to sliding or rolling so that as little energy as possible is lost to friction. Vice versa, in other components, such as brakes and clutches, maximum sliding resistance is required, in order to limit the relative motions and sliding [42].

## b. Adhesion theory of friction

The theory was explained by Bowden and Tabor [43] on the basis of the observation that two clean surfaces that are loaded against each other, in dry conditions, are in contact only for a fraction of their apparent area. Regardless the surface roughness, at a microscopic level (see Fig. 2.1 ) the load is supported only by the contacting asperities, whose sum represents the real area of contact $A_r$.

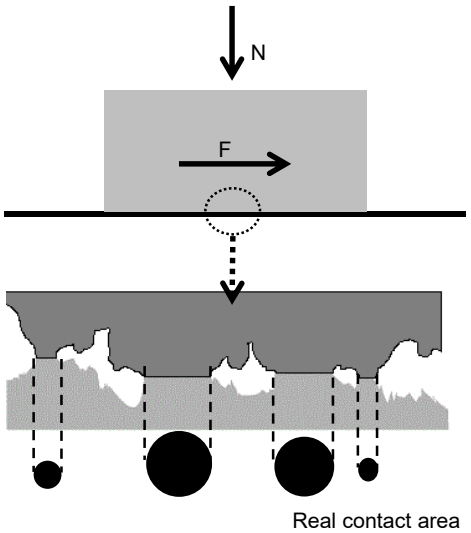


Fig. 2.1 Real area of contact of two surfaces in contact.

If the level of local pressure is kept lower than the material yield strength, the local deformation is elastic, while, as the pressure increases and overcomes the material yield stress, the contact asperities deform plastically with an increase of the contact area until the real area of contact $A_r$ is sufficient to support the load. Eventually new junctions are formed with other asperities of the two surfaces in contact with each other.

## c. Coefficient of friction

The coefficient of friction usually described by the letter $\mu$, is a dimensionless scalar value which represents the ratio of the tangential force $F$ and the normal force $N$ applied between two bodies in contact:

$$\mu = \frac{F}{N} = \frac{\tau Ar}{\sigma Ar} = \frac{\tau}{\sigma} \qquad \text{Eqn. (1)}$$

where $\tau$ is the shear stress of the junction and $\sigma$ is the normal stress [44]. The equation is often referred to as Coulomb friction model. In case of plastic deformation of the contacting asperities, $\sigma$ is the material yield stress and, for low values of normal load $N$, the real contact area $A_r$ is much lower than the nominal area $A$. This condition is typical of simple sheet metal forming processes such as bending. When the normal load increases, the number of asperities that are plastically deformed increases and the ratio between the real contact area $A_r$ and the nominal area $A$ increases too. Consequently, the relationship between the tangential and normal loads departs from linearity as it may be experiences in complex sheet forming processes such as deep drawing or stretch forming. If the normal load is increased further, $A_r$ ideally becomes comparable to the value of the nominal area of contact and the shearing force reaches a plateau maximum value, see Fig. 2.2.

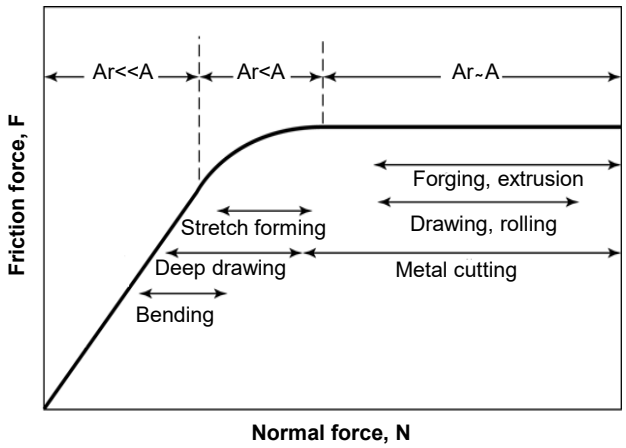


Fig. 2.2 Relation between friction force F and normal force N. Adapted from [44].

To describe the friction at the interface of two contacting bodies when high normal pressures are applied, a friction factor (or shear factor) is defined as:

$$m = \frac{\tau_i}{k} \qquad \text{Eqn. (2)}$$

where $\tau_i$ is the shear stress of the interface and $k$ is the shear yield stress of the softer material. The last equation is often referred to as Tresca friction model. According to such

definition, the magnitude of *m* does not depend on the normal force or stress, since the the shear yield stress of a thin layer of the material near the interface of two contacting bodies is unaffected by the magnitude of the normal stress [44].

### 2.1.2 Wear

Wear is defined as "damage to a solid surface, usually involving progressive loss or displacement of material, due to relative motion between that surface and a contacting substance or substances" [45].

#### a. Types of wear

The following main type of wear mechanisms can be distinguished:

- ✓ *Adhesive wear:* this term indicates the wear mechanism between two bodies in contact, where plastic deformation phenomena and adhesion between the contacting asperities play a predominant role in the fragment formation. Historically, this mechanism is described by the Archard theory, even if the current interpretation has been modified compared to the original theories, because of developments in techniques Observation of fragments and wear surfaces, which have allowed to understand in more detail the real phenomena. The starting point of Archard theory is the hypothesis of plastic deformation of the asperities in contact with the consequent formation of plastic junctions by adhesion [46]. The fracture path depends on whether or not the strength of the adhesive bond of the asperities is greater than the cohesive strength of either of the two sliding bodies. Some possible causes are the strain hardening of the asperity contact, diffusion etc. which make the adhesive bond stronger than base material. Thus, during sliding, fracture at the asperity usually follows a path on the weaker or softer component and a wear fragment is generated.
- ✓ *Abrasive wear:* in case of large difference in the surface hardness of the two bodies, the harder one tends to scratch the softer material, causing the phenomenon known as plowing. In such case, adhesion between the asperities is less relevant and portions of the softer materials can be ripped [44]. The abrasive resistance is directly proportional to material hardness, so in order to reduce abrasive wear, it is possible to increase the hardness of materials or reduce normal load applied. Furthermore, there are two basic types of this wear mechanisms:

- If there are only two rubbing parts involved in the friction process the wear is called *two body wear*. In this case the wear of the softer material is caused by the asperities on the harder surface.
- If the wear is caused by a hard particle trapped between the rubbing surfaces it is called *three body wear*. The particle may be either free or partially embedded into one of the mating materials.

- ✓ *Fretting wear:* this type of wear occurs when two surfaces in contact are subjected to high loads and oscillatory movement with small amplitude and high frequency rate, to reciprocating motion of small displacement amplitude in the order of microns, whereas the conventional reciprocating motion relative to wear is known to occur at much larger displacement amplitude [47], namely higher than 300 microns [48][49]. This causes the generation of wear particles which are unable to escape from the contact and give rise to more wear.
- ✓ *Fatigue wear:* this phenomenon is caused when the surface of the tribo-body is subjected to cyclic loading, such as in a rolling contact in bearing.
- ✓ *Trib-oxidative wear:* this wear, also known as *corrosive wear* or *tribo-chemical wear*, indicates wear that is caused by chemical or electrochemical reaction between the surface and the environment. The fine corrosive products on the surface constitute the wear particle. When the corrosive layer is destroyed or removed, as by sliding or abrasion, another layer begins to form, and the process of removal and corrosive-layer formation is repeated. This process is influenced by atmosphere gases (oxygen) and temperature.

### 2.1.3 Lubrication

The reduction of friction and wear between two bodies in contact and in relative sliding can be obtained by interposing between the two surfaces a substance capable of reducing the shear stress needed to allow the sliding of the same. This substance, which can be solid, liquid or gaseous, is called lubricant. Consequently, lubrication is the process or technique employed to reduce friction and wear of one or both surfaces moving relative to each other, by interposing a lubricant.

#### a. Types of lubrication

The most common lubricants are the liquid ones, such as oil, which consist of a base fluid and different additives which are added to improve certain properties such as load carrying capacity, viscosity or oxidation resistance. Other widespread lubricants are greases, which are considered as semi-solid and consist of oil mixed with a thickener. They are characterized by very high viscosity at room temperature and they are usually employed where oils would not be able to remain in place. Furthermore, they provide sealing against contaminants. The lubricant can also be a solid material with a lamellar structure that allows easy shearing e.g. graphite, molybdenum disulphide or boric acid.

By using liquid lubricants, depending on contact situation, a classification between the surfaces lubricated into different regimes is common. By using the Stribeck curves, schematically represented in Fig. 2.3, lubrication regimes are distinguished into three principal mechanisms:

- ✓ *Boundary Lubrication* (BL): this phenomenon occurs when the interaction load is supported by asperities and friction and wear are governed by the surface films that are formed during sliding through reactions between the surfaces and the additives/environment [50];
- ✓ *Mixed Lubrication* (ML): in this case, as the speed and viscosity of the fluid decrease, or as the normal load increases, the film thickness is reduced to about three to five times the surface roughness. There may be some metal-to-metal contact at the higher asperities; this contact increases friction and leads to slightly higher wear. A hydrodynamic pressure starts to build up and the load is partially carried by an oil film [50];
- ✓ *Hydrodynamic Lubrication* (HL): when fluid lubricant is present between two rolling and/or sliding surfaces, a thick pressurized film can be generated by the surfaces velocities to reduce friction and wear. In this case the two surfaces are completely separated and the entire load is carried by a lubricant film. A pure hydrodynamic lubrication strongly relies on continuous high sliding velocities and subsequently pressures and temperatures remain low. Hence the mechanism only appears in case of ideal conditions [50].

The Stribeck curve shows the relation between coefficient of friction μ as function of the parameter

$$H = \frac{\eta v}{p} \quad \text{Eqn. (3)}$$

where η is the lubricant viscosity, v the relative velocity and p the contact pressure. The H parameter is often referred to as the Hersey or Sommerfield parameter.

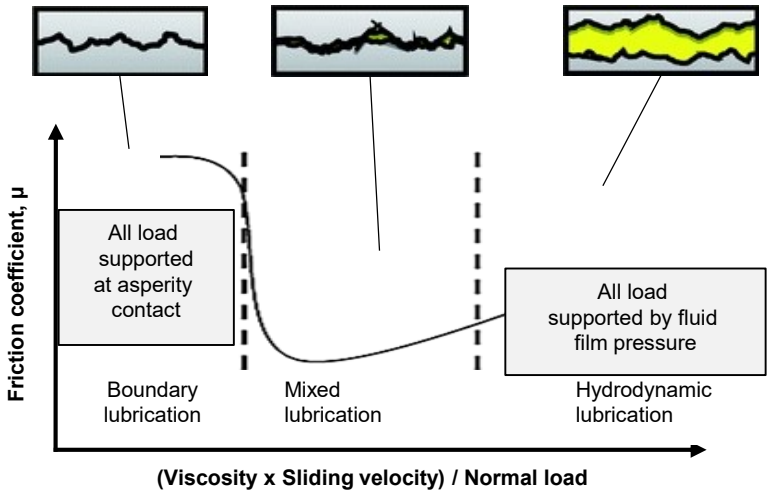


Fig. 2.3 The Stribeck curve. Adapted from [51].

With solid lubricants, the sliding mechanisms are different from the liquid one and can be classified in three ways, Fig. 2.4;

- ✓ *Intrafilm flow:* it occurs when the film adheres to both surfaces and flows like a viscous fluid to accommodate relative displacements of the two surfaces. Although

normally associated with non-crystalline materials, shear flow can also take place with crystalline materials at relatively high temperature.

- ✓ *Interface sliding:* it allows the two original surfaces to slide over one another only if there is no adhesion to the upper surface.
- ✓ *Inter-film sliding:* it occurs when the lubricant adheres to both surfaces but separates into two distinct films that slide across one another. In this case neither of the two original surfaces is in contact. The shear strength is, therefore, the one that permits the two films to slide against one another.

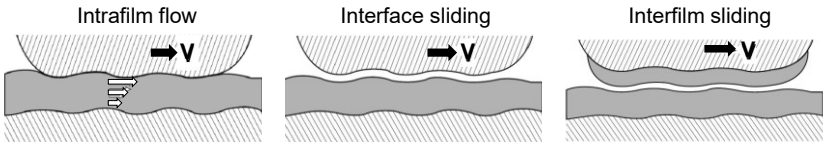


Fig. 2.4 Schematic representation of three ways by which sliding can be accommodated between an uncoated and a coated surface. Adapted from [52].

### 2.1.4 Parameters influencing friction and wear

The most relevant parameters that can affect the friction and wear at the interface between the tools and the workpiece during a sheet metal forming process are the following:

*Tool/Workpiece Parameters*

- ✓ *Properties of the workpiece material:* i.e., flow stress influences how the workpiece deforms and thus how the lubricant must flow. Consequently, the properties of both the die and workpiece material influence how the lubricant reacts with the surfaces.
- ✓ *Geometry*: i.e., the geometry of the die influences how the workpiece deforms and thus how the lubricant must flow.
- ✓ *The surface finish:* both the tool and the workpiece surface roughness influence how hydrostatic lubricant pockets are formed.
- ✓ *Oxidation*: the scale on the workpiece surface influences the interface conditions. If the scale is soft and ductile, it may act as a lubricant. If it is hard and brittle, it may cause an abrasive wear mechanism.

*Lubricant parameters*

- ✓ *Type of lubricant:* the composition of the lubricant influences the viscosity and how the viscosity changes when subjected to extreme heat and pressure. The lubricant composition also influences how the lubricant reacts with both the die and the workpiece.
- ✓ *Amount of lubricant*: this variable influences how the lubricant spreads as the workpiece is deformed and how hydrostatic lubricant pockets are formed.

- ✓ *Coatings:* the type of coating used, for example metallic or polymeric, may establish different mechanisms of lubrication to the interface tool-metal sheet and the possibility of oxidation of the surfaces due to heating.

*Process parameters*

- ✓ *Pressure:* load exerted by the die on the workpiece influences the viscosity of the lubricant and the deformation of the surface asperities, which affects the formation of hydrostatic lubricant pockets.
- ✓ *Sliding velocity:* velocity at which the die moves relative to the workpiece influences the heat generation at the die/workpiece interface.
- ✓ *Sliding length:* length at which the die moves over the workpiece influences the heat generation at the die/workpiece interface, the extent to which the lubricant must spread out, and the extent to which the lubricant will break down.
- ✓ *Temperature:* the heat generated due to the deformation process and the machine operation influences the material properties (i.e., flow stress) of both the die and the workpiece and the viscosity of the lubricant.

### 2.1.5 Tribological tests for sheet metal forming

When characterization of the tribological performance is required during a sheet metal forming process, a high level of control of the conditions that can be established is necessary. The conditions at the interface dies-metal sheet may vary significantly in different zones of the dies and during different phases of deformation, thus making it complicated to reproduce them in simple laboratory experiments. For this reason it is not appropriate to use a single test to characterize the tribological performance and the choice of the most appropriate test requires careful assessment of parameters for which the tribological analysis is desired. As a consequence, different tribological tests have to be considered, and they can be divided into three main categories according to their capabilities in both replicating and controlling the process parameters [8]:

- material testing;
- simulative testing;
- process-type testing.

- ✓ *Material testing:* Material testing is usually performed on commercially available friction testers that are configured to realize traditional pin-on-disk or ball-on-disc experiments. In the test, a pin/ball is pressed against a rotating disk to evaluate the friction coefficient between two bodies. The pin/ball is mounted on a controlled head, while the disk is fixed to a rotary drive, see Fig. 2.5.

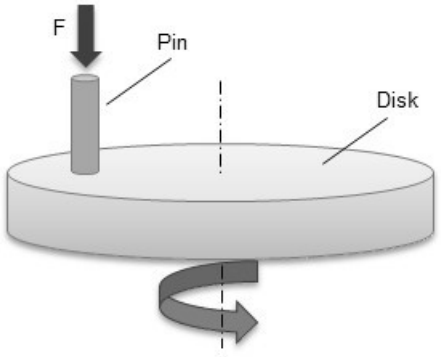


Fig. 2.5 Schematic illustration of the pin on disk test.

A load-control mode may be adopted to apply a constant pressure at the interface between the pin and the disk during the test [53]. Consequently, the Coulomb friction coefficient is calculated according to Eqn. (1).

- ✓ *Simulative testing:* With this type of test it is possible to have complete control of the conditions that are established at the interface die-sheet arising during a sheet metal–working operation, with the full control of the relevant process parameters, such as the normal pressure, sliding length, sliding speed, and workpiece–tool interface temperature. This approach allows reproducing the process conditions, but the simulative testing apparatus has to be designed as a dedicated piece of equipment, embedding the measurement sensors for the test control and the acquisition of the test parameters. The flat die drawing test is probably the most popular simulative type of testing [8]. The test allows the measurement of the coefficient of friction for a wide range of normal loads $F_N$ and drawing speed, v. During the test, a strip is drawn between flat dies, which can be at room temperature or heated up to the temperature of the dies in the industrial reference process, see Fig. 2.6. The equation used for the calculation of the friction coefficient is Eqn. (1), where $F_T$ defines the drawing force (tangential force). This typology of test allows an independent control of the most critical process parameters, such as the normal pressure at the sliding interface, sliding speed, interface temperature, and surface texture.

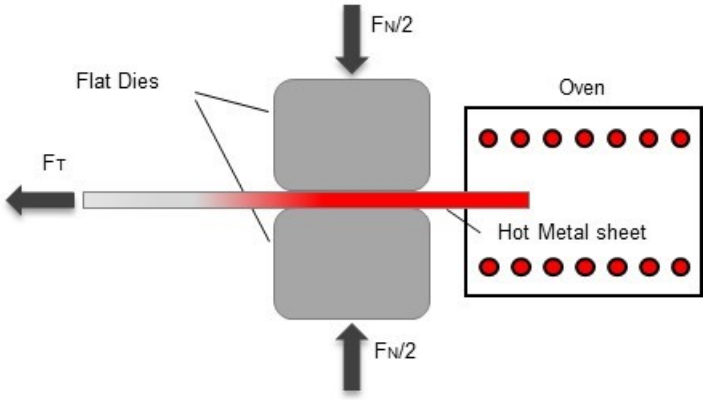


Fig. 2.6 Schematic illustration of the strip drawing test.

- ✓ *Process-type testing:* These tests are generally based on equipment similar to that utilized in industry, reproducing sheet metal – working process operations without changing the basic process kinematics. Due to their simplicity and immediate information, such tests are especially attractive for industry, because of the possibility of reproducing exactly the conditions of the process. The testing procedure seldom requires special equipment and accurate control of the testing conditions. Friction data are usually obtained through indirect measurement of the specimen deformations [8]. Examples of process type testing is the cup drawing test (see Fig. 2.7). In the deep drawing test, if the friction is not significantly high, the final formed cup will not present tears and/or excessive necking. The method is relatively insensitive to changes in friction regarding the forming force, but the maximum drawing ratio, defined as the largest blank diameter possible to draw divided by the punch diameter, yields information about the friction level, thus permitting to rank the lubricant performance and therefore providing qualitative information. However, quantitative measurements have been developed, for example based on a divided blank-holder system.

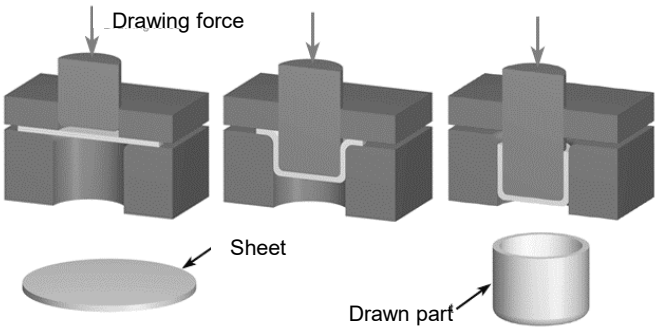


Fig. 2.7 Schematic illustration of cup drawing test.

The tests presented above are among the most common used in tribological evaluations for the processing of sheet metal forming; anyway, in order to study the tribological phenomena during any metal forming process, appropriate tests that can replicate the interaction surfaces are needed. Many parameters are implied in tribological conditions, so the prediction of frictional forces only on the basis of theoretical calculation is impossible. Therefore experimental testing must be chosen and used in order to evaluate the frictional, lubrication and wear effect either in qualitative or quantitative terms.

## 2.2. Tribology in hot stamping of HSS

In this Section the literature review on the innovative hot stamping process of High Strength Steels for car manufacturing was analyzed in detail from the preliminary studies until the recent process evolutions. In the first part a short introduction is developed to provide a general outline of the issues addressed and under review within this research work and, subsequently, particular attention is given to a survey of the existing research works concerning

tribological investigation of coated and uncoated HSS for hot stamping process in terms of heat transfer phenomena, friction and wear.

One of the parameters that most influence the behaviour of the friction coefficient and the wear mechanisms that are established at the interface die-metal sheet is thermal cycle applied on die surface and blank. The cooling strategy and above all the tool material thermal conductivity are among the factors that most affect the thermal state during the contact between die and metal sheet, supposing that the sheet-tool contact and the cooling fluid properties are constants. Moreover, an important aspect of hot stamping is cycle times and, tool steels with a High Thermal Conductivity improve product quality and the productivity of the hot stamping process because heat can be transferred much faster from the sheet metal into the tool, decreasing the quenching time. Additionally, steel grades used for hot stamping dies should offer an elevate hardness and good wear resistance to withstand severe tribological condition during service life, since the major failure is abrasive and adhesive wear which is caused by sliding of the sheet metal against the tool surface.

### 2.2.1 Thermal aspects in stamping of HSS at elevated temperature

In [54] Authors presented a method to estimate the thermal conductance to improve the Usibor 1500P® blank cooling during the hot stamping process. In this research work an experimental equipment was presented with the purpose to evaluate the thermal contact resistance at the die-metal sheet interface. The testing set up is composed of a die and a punch made in Z160CDV12 steel with an omega shape. The most interesting locations in the tools and samples are thermally instrumented with thermocouples type K sheathed with silky glass, forming heat-flux meters. By using these values the thermal contact resistances RC at the contact interfaces were estimated experimentally through a non-linear 1D inverse technique founded on sequential method of Beck. The results show that the thermal contact resistance at blank/tools interfaces is as a function depending on the global contact pressure. For his reason, results of thermal conductance during the quenching phase show that the heat transfer is three times more intense at the bottom of the part interface than at the vertical interface.

M. Merklein in [55] is focused on the determination of the thermal properties of 22MnB5 sheets coated with Al-Si and Zinc coatings Fig. 2.9, used during the hot stamping process.

| Classification | Base material | Sheet thickness | Coating system | Supplier |
|---|---|---|---|---|
| Material A | 22MnB5 | 1.75 mm | Al/Si | A |
| Material B | 22MnB5 | 1.75 mm | Al/Si | B |
| Material C | 22MnB5 | 1.8 mm | Zinc | C |

Fig. 2.8 Investigated materials and their specification and classification. Adapted from [55].

For the determination of the heat transfer coefficient, an equipment with two rectangular exchangeable water cooled contact plates and thermocouple equipped specimens was used. The sample was placed between the two plates after undergoing a previous homogeneous austenitization at temperatures between 850 °C and 950 °C in a furnace under atmospheric conditions. After positioning of the sample, the specimen can be loaded during quenching with a defined contact pressure up to 40 MPa. During the test, the temperatures of the blank and

both contact plates are recorded by using integrated thermocouples. With this research work, the authors found a strong dependence of the heat transfer coefficient with the applied pressure at the interface die-metal sheet; all the test conditions exhibit a significant increase of the occurring heat transfer between tool and workpiece with increasing contact pressure, Fig. 2.9.

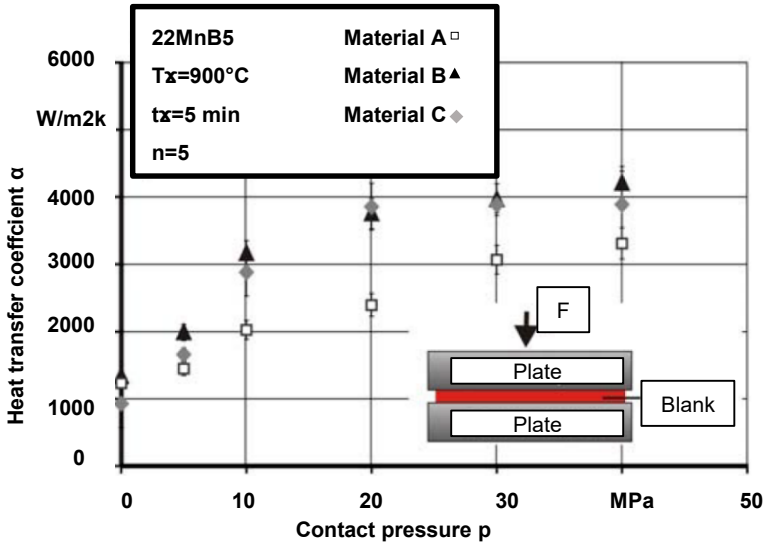


Fig. 2.9 Evaluation of the heat transfer coefficient as function of the contact pressure p in dependency of the applied corrosion preventing coating system. Adapted from [55].

Furthermore, the results show that the dependency of the heat transfer coefficient is strongly influenced by the applied coating system of the blanks in terms of supplier, thickness and type of coating.

Authors in [56] analysed influence of two important parameters, tool temperature and punch speed in hot stamping technology, on effects of the temperature distribution and thus the microstructure and the final properties of hot stamped part (22MnB5), by combining the experimental and simulation results. Three levels of tools temperature were selected (room temperature RT, 110 °C and 250 °C) and punch speed from 35 to 350 mm/s. With regard to effect of tool temperature, results show that the higher temperature difference between workpiece and tools results in a higher cooling rate of workpiece and better quenching effectiveness while, the punch speed seriously affects the final properties of hot formed part; the higher punch speed, leads to higher tendency of crack despite the high punch speed increases production efficiency.

With the aim to calculate the Interface Heat Transfer Coefficient (IHTC), and the factors that influence this last, in [57] Authors developed a cylindrical-die experimental model (Fig. 2.10) in order to carry out experiments on boron steel 22MnB5 during hot stamping operations.

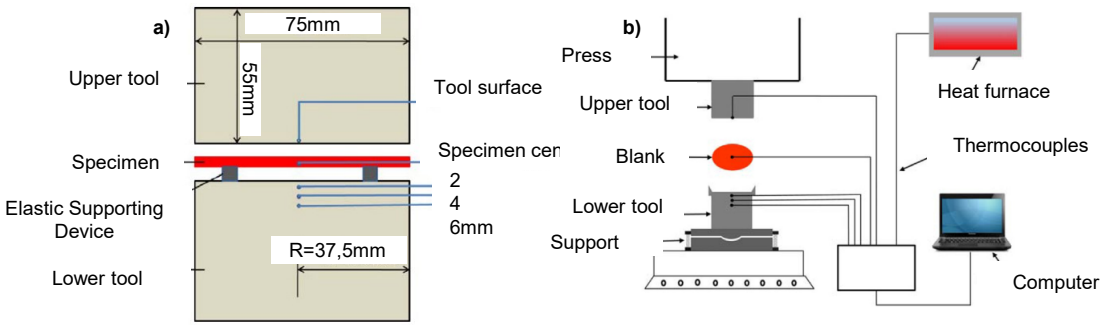


Fig. 2.10 a) Dimensions of the heat transfer device and the thermocouple positions and b) schematic illustration of the experiment setup. Adapted from [57].

The influence of both contact pressure and blank surface roughness were studied, because these affect the actual contacting area, which impacts the interfacial heat flow resistance and consequently the value of IHTC. Also in this case, results show that the IHTC is strongly influenced from contact pressure (Fig. 2.11a); it also increases significantly with decreasing surface roughness but slows down when the roughness is less than 1 μm and saturates at high contact pressure as it is possible to observe from Fig. 2.11b.

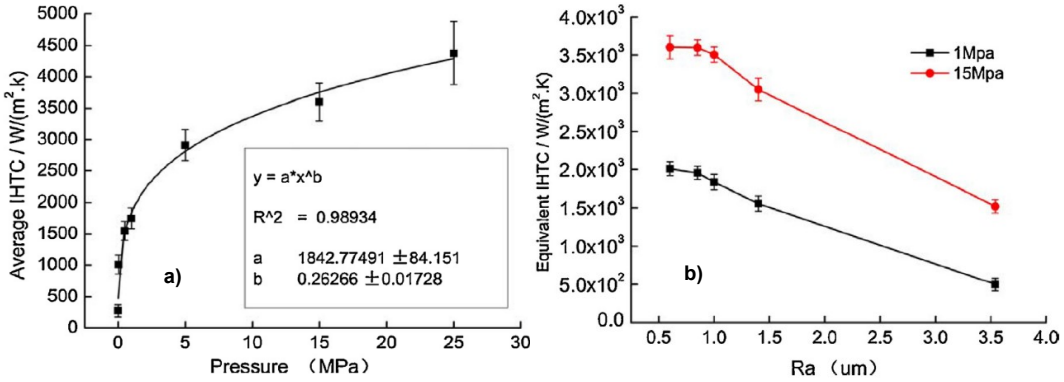


Fig. 2.11 a) Curve fitting for the equivalent IHTC versus contact pressure and b) relationship between the equivalent IHTC and surface roughness. Adapted from [57].

In [58], the characteristics of the Interface Heat Transfer Coefficient between sheet blank (boron steel) and tools (SKD 61 steel) were investigated using an experimental platform and at the same time, the performance of cooling system design were studied as a function of distance from tool surface to cooling channel edge (three distances 5, 10 and 15 mm), channel diameters (three diameters 10, 15 and 20 mm) and number of cooling channel in a unit cell. From the experimental results, it reveals that the interface heat transfer coefficient is proportional to contact pressure; as the contact pressure increasing, the IHTC is also increased. In the analysis of cooling system, the finite element simulation results reveal that the distance from tool surface to cooling channel has a significant influence on the cooling rate for all three channel diameters selected; the greater the diameter used, the greater the cooling rate. It also shows that as the number of channel increases, the cooling rate performance become steady and a more uniform cooling rate in the sheet metal can be achieved.

The characteristic of the Heat Transfer Coefficient of the boron steel for hot stamping process was studied in [59]. In this research work, an experimental platform was built, and an inverse calculating method was used for obtaining the heat transfer coefficient as a function

of contact pressure at interface die-metal sheet (SKD61 die steel and boron sheet steel). The experiment and analysis results show that the heat transfer coefficient increases as the contact pressure increases, Fig. 2.12 and that using the heat transfer coefficient as a function of time in FEM model can obtain more accurate results compared to using the constant heat transfer coefficient in FEM model.

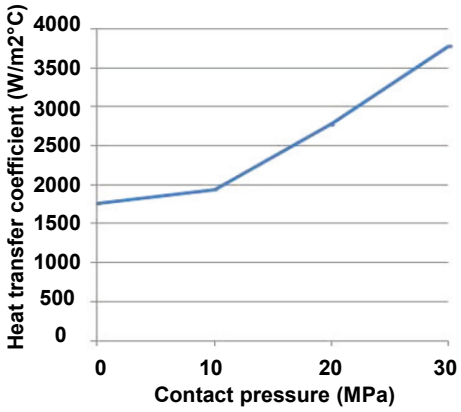


Fig. 2.12 Heat transfer coefficient of blank and tools at different contact pressures. Adapted from [59].

In [60], with the purpose to present a systematic method to design hot stamping tools with cooling systems, a series of hot forming processes (of a stamped component, Fig. 2.13a) was simulated thermally as well as thermo-mechanically (in terms of time cycle and process parameter) to observe the heat transfer and the cooling rate through the optimized cooling system, without considering the tool motion, which could be sufficient with reasonable accuracy and shorter computation time for quick design of the hot stamping tools with cooling system. On this base, the cyclical tools surface temperature evolution of two different configurations were evaluated, and then the thermo-mechanical analyses was carried out on the best cooling system configuration in order to enhance the accuracy of the predictions, Fig. 2.13b.

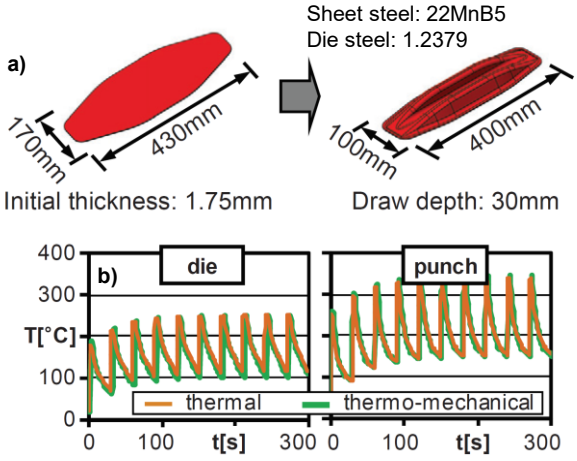


Fig. 2.13 a) Initial blank and drawn part and b) temperature changes for 10 cycles. Adapted from [60].

In [61] F. Sheick, by means of simulation environment, analysed the flow conditions in the cooling channels involving the use of two different cooling concepts (punch, die), in order to gain knowledge about the distribution of heat transmission during the press-hardening

process and the analysis of the influence of flow parameters such as, velocity and direction of flow on the surface temperature of the active parts. The main results coming from the simulation are shown in Fig. 2.14.

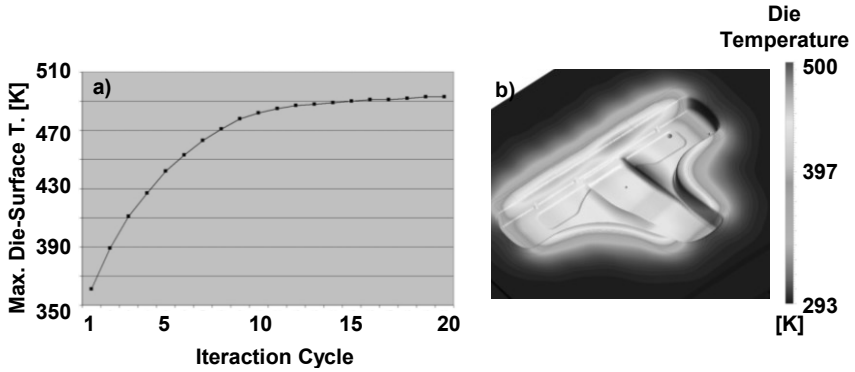


Fig. 2.14 a) Maximum surface-temperature (die) for each iteration cycle and b) die surface-temperature – cycle 20. Adapted from [61].

The results of the simulation show the rise in temperature over and above the individual process iteration loops until a steady state operating condition has been more or less achieved for the tool (process parameters approximating to those in use in volume production); the evolution of the maximum surface temperature on die surface as a function of the iterations cycles is shown in Fig. 2.14a. Figure Fig. 2.14b highlights a non-constant surface temperature distribution, with the maximum one of 493 K. The simulation had demonstrated its potential in optimizing tool design but depending on the individual application often cannot be implemented because of a lack of sufficient characteristic data and adequate computer performance.

### 2.2.2 Friction and wear in stamping of HSS at elevated temperature

A review of literature reveals that A. Yanagida in [62] proposed the first development of experimental apparatus to evaluate friction coefficient in hot stamping condition, Fig. 2.15.

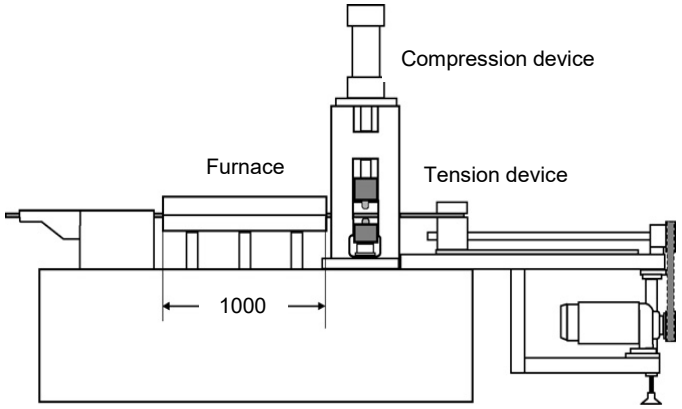


Fig. 2.15 Schematic representation of hot flat strip drawing test machine. Adapted from [62].

This test machine consists of a compression device driven by a hydraulic actuator, a furnace and a drawing device driven by a ball screw using a 2.2 kW vector control AC motor. As shown in Fig. 2.15, the strip is first set on the table then the strip edge is clamped with the chuck part

of the tension device. The strip is heated to a given temperature using an infrared image furnace. As shown in Fig. 2.16b, secondly the strip with a front tension moves to the compression device by the tension device.

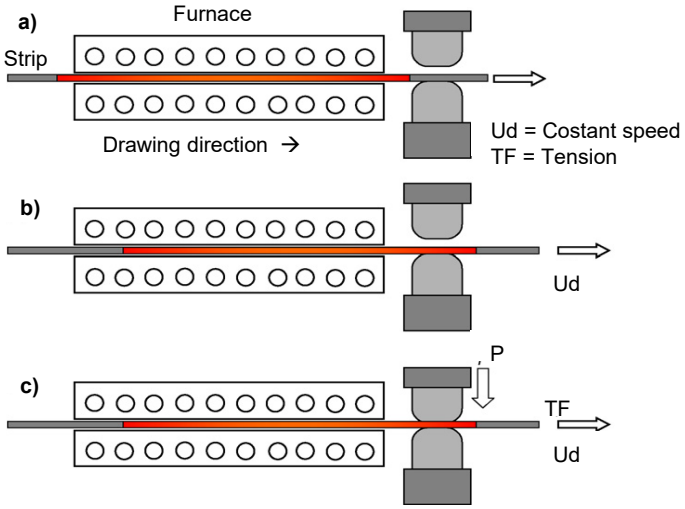


Fig. 2.16 Schematic representation of test method. Adapted from [62].

As shown in Fig. 2.16c, as the heated zone of the strip reaches the entrance of the die, the heated strip is compressed at a given compression load by the upper die and simultaneously moved at a constant drawing speed. Under these conditions, the compression load P and the tension load TF are measured. The coefficient of friction can be calculated from P and TF using the equation $\mu = TF/2P$. The first results obtained regarded the heating and cooling performances (equipment calibration phase), which were evaluated with K-thermocouple spot-welded on metal strip surface.

In [63], the Authors, by mean the machine presented in [62], measured the friction coefficient using SPHC (0.15 C-0.6 Mn steel) steel and 22MnB5 steel (Al-Si coating) under dry and lubricated conditions, by investigating the influence of several process parameters. A sliding speed of 10 mm/s, two levels of pressure (32 and 9 MPa), two range furnace temperature (600-800 °C) and two lubricants (both water based) are tested. Under lubricated conditions, the dies (SKD61 steel) were removed from the simulator and preheated to 200 °C then the lubricant was sprayed on the die surface before drawing in order to form the lubricant film. Results shown that in dry condition, coefficient of friction of 22MnB5 steel is higher than that of SPHC steel, Fig. 2.17a. The mean coefficient of friction of 22MnB5 steel increases with increasing temperature. For SPHC steel, the mean coefficient of friction is independent of the die pressure, Fig. 2.17b. In case of lubricated condition, the mean coefficient of friction of 22MnB5 steel is higher than that of SPHC steel and the mean coefficient of friction is independent of the temperature. The coefficients of friction of both steels under lubricated conditions are lower than those under dry conditions. Lubricants highly affected the friction coefficients, since it was registered a drop from 0.58 to 0.3 with the Al-Si coated 22MnB5 steel and from 0.43 to 0.15 with the SPHS one, Fig. 2.17c.

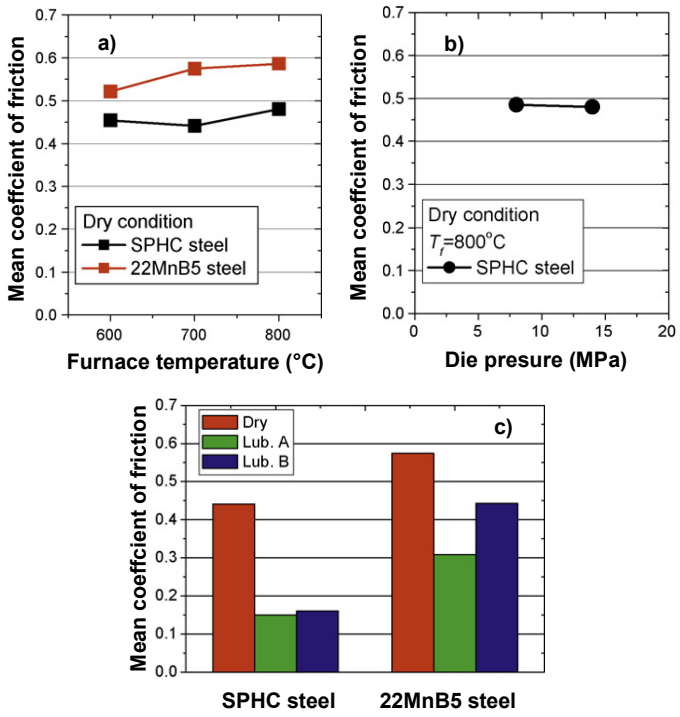


Fig. 2.17 a) Effects of temperature on mean friction coefficients under dry conditions b) Effect of die pressure on mean friction coefficients under dry conditions and c) Effect of lubricant on mean coefficient of friction. Adapted from [63].

Again, by means of the machine presented in [62], the Authors in [64], analysed the friction coefficient for various surface roughness of the die (0.07, 0.2 and 0.5 μm Ra values), against aluminium-coated HSS in dry and lubricated conditions with metal sheet temperature 720 °C, a drawing speed of 10 mm/s and 3.5 kN of compressive load. Results shown that, in dry condition, coefficient of friction is independent of the surface roughness of die and remains at about 0.55 regardless of the sliding distance but affected adhesion tendency of Al-Si coating on die surface, Fig. 2.18a. In lubricated condition, coefficient of friction depends on the surface roughness of the die and is lowest for a die surface roughness of 0.2 μm Ra, Fig. 2.18b. The coefficients of friction under lubricated condition are considerably lower than those under dry condition as shown in Fig. 2.18 and at same time, adhesion phenomena were less pronounced than in dry condition.

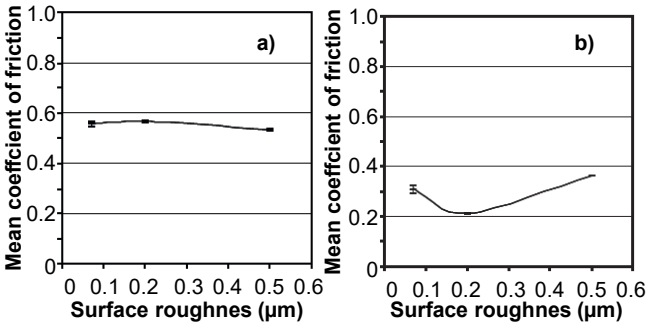


Fig. 2.18 a) Relationship between mean coefficient of friction and surface roughness under dry condition and b) Relationship between mean coefficient of friction and surface roughness under lubricated condition. Adapted from [64].

Also A. Ghiotti in [65] presented a novel experimental apparatus suitable for reciprocating sliding wear tests at elevated temperatures in order to study friction and wear in hot stamping process of HSS sheets, Fig. 2.19.

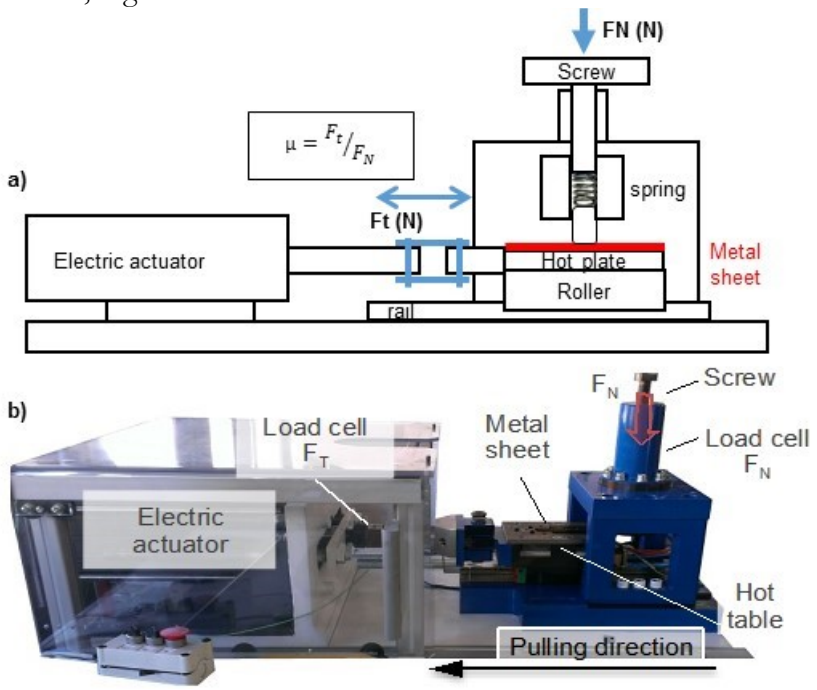


Fig. 2.19 a) Schematic representation of flat strip drawing test and b) the real version. Adapted from [65].

In this tribotester, a carriage, where the sheet sample is fixed, see Fig. 2.19a, is mounted on linear roller guideways and moved by the electric linear actuator. The load sensor, placed on the drive shaft, is used to measure the pulling force FT during the test. The normal load FN is applied on the metal sheet by a screw mechanism that embeds a piezoelectric sensor to monitor the applied normal pressure. A spring is sited between the die and the load sensors, which enables a high control and stability of the normal load applied, see Fig. 2.19a. The hot table, which provides the temperature control during the test, integrates three 800 W electric cartridges to heat up the metal strip and maintain the temperature constant during the test. Compared to the state-of-the-art laboratory tests, the developed set-up allows reproducing in a laboratory environment the loading and temperature conditions typical of the industrial process, so that to provide information similar to those that can be achieved through industrial trials.

J. Hardel [66], by using a high-temperature version of the Optimol SRV reciprocating friction and wear tester, analysed friction and wear behaviours of different tool steels sliding against Al–Si-coated High-Strength Steel at elevated temperatures, 40, 400 and 800 °C. The tools\pins specimens were used both with and without surface treatment. In case of surface treated tool steels, the pin specimens were nitrided by plasma nitriding, gas nitro-carburising and oxidation. Two sets of experiments were conducted. In the first set of experiments, the friction and wear characteristics of different tool steel and High-Strength Steel tribological pairs were studied during a temperature ramp from 20 °C up to 800 °C. These temperature ramp experiments were mainly aimed at studying the influence of increasing temperature on frictional behaviour. Wear measurements were carried out at the end of each temperature ramp

test and did not pertain to any specific temperature. The second set of experiments were conducted at three different constant temperatures with a view to studying the influence of temperature on friction and wear characteristics of tool steel and High-Strength Steel. In this case only the sheet specimen was heated, once it reached the desired temperature the tool specimen was brought in contact and loaded against the sheet metal specimen and the test was started. The low temperature of 40 °C resulted in low wear on the tool steels. At 400 °C, the tool wear increased. At 800 °C, the change in wear characteristics of plasma nitrided tool steels, as compared to those at 400 °C, were small but the wear on the Al–Si-coated High-Strength Steel was significantly lower. The principal material removal mechanism appears to be adhesive wear at all temperatures coupled with contribution from abrading action of oxidised wear debris at elevated temperatures. The wear characteristics of different plasma nitride tool steels are quite similar indicating that the compositions of the tool steels have hardly any influence on wear. Furthermore, the Al–Si-coated surface underwent surface morphological changes when heated to 800 °C. Concerning the friction analysis, the frictional behaviours as a function of temperature for different tribological pairs were quite similar. The initial friction coefficients in the first part of the test were about 0.8. These then quickly decreased to values of about 0.6. This trend was observed for all the plasma nitrided tool steels as well as for the untreated tool steels implying that the initial friction coefficients are neither dependent on the composition of the tool steel nor the surface treatment.

In [67] the Authors are focused on tribological investigations on both High Strength boron Steel – tool steel tribological pairs at elevated temperatures – as well as self-mated hardened High Strength boron Steel tribological pairs. Two different experimental equipments have been used in this study. For tribological studies at high temperatures, the Optimol SRV reciprocating friction and wear test machine was utilised. The other test equipment (Wazau UTM2000) is based on two-disc machine, used in the studies pertaining to fundamental tribological properties of self-mated hardened HSS, Fig. 2.20.

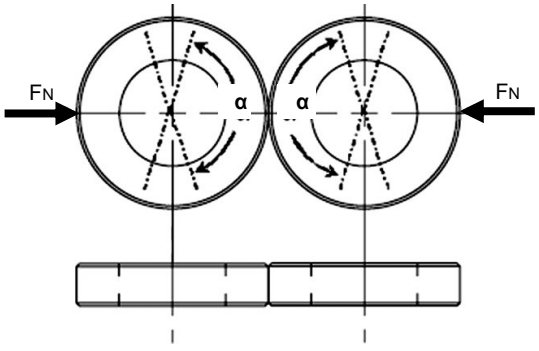


Fig. 2.20 Orientation of the discs relative to each other. The arrows show the direction of rotation (rotational angle $\alpha = 150^{\circ}$). Adapted from [67].

The metal sheet material under investigation was the boron steel 22MnB5 both uncoated and coated with 25 μm of hot-dip galvanized Al-Si. On tool side, three different types of materials were used and their surface were plasma nitrided to increase wear resistance. The tribological studies at high temperatures, with SRV test indicate that the operating temperature considerably influences the friction and wear behaviour during the tribological interaction of High Strength boron Steel and tool steel. The plasma nitriding of the tool steel specimens is effective in reducing friction and providing protection against severe adhesive wear during

rubbing against high strength boron steel. The Al–Si coating on boron steel has been effective in reducing friction during rubbing against plasma nitrided tool steel 1 at 800 °C but resulted in significantly higher friction at 500 °C. Further, the Al–Si coated boron steel has generally resulted in lower wear of plasma nitrided tool steel. On the other side, the Authors by means two-disc machine test, have shown that the friction and wear characteristics of the hardened High Strength boron Steel are considerably superior to that of the 900A steel, a common rail steel grade, chosen as a reference material since it is a well-known wear resistant rail material. The influence of sliding speed on the frictional behaviour of self-mated high strength boron steel pairs was marginal but friction tends to decrease at higher contact pressures. The specific wear rates of the high strength boron steel pairs decreases with increasing sliding speed whereas the influence of contact pressure on the specific wear rate do not reveal any clear trend.

In [68], M. Geiger presented an evaluation method for the determination of the friction coefficient for the direct hot stamping process of boron-manganese steels, basing on cup deep drawing tests at elevated temperatures, Fig. 2.21, on the base of the time-temperature-characteristic of the hot stamping process. Authors used, in this research work, aluminium-silicon coated boron-manganese steel 22MnB5 blanks, exposed to a heat treatment of 5 minutes at an austenitization temperature of 900 °C and 950 °C before being transferred manually to the cold or defined heated tooling device and subsequently being drawn. Regarding the validation of the numerical prediction of the outer cup diameter different specimens with an initial diameter d0 of 90, 85, and 80 mm were drawn up to varying punch strokes between 0 and 35 mm. Afterward the respective current outer diameter of the cups had been measured. Different temperatures at the moment of the maximum punch force were realized by varying the tool temperature in a range between 25 °C and 500 °C.

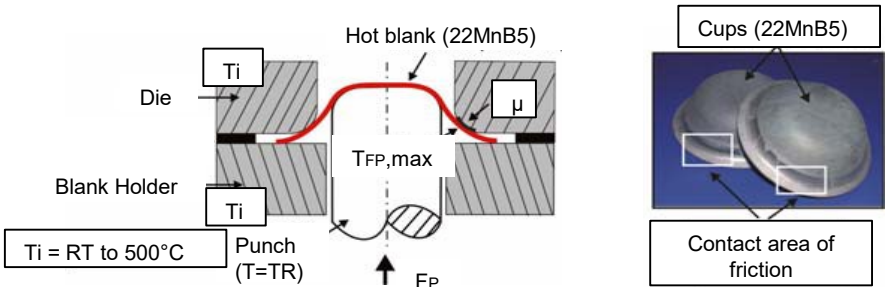


Fig. 2.21 Schematic sketch of the experimental setup of the cup deep drawing test (left) and two drawn cups at elevated temperatures with the contact areas of the main friction between blank and tool pointed out (right). Adapted from [68].

Fig. 2.22 reports the main results in terms of friction.

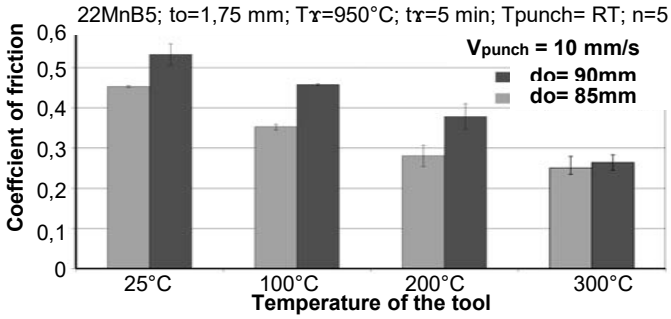


Fig. 2.22 Evolution of the friction coefficient in dependency of the tool temperature during the temperature of the punch remains at room temperature. Adapted from [68].

From this study, a decrease of the friction coefficient with increasing tool and so the sheet temperature was detected, with the values lie in a range between μ=0.55 at a tool temperature of 25 °C until μ=0.28 for tool temperature of 300 °C, Fig. 2.22. This type of approach, is very close to the real conditions present in the hot stamping process, both as regards speed of the punch and for the analysed temperatures.

The research work reported in [69] is aimed at evaluating the influence of different surface topography parameters, besides the commonly used Ra/Sa parameter, on the occurrence of galling during the tool steel/Al-Si-coated UHSS interaction at elevated temperatures. The parameters considered for this study are Rp, Rv, Rsk and Sm. Authors have focused on investigations of parameters that can be used to characterise the galling resistance of untreated tool steel surfaces. The experimental work in this study was carried out using an Optimol SRV high-temperature reciprocating friction and wear test machine; in this test, the specimens used for the tribological experiments were an upper pin made from quenched and tempered hot work tool steel with hardness of 52 HRC. The surface corresponding to the refurbished tools will be referred to as coarse grinding. The lower disc specimen was made from Al-Si-coated UHSS. Fig. 2.23a shows the surface roughness parameters and the values that correspond to each test specimen.

a)

| Type of surface | Sa (μm) | Rp (μm) | Rv (μm) | Sm (μm) | Rsk | Rku |
|---|---|---|---|---|---|---|
| Coarse grinding | 1.2–2.7 | 2.9 | −5.0 | 127 | 0.9 | 4.4 |
| Mild grinding, grit #60 | 0.7–0.8 | 1.8 | −1.9 | 99 | 0.1 | 2.7 |
| Mild grinding, grit #120 | 0.47–0.49 | 0.8 | −1.4 | 78 | −0.7 | 4.6 |
| Mild grinding, grit #240 | 0.34–0.39 | 0.4 | −0.6 | 90 | −0.6 | 3.2 |

b)

| Test parameters | Value |
|---|---|
| Normal load | 31 N |
| Nominal contact pressure | 10 MPa |
| Temperature | 900 °C |
| Stroke length | 4 mm |
| Frequency | 12.5 Hz |

Fig. 2.23 a) Surface roughness parameters and the values that correspond to each test specimen, while b) experimental plan. Adapted from [69].

The tribological tests were carried out following the experimental plan shown in Fig. 2.23b. The highlights of this research work results are that (i) the orientation of surface roughness lay

with respect to the sliding direction significantly influences the galling behaviour; parallel sliding with respect to the surface lay tends to reduce material transfer and the galling tendency. (ii) Surface roughness parameters, such as Rsk, Rv, Rp and Sm, influence on the occurrence and severity of the transfer of the Al-Si coating onto the tool steel. (iii) The surface roughness of the tool steel obtained after grinding with different grit sizes of abrasive paper resulted in reduced galling at elevated temperatures; this because the conditions for the occurrence of severe galling were not met on the specimens ground with abrasive paper.

Another deep study regarding adhesive wear and high temperature galling mechanisms occurring in hot stamping of HSS was done in [70] always by L. Pelcastre; in this research work only galling damage mechanisms were analysed, without taking into account other wear phenomena, as in [69]. The same Optimol SRV high-temperature reciprocating test and materials presented in [69], are used in this experience. The specimens (tools) used for the investigation had hardness values of 44, 48, and 52 HRC and the differences in hardness levels were achieved through heat treatments. At the same time, the surfaces of the tool steel specimens were produced using grinding, milling, and polishing processes. Tests at 10 and 20 MPa were carried out for each hardness level and surface roughness of the tool steel specimens, with the metal sheet at 900 °C. A stroke of 4 mm, a test duration of 30 s and a frequency of 12.5 Hz were used as test parameters. In this way, the influence of contact pressure, hardness, and surface roughness was then evaluated. The main results of this study are focused on the evolution of the wear mechanisms to vary the hardness of the inserts and the relative roughness; at low nominal contact pressure, the role of surface roughness is very significant in the occurrence of galling. The rougher surfaces result in more material transfer and the effect of the tool hardness on the galling process is not very significant. Vice versa, at a greater nominal contact pressure of 20 MPa, the role of surface roughness is not as significant as that at 10 MPa and the higher hardness seems beneficial in reducing the material transfer.

Also X. Tian in [71], as A. Yanagida in [62] and A. Ghiotti in [65], developed a hot strip drawing tribo-simulator in order to investigate the friction and wear behaviour of High Strength Steel in hot stamping process. Compared to others Authors [62][65], X. Tian introduced an induction heating ($T_{max}$=1000 °C) to ensure high heating rate and hence less oxidation of the strip, Fig. 2.24.

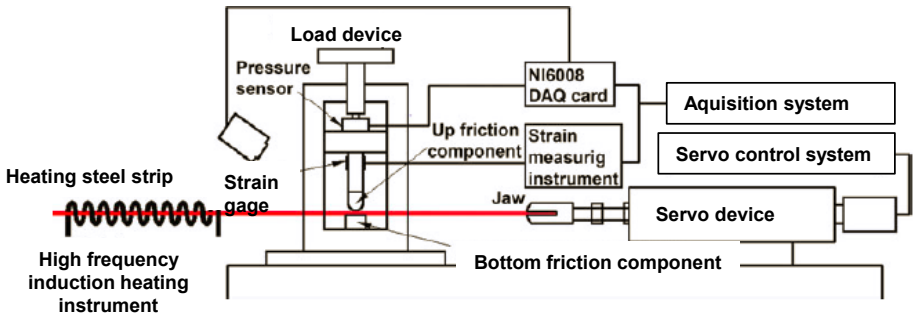


Fig. 2.24 Schematic representation of hot strip drawing tribo-simulator. Adapted from [71].

Tool steel H13 was selected for fabrication of the top and bottom friction components that generate friction with the hot steel strip. A High Strength Steel Advanced 1500 was used as sample for friction measurement. Friction coefficient as functions of temperature and drawing

speed was measured, respectively, to simulate the hot stamping processes, and a constant load of 215 N was applied for all the measurements. The main results are reported in Fig. 2.25.

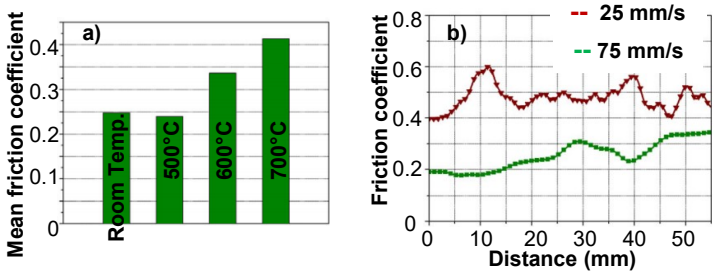


Fig. 2.25 a) The friction coefficient of steel Advanced 1500 at temperatures of room temperature, 500 °C, 600 °C and 700 °C and b) friction coefficient as a function of sliding distance at 550 °C and various drawing speeds. Adapted from [71].

As is possible to see, the results have shown that the friction coefficient remains almost unchanged until temperature reaches 500 °C. Further increasing the temperature from 500 to 600 °C, the coefficient of friction greatly increases, Fig. 2.25a. Fig. 2.25b, shows that by increasing the sliding speed the friction coefficient decreases, and this was mainly due to the different wear mechanism activated on metal sheet surface, adhesive wear at 25 mm/s and slight surface grooves at 75 mm/s.

J. Kondratiuk in [72] is focused on investigating in friction and wear between tool steel and Al–Si coated or electro-plated zinc nickel boron steel sheet at elevated temperature, using a hot strip drawing simulator, Fig. 2.26, which calculates the friction coefficient μ according with $\mu = F_t/2F_C$ and permits to use different tool geometries.

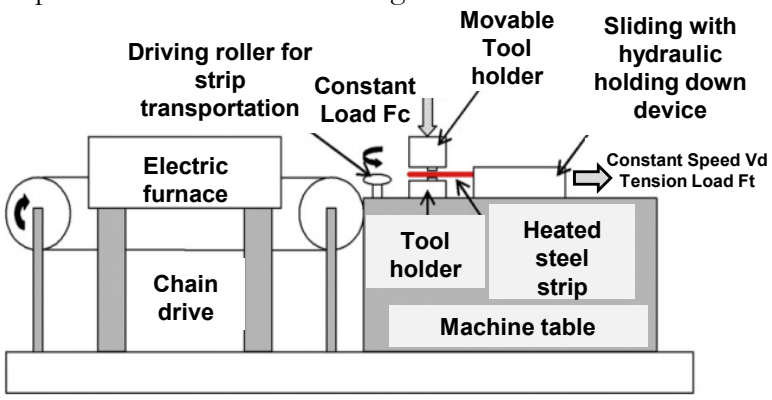


Fig. 2.26 Schematic representation of hot strip drawing simulator. Adapted from [72].

The experiments were conducted with two different load levels (2.5 and 4 kN), two tool geometries (material is 1.2379), two levels of temperature (880 °C and 920 °C) while the sliding speed was kept constant at 60 mm/s. Fig. 2.27 represents the average coefficient of friction for all tested conditions.

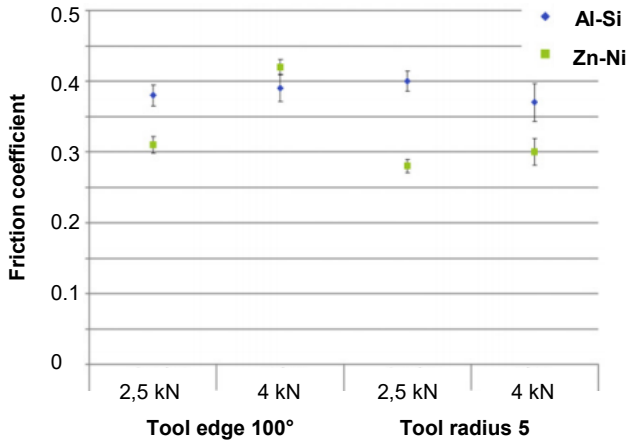


Fig. 2.27 Coefficients of friction for Al-Si and Zn-Ni coatings at different tested conditions in comparison. Left hand side: tool geometry edge 100° with loads 2.5 kN and 4 kN; right hand side: tool geometry radius 5 with loads 2.5 kN and 4 kN. Adapted from [72].

Results shown that the mean coefficients of friction for the electro-plated Zn–Ni coating are ranging from 0.28 to 0.42. The reason for the lower friction coefficients might be attributed to the oxidised top layer of the zinc based coating. It consists mainly of ZnO, which is known to act as "lubricious oxide" under certain conditions at elevated temperature. The average friction coefficients for the Al–Si coatings vary from 0.37 to 0.40 depending on the test conditions as displayed in Fig. 2.27. From these results it is possible affirm that the tool geometry and the applied compression load do not seem to have significant influence of friction behaviour in hot strip drawing. Other at friction behaviour, the present study is focused on the assessment of wear behaviour and test to quantify the amount of wear by gravimetric methods, by means metal forming tests performed on a hydraulic double-sided press. The tool materials are 1.2080 for the punch and 1.2379 for the die. Both parts have been hardened and tempered at a hardness of 61 HRC. After heat treatment and surface finishing some tools have been plasma nitrided and coated with different coatings. In this study, coatings applied are a TiN/TiB2 multilayer system and an AlCrN coating system. Metal sheet temperature were the same of the friction tests (880 and 920 °C). The analysis of each die material was performed after 150 strokes by using SEM equipped with EDX detector. Detailed metallographic and chemical analysis of material transferred from workpiece to die surface during hot forming operation revealed that mass transfer and persistent material build-up on the die is significantly lower when Zn–Ni coatings are used. Moreover, the transferred material on the dies originating from the Al–Si coating is in metallic state, thus implying adhesive wear characteristics in that particular case. Furthermore, increasing the furnace temperature to 920 ◦C is favourable for reducing adhesive wear when Al–Si coated blanks are used. Due to the formation of zinc oxide layers on the Zn–Ni coated blanks, a pure metallic build-up of coating material on the die is reduced. Thus ZnO formation is beneficial for reducing (i) the coefficient of friction and (ii) undesired adhesive metallic build-up of coating material on dies in hot forming operations.

In [73][74], the wear damage of 3 different tool steel grades are investigated in the hot sheet-metal-forming process, by means successive sliding of a pre-alloyed Usibor1500P® strip heated at high temperature. The three steels used in this experience were: an X50CrMoV5

alloyed nitride steel (called SG1), a 60CrMoTiV16 alloyed steel (SG2), and a Mo alloyed steel (SG3). Wear criteria, determined from 2D profiles, are used to quantify the adhesive and abrasive wear magnitude of the die-radii. During the drawing process, an experimental friction laboratory pilot, the steel strip, unrolled directly from a coil, was heated by Joule effect with a resistance heating system. When a prescribed temperature was reached, the heated zone of the strip was moved towards the tool, and slid on the die radius under normal loading (20-30 MPa). The strip was maintained in contact on the die radius by a special flat blank-holder during a few seconds, and then pulled through the working system by the rolling-up engine at a constant velocity of 250 mm/s. For the experiment, the pre-alloyed strip was heated up to 875 °C, and maintained at this temperature for 10 s before entering the working system. When the strip slides on the tool, its temperature, measured by a pyrometer, was about 730 °C. Two test campaigns were carried out; a first test campaign (test 1) was under taken up to 5000 cycles with cycling interruptions at each 1000 cycles. A second trial (test 2) was conducted up to 2000 cycles, with shorter interruption intervals at 200, 500 and 1000 cycles. At each test interruption, non-destructive investigations were carried out by using SEM observation and 2D profile measurement at different batch, in order to asses adhesive and abrasive wear by using three quantitative criteria. The results shown that the major damage observed on the die radii is a material transfer mechanism, resulting from the adhesion of the strip-coating particles during the hot-strip sliding. Abrasive wear appears as a minor phenomenon. The surface damage exhibits a rapid kinetic, only a few hundred cycles being necessary to obtain a significant transfer layer on the die radius. The three grades of steel investigated present different adhesive and abrasive behaviours but the transferred layer is more or less compacted depending on the steel grade, Fig. 2.28a. On the nitrided SG1 die radius, a compact and glazed transfer layer forms and stabilizes rapidly from 500 cycles onwards. SG2 generates a smaller and less continuous transfer layer, but seems more degraded by loss of material, which could be explained by the presence of hard and large titanium precipitates near its surface. SG3 is sensitive to material transfer, even in the die-radius exit, and produces less abrasive wear linked to the smaller size of the hard precipitates included in the matrix. Like SG2, the evolution of the transferred layer, formed by particles that are not totally agglomerated, is cyclic. This cyclical evolution has been by a cumulated cyclic plastic deformation of the sub-surface of the substrate. The smoothest steel grades (SG2 and SG3) exhibit a strong plastic deformation in the sub-surface, especially at the die radius exit, whereas for SG1, the plastic deformation is hindered by the nitriding layer on the tool surface. SEM cross-sections highlight that the thickness of the transfer layer is thinner and less uniform on SG2 (Fig. 2.28b).

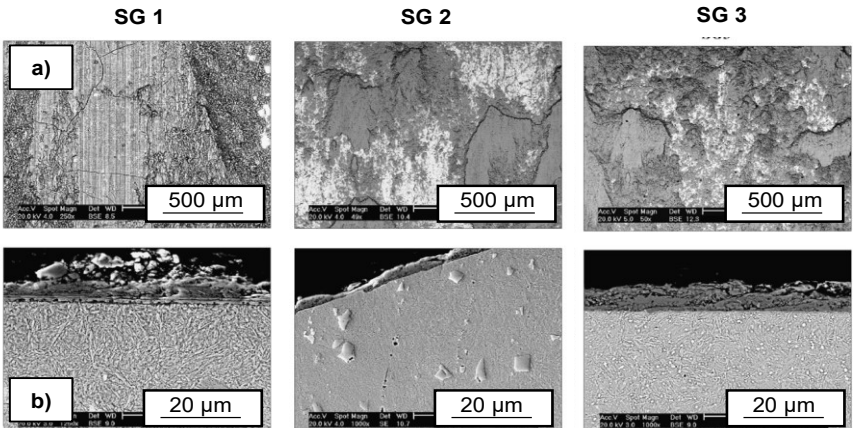


Fig. 2.28 SEM observations showing the transferred layer on SG1, SG2 and SG3: (a) back-scattered images of the die radius surface after 2000 cycles (the transferred layer is in grey, the steel in white) and (b) transverse cross-sections after 5000 cycles. Adapted from [73].

Also A. Ghiotti in [75] presented a fundamental study about the sheet coating characteristics in terms of morphology, surface roughness and tribological behaviour as a function of the process parameters typical of industrial hot stamping processes. The Authors focused their attention on two aspects: (i) investigation of the influence that the thermal parameters exert on the Al–Si coating during hot stamping and (ii) analysis of behaviour of friction at high-temperature. In order to fulfil the first aspect, Authors used an experimental set-up that is arranged on a MTS machine equipped in the tensile mode, where a tensile-type sheet sample is heated by a frontal inductor, and maintained at the target temperature for a certain amount of time (holding time) in order to get a complete microstructure homogenization. The sample is finally quenched to room temperature by means of compressed air nozzles. In order to assure the control of the heating and the cooling down steps, a K-type thermocouple is spot-welded on the specimen in the middle of the heated zone. With regards to second aspect, the evaluation of the tribological characteristics was carried out by performing pin-on-disk experiments, on a universal mechanical tester (UMT), specially equipped to work at elevated temperatures. In order to reproduce the tribo-system typical of hot stamping, the material used for the pin is the hardened hot working tool steel AISI H11, while the counter material is a disc made of the 22MnB5 with the Al–Si coating. The metal disc is heated up to 900 °C in order to have its complete austenitization inside the heating chamber at a constant heating rate; then, it is cooled down to the target temperature with a constant cooling rate. In Fig. 2.29 are reported experimental plans for thermal test and for high-temperature pin-on-disk test.

a)

| Heating temperature (°C) | Heating rate (°C/s) | Holding time (s) | Cooling rate (°C/s) |
|---|---|---|---|
| 600 ± 10 | 7.3 ± 0.1 | 180 ± 0.1 | 300 ± 5 |
| 900 ± 10 | 7.3 ± 0.1 | 180 ± 0.1 | 300 ± 5 |

b)

| Heating temperature (°C) | Heating rate (°C/s) | Holding time (s) | Cooling rate (°C/s) |
|---|---|---|---|
| 900 ± 10 | 7.3 ± 0.1 | 10 ± 0.1 | 300 ± 5 |
| 900 ± 10 | 7.3 ± 0.1 | 180 ± 0.1 | 300 ± 5 |

c)

| Heating temperature (°C) | Heating rate (°C/s) | Holding time (s) | Cooling rate (°C/s) |
|---|---|---|---|
| 900 ± 10 | 7.3 ± 0.1 | 180 ± 0.1 | 50 ± 5 |
| 900 ± 10 | 7.3 ± 0.1 | 180 ± 0.1 | 300 ± 5 |

d)

| Factors | Low level | High level |
|---|---|---|
| Normal pressure (MPa) | 5 | 25 |
| Temperature (°C) | 500 | 800 |
| Sliding velocity (mm/s) | 1 | 10 |
| Surface condition | Turned | Polished |

Fig. 2.29 a, b, c) Experimental plan to investigate the influence of the heating temperature and d) DOE experimental plan to investigate friction conditions. Adapted from [75].

From this experiments it was found that the heating temperature governs the diffusion phenomena of the iron to the coating surface giving origin to an Al–Fe–Si ternary alloy and that the surface topography and roughness vary with the heating temperature. The holding time must be adequate to allow the iron diffusion into the Al matrix and the formation of the Al–Fe–Si alloy system; a longer holding time allows more homogeneous surface characteristics in terms of chemical elements and topography. Instead the cooling rate does not affect the surface characteristics, in the range variations typical of the hot stamping. For the tribological test, the blank temperature and contact pressure are the process parameters that have the larger influence on the friction coefficients as it is possible observe from Fig. 2.30.

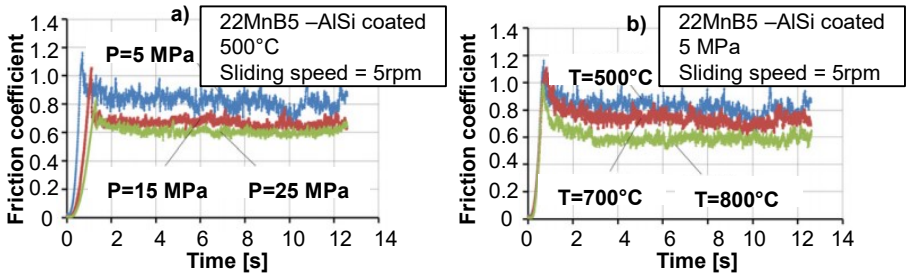


Fig. 2.30 a) Friction coefficient at the lower contact pressure (5 MPa) and b) influence of the contact pressure on the friction coefficient at the lower temperature (500 °C). Adapted from [75].

By increasing normal pressure friction coefficient passes from 0.74 with 5 MPa at 0.64 with 25 MPa, while by increasing metal sheet temperature it passes from 0.735 at 500 °C to 0.635 at 800 °C.

At a laboratory scale, J. Hardell et al. carried out an extensive research on tribological characterisation at high temperature of hot stamping of steels, by using reciprocating friction and wear ball-on-disc tests.

In [76], J. Hardell analyzed tribological behaviour of surface coatings (PVD coatings) applied on the tool steel, TiAlN and CrN, during sliding against ultra-high strength boron steel (UHSS) at elevated temperatures, in order to control friction and reduce wear/oxidation issue. The tribological studies were conducted by using both a reciprocating tribometer as well as a pin-on-disc machine at temperatures in the range from ambient to 800 °C. The frictional results from unidirectional sliding tests of the TiAlN coating have shown that friction increases with temperature, Fig. 2.31a. A similar behaviour is also seen for the CrN coating. The increase can be explained by increased oxidation of the coatings, increased softening and plastic deformation, as result of increased temperature. Under reciprocating sliding conditions, Fig. 2.31b, the TiAlN coating shows quicker stabilization and lower initial friction values compared to the CrN. The increase in friction from 40 °C to 800 °C is attributed to higher plastic deformation of the hot UHSS disc resulting in large contribution from ploughing.

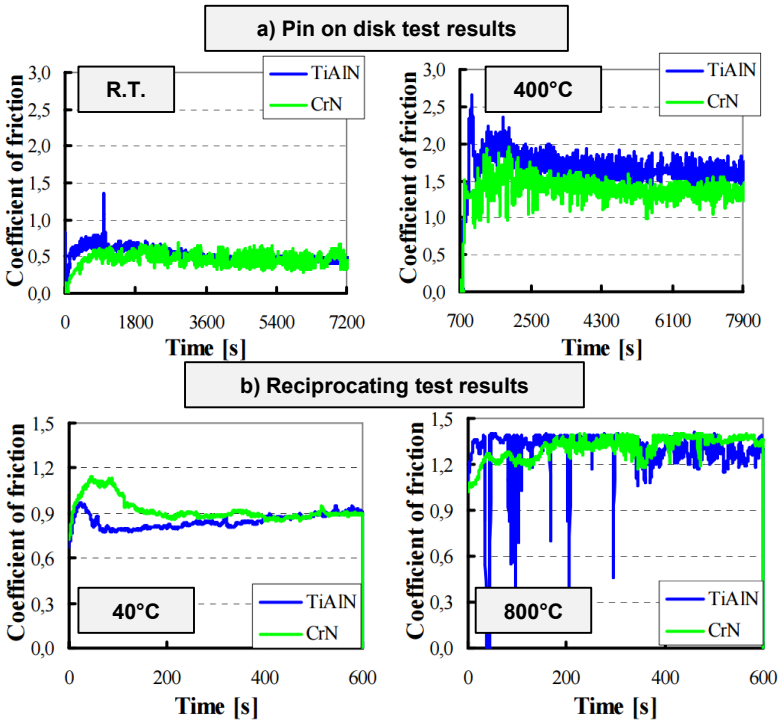


Fig. 2.31 a) Coefficient of friction as function of time from unidirectional tests at R. T. and 400 °C (Load: 25 N; Sliding speed: 0.2 m/s; Duration: 7200 s) while b) Coefficient of friction as function of time from reciprocating tests at 40 °C and 800 °C (Load: 50 N; Stroke: 1 mm; Frequency: 50 Hz; Duration: 600 s). Adapted from [76].

Both coatings experience no wear in unidirectional sliding at room temperature and a thin layer is built up inside the wear track. This layer is composed mainly of oxidised wear debris from the UHSS pin specimen. At 400 °C the TiAlN coating again shows no wear and only a mild polishing wear occurs. However, the CrN coating is removed to large extent by abrading action of hard oxidised wear debris from both surfaces. In reciprocating sliding at 40 °C, the coatings are mainly worn due a combination of high contact pressure and interaction with hard oxidised wear debris. However, the coatings are not removed completely. At 800 °C, none of the coatings can withstand the tough conditions, including thermal softening and large ploughing, and are completely removed.

M. Vilaseca in [77] focuses at investigating the effect of PVD coatings on the performance of hot stamping tools, in order to characterise and compare the tribological behaviour of a B-pillar production tool with two surface conditions: uncoated and with a PVD coating. Two sets of B-pillar tools were studied: the usual production set, made of hot work tool steel, and an additional tool set made of hot work tool steel coated with commercial cathodic arc PVD hard coatings. Punch was coated with an AlCrN coating and die was previously plasma nitrided and coated with a CrN coating. Usibors Al-Si blanks were heated and austenitised (900 °C, 7 min) in an atmospheric oven and formed and quenched in a direct hot stamping process. Punch was located in the lower position and die in the upper position in the press shop (300t) and the same press shop was used for both sets of tools. Coated tools were inspected in its initial status, 0 cycles, and after 1350 and 2200 cycles. Uncoated tools were inspected after 1970 cycles. The tribological analysis were performed in several zone of the B-pillar die that were selected as the most critical in terms of wear, Fig. 2.32.

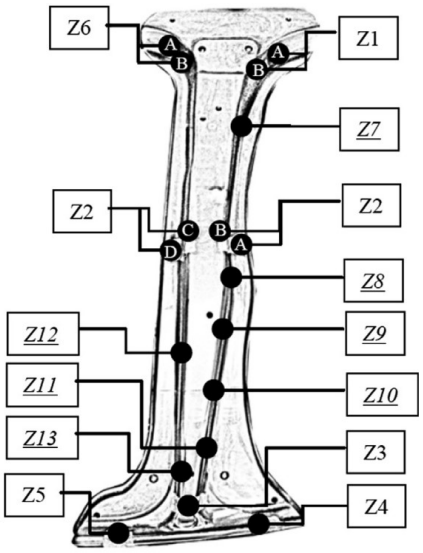


Fig. 2.32 Scheme of the B-pillar tool (punch) with the identification of inspected zones (Z). Underlined and italics: additional zones inspected in uncoated tool. A, B, C and D correspond to different replicas in the same zone. Adapted from [77].

During hot stamping of Al-Si coated 22MnB5, adhesive wear is the main acting mechanism on tools surface. It was identified in form of rougher layers and localised lumps, with thicknesses of tens of microns. AlCrN and CrN coated tools show less adhered material than uncoated tools, in terms of affected zones and thickness of compact lumps. No cracking or spallation was detected in none of the coatings. Also tool position (upper tool, lower tool) in the press shop has an impact on the quantity of stuck material: lump thickness is higher in uncoated punch (lower position) compared to uncoated die (upper position). The same trend was observed with coated tools; Al-Si dust coming from the sheet coating remains in lower tools because of gravity and contributes actively to material adhesion. Moreover, results showed that the replicating technique allows studying the roughness and wear related phenomena of large industrial tools without removing them from production. By means of the replicating technique, the tribological behaviour of both tool sets can be determined down to microscale level and objectively compared.

A. Ghiotti in [78] investigates on tribological behaviour of a hot working tool steel sliding against High Strength Steel blanks coated with the Al–Si coating under dry reciprocating sliding conditions, by means a universal UMT tribometer by Bruker equipped with a pin-on-disk configuration and with a heating furnace that was utilized to carry out the wear tests at elevated temperature. In order to cool down the pin during the test and simulate the thermal cycle to which the forming dies are subjected during the process, an air nozzle is used, which is placed outside the heating chamber and can be positioned, in conjunction with the air flow, to impart the desired cooling rate on the pin sample. The pin material is the hardened hot working tool steel AISI H11 and the metal sheet material is the boron steel 22MnB5 coated with the Al–Si coating. In Fig. 2.33 the experimental plan of this experience.

| | |
|---|---|
| Sheet heating rate | 0.43 °C/s |
| Sheet temperature | 800 ± 1 °C |
| Normal load (contact pressure) | 50 ± 2 N (7 ± 0.1 MPa) |
| Sliding speed | 15 mm/s |
| Sliding distance per cycle | 75 mm |
| Pin cooling time | 15 s |
| Pin cooling rate | 3.6 °C/s |
| Duration | 2000 cycles |

Fig. 2.33 Testing parameters. Adapted from [78].

The worn pin surface analysis by SEM/EDX and 3D profilometer showed that both adhesive and abrasive wear mechanisms take place; the adhesion can be attributed to the aluminium transfer from the sheet protective Al-Si coating, whereas the formation of oxide particles acting as wear debris can provoke the occurrence of abrasive wear.

In [79], Authors presented the approach and the results in evaluating a Zinc-based coating applied to boron steel sheets in hot stamping operations. Thermal and physical-simulation experiments were carried out to evaluate the chemical interactions between the coating and the metal sheet and the tribological performances during the process. The steel grade used in this investigation is the boron steel 22MnB5, covered with a Zn coating deposited by hot-dip galvanizing process while, the tool steel grade used is the AISI H11. To evaluate the influence of the process thermal parameters on the changes in the chemical composition of the Zn coating and surface topography, thermal experiments were designed and carried out on a Gleebles 3800 thermo-mechanical simulator equipped in the tensile mode. A tensile-type sheet sample was heated by Joule effect and maintained at the target temperature for a fixed amount of time (soaking time) to get the full microstructure homogenization. The tests were performed without applying any load to the specimen thus allowing its thermal dilatation. The sample was finally quenched by means of compressed air nozzles. The temperature was controlled through a type-K thermocouple spot-welded on the specimen gauge length. The frictional behaviour of the Zn coating during sliding against the tool steel was investigated by means of Hot Flat Strip Drawing Tests presented in [65] while the wear mechanisms at high temperatures were investigated by means of hot pin-on-disk tests carried out on a Bruker UMT-3 presented in [78]. In Fig. 2.34 the experimental plans for the three typology of test.

a)

| Heating temperature (°C) | Heating rate (°C/s) | Soaking time (s) | Cooling rate (°C/s) |
|---|---|---|---|
| 500, 600, 700, 800, 900 (±0.1) | 10 (±0.1) | 60; 120; 180; 240; 300 (±0.1) | 40 (±1) |

b)

| Strip temperature (°C) | Tool temperature (°C) | Sliding speed (mm/s) | Normal pressure (MPa) |
|---|---|---|---|
| 500, 600, 800 (±13) | 500, 600, 800 (±2) | 10, 30, 60 (±1) | 6.5, 15.0 (±0.1) |

c)

| | |
|---|---|
| Sheet heating rate (°C/s) | 0.43 |
| Sheet temperature (°C/s) | 800(±3) |
| Contact pressure (MPa) | 10(±0.1) |
| Sliding speed (mm/s) | 15(±0.1) |
| Sliding distance per cycle (mm) | 75 |
| Pin cooling time (s) | 15 |
| Pin cooling rate (°C/s) | 3.6 |
| Test duration (cycles) | 2000 |
| Repeatability | 5 |

Fig. 2.34 a) Plan of the thermal experiments, b) plan of the HFSDTs and c) plan of the hot wear tests. Adapted from [79].

The results regarding the thermal experiments shown that the heating temperature is the most influencing parameter: the higher the temperature, the higher the diffusion of iron in the coating, with values of Fe wt% ranging from 26% at 700 °C up to 75% at 900 °C, whereas the influence of the soaking time is negligible. In particular, starting from the temperature value of 800 °C the diffusion rate becomes more significant with a value of 62 wt% Fe. As the testing temperature rises up to 800 °C, larger areas with dense small peaks start appearing, with a roughness increase. Such evolution of the surface topography is related to the proximity of the Zn boiling temperature at 903 °C. For the testing temperatures above 900 °C, this results in a typical cratering topography of the surface, which sets the upper bound temperature to 900 °C for the investigated Zn coating and limits the blank austenitization temperature to this value (less than the industrially utilized 950 °C). In the analysis of the friction, the Authors observed that for both the investigated pressure levels, when applying a sliding speed equal to 10 mm/s the friction coefficient appears not influenced by the temperature, while for the other two values of the sliding speed the temperature increase determines the decrease of the friction coefficient. Concerning the influence of the sliding speed and normal pressure, although with different levels of interactions, the higher the values of the testing parameters, the lower the friction coefficient. The pin wear appears to be dominated by a combination of adhesion-and abrasion-based wear mechanisms. Since the beginning of test, the Zn coating appears to adhere to most of the pin surface but although adhesive phenomenon is detected, the predominant wear mechanism is the abrasion, which becomes more important over 600 cycles, due to the presence of oxides in the form of debris between the pin and the sheet metal surface.

L. Pelcastre in [80] analysed the material transfer from Al–Si coated work-piece to the tool material. The main aim of this work is therefore to clearly describe the galling mechanisms that are encountered during the interaction of Al–Si coated UHSS with tool steels, with and without surface modification. The surface modifications studied in this work were hard PVD coatings and plasma nitriding. Three variants of the pin specimens were used; uncoated tool steel specimens, PVD coated specimens and plasma nitrided specimens. The chemical composition of the tool steel is the same as that commonly used in the actual hot stamping process and it

is a quenched and tempered tool steel. The counter material specimen for the tribological tests was an Al–Si-coated UHSS. Tribological tests were carried out using an Optimol SRV high temperature reciprocating friction and wear tester, presented in [66]. The test conditions used for the tests carried out in this work are presented in Fig. 2.35.

| Test parameters | Value |
|---|---|
| Normal load | 31 N |
| Nominal contact pressure | 10 MPa |
| Temperature | 800 °C |
| Stroke length | 4 mm |
| Frequency | 12.5 Hz |
| Duration | 30 s |

Fig. 2.35 Test parameters. Adapted from [80].

During tribological tests with uncoated tool steels severe galling occurred on the ground tool steel surface whilst some sparse and thinly smeared layers of transferred material were observed on the milled tool steel surface. For the uncoated tool steel specimens, galling always occurred and only the severity varied. Compaction galling was more severe than adhesive galling. Authors used term "compaction galling" to identify when wear debris is easily accumulated within valleys in the surface or surface defects while "adhesion galling" is used to identify adhesion when the surface topography is such that it does not provide for sites where debris can be accumulated, essentially in regions where contact pressure is high, such as the tip of asperities. In the case of PVD hard-coated tool steel, all coatings showed severe material transfer. Not only the severity of the material transfer is more significant for the PVD coated tool steel specimens compared to uncoated tool steel, but the galling mechanisms also appear to be different. For all these coatings, adhesive galling seems to be the main mechanism for the occurrence of severe galling and not the compaction of debris as seen in case of uncoated tool steel. Galling on nitrided tool steel specimens was considerably reduced compared to the PVD coated tool steel and the uncoated tool steel. It seems that in general, for both of the plasma nitride specimens, material transfer was reduced due the absence of direct contact between the tool steel and the Al–Si coating; the contact was between an oxide layer (formed subsequent to the nitriding) and the Al–Si coating. Under these conditions, primarily wear of the oxide layer takes place thus reducing galling onto the tool surface.

In [81] Authors have focused their studies in order obtaining an in-depth understanding of the different phenomena involved in the failure of form fixture hardening tools. Two different tools having different hardness values and microstructures that had been used in production were analysed, namely, tool 1 (T1, AISI P20 modified) and tool 2 (T2, Premium AISI H13); in the case of T1, the tool was provided with a nitrided layer and in the hardened and tempered condition. Tool T2 was also nitrided but it was in an unhardened state. T1 presented a martensitic structure whereas T2 had a ferritic structure. T1 and T2 have been in production in the same hot stamping process of HSS coated, until they were considered unusable. The tool is considered unusable when the work-pieces no longer fulfil the quality demands. T1 was used for about 1.5 years in production with estimated cycling repetitions in the range of 80.000–100.000 cycles while T2 was used for 150.000–200.000 cycles. Section cut, polishing and etching were carried out in order to prepare samples. Based on the observations in this work, selecting a tool material that can withstand the stresses generated by friction

during forming will minimise the damage due to mechanical fatigue. The analysis results show the following conclusions; (i) the two tool steels differ in their microstructures as well as hardness depth profiles. The microstructure of T1 is mainly martensitic and has a thick nitrided layer. On the other hand, T2 has ferritic microstructure and its nitrided layer thickness is also considerably smaller. (ii) The damage to the form fixture hardening tools occurs due to several mechanisms. However, the dominant mechanisms observed are fatigue and corrosion. The contribution from adhesive and abrasive wear appears to be relatively small. (iii) The mainly ferritic microstructure of T2 appears to facilitate deformation of the grains and enhances its resistance against crack propagation. The martensitic tool steel T2 has shown the tendency of brittle cracking. (iv) Despite their different microstructural and hardness depth profile characteristics, both tool steel are able to work at elevated temperatures encountered in the form fixture hardening process for sufficiently large number of cycles.

A. Tomala in [82] studied the reliability of combined model and component tests under solid lubricating conditions of HSS coated with Al-Si layer. The investigated sheet specimen is a 1.5 mm thick Al–Si coated 22MnB5 alloy steel. The lubricants used for the present work were three commercially available solid lubricants (Lub A is based on bismuth, Lub B is based on MoS2 and Lub C is based on graphite and boron nitride) suitable for high temperature metal forming applications. In order to conduct tribological tests that closely simulate the conditions in the actual sheet metal forming process, a specially modified High Temperature Disc on Disc Tribometer (HT-RRT) and a High Temperature Forming Tribometer (HT-FT) were used, see Fig. 2.36.

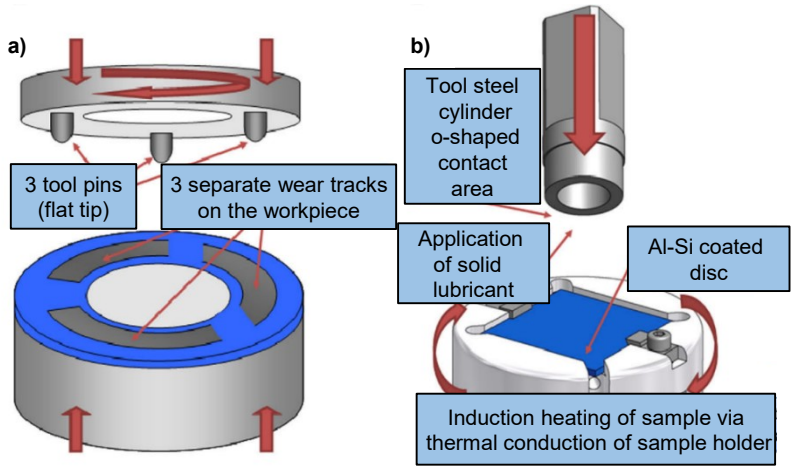


Fig. 2.36 Schematic drawing of high temperature test setups used for the experiments: (a) HT-RRT, (b) HT-FT and c) parameters used for the tests (HT-RRT and HT-FT). Adapted from [82] .

The HT-RRT test facility, Fig. 2.36a, is a disc-on-disc tribometer. In this case however, the upper disc was replaced by three equi-spaced pins while the workpiece specimens (disc) were cut out of the Al–Si pre-coated flat 22MnB5 metal sheets. The tool steel pins were tested without and with solid lubricant sprayed layer. Approximately 1h before the test, solid lubricant was sprayed and heated on the pins surface, so that a dry film was formed. Prior to the tests, the entire chamber with mounted samples was heated up to 500 °C. The test disc and pins were brought into contact, then the desired normal load was applied and finally the motor started to cause the sliding of the workpiece disc against the tool pin specimens. A second series of tests was performed on an HT-FT high temperature reciprocating friction and wear

test machine. In this equipment, an upper tool steel cylindrical specimen is pressed against a lower Al–Si coated 22MnB5 disc specimen as shown in Fig. 2.36b. The workpiece disc was heated via thermal conduction over the lower section of a sample holder. The lower disc specimen was kept separated from the upper tool steel cylinder during heating. The tool specimens and workpieces used in this testing approach were made out of the same materials as in the HT-RRT tests. Fig. 2.37 shows the experimental plan used.

| Technical specification | **HT-RRT** (High Temperature Disc on Disc Tribometer) | **HT-FT** (High Temperature Forming Tribometer) |
|---|---|---|
| Type of movement | pure sliding | pure sliding |
| Contact geometry | non-conformal: circle | flat on flat |
| Spatial configuration | vertical disc rotation axis | verical workpiece rotation axis |
| Tool diameter (mm) | Pins–4 | outer 22, inner 15 |
| Workpiece diameter (mm) | 90 | 35 |
| Sliding velocity (mm/s) | 30 | 30 |
| Temperature | 500 °C | Workpiece at 800 °C, Tool at room temperature |
| Normal load (N) | 1000 | 4068 |
| Contact pressure (MPa) | 6.6 | 20 |
| Duration (s) | 2 | 5 |
| Lubricants | A, B, C | A, B, C |

Fig. 2.37 Parameters used for the tests (HT-RRT and HT-FT). Adapted from [82]

This work has highlighted the fact that application of the solid lubricants allows to balance and control the coefficient of friction during the tribotests, what is most desired action in the metal forming processes. HT-FT results are in good correlation with the HT-RRT tests. Unlubricated tests had very unstable friction and wear characteristic, when compared with the lubricated ones. For the unlubricated test, the tool failed after 4 cycles, while lubricated ones tools operated for much longer lifetime. The coefficient of friction for solid lubricants A and B was very low and stable for all cycles, while for lubricant C it rose continuously. Furthermore, measured wear characteristics show the growing values for lubricant C and massive adhesion from the workpiece onto the tool. Model tests (HT-RRT) showed that the application of solid lubricants A and B not only reduced the coefficient of friction, but also completely protected the tool from adhesion of Al–Si coating from the workpiece. The deposited lubricant layer separated the tool and workpieces surfaces and acted as a sacrificial layer during tribotests.

L. Pelcastre in [83] investigated different heat treatment parameters and the influence they had on the microstructure of the Al-Si coating and the galling behaviour. In this work, two temperatures (700 °C and 900 °C) were chosen for the investigations with a given soaking time for alloying of the coating. From a fundamental point of view, the selected temperatures allow the formation and evolution of typical phases encountered in the forming process and others that are not often seen in the process but that are also typical in the Al-Si-Fe system. Tribological tests were carried out using an Optimol SRV high-temperature reciprocating friction and wear tester, presented in [66]. The upper pin (tool steel) specimen was kept separated from the lower disc (Al-Si coated UHSS) during heating. Once the desired temperature was reached, the lower specimen was retained at that temperature for a given time while still separated from the upper specimen. The holding times used for the tribological tests were 0, 4 and 20 min. When the holding time had elapsed, the pin was loaded against the disc and the test was started. On completion of the test, both specimens were left to cool in air and then removed and analysed. Repeat tests for all conditions were carried out with new

specimens, tool steel pin and work-piece disc, in order to assess repeatability of the galling mechanisms. The conditions used for the tests carried out in this work are presented in Fig. 2.38.

| Test parameters | Value |
|---|---|
| Normal load | 31 N |
| Nominal contact pressure | 10 MPa |
| Temperature | 700 and 900 °C |
| Stroke length | 4 mm |
| Frequency | 12.5 Hz |
| Duration | 30 s |

Fig. 2.38 Test parameters. Adapted from [83].

At 700 °C, an interlayer with the appearance of a continuous thin line is formed. This phase is Fe2Al2Si and it is characterised by a high hardness. Surrounding this interlayer, FeAl2 and/or Fe2Al5 are formed which also have a high hardness and the outer layer was unalloyed Al and Si. Longer soaking time at 700 °C allowed more diffusion of Fe and when 4 min had elapsed, the unalloyed Al and Si layer had already disappeared and the whole coating had transformed into inter-metallic phases. Similar microstructure was observed for longer soaking times; the main difference was that the Fe2Al7–8Si layer was thinner whilst the FeAl2/FeAl5 layer had grown. At 900 °C, the layer with unalloyed Al and Si was not observed for any soaking time and the Fe2Al2Si phase was already at the middle of the coating when 0 min soaking time was used and it was present for all of the soaking times. When 20 min soaking time had elapsed, this layer shifted further out-wards in the coating. The Fe2Al7–8Si phase was observed only when 0 min soaking time was used. For all of the other cases, this phase had dissolved and only layers containing Fe2Al2Si and FeAl2/Fe2Al5 were observed. Concerning the influence of the heating conditions on the tribological behaviour, the soaking time had a significant effect on the friction behaviour. For the specimens heated up to 700 °C, the coefficient of friction had in general an unstable behaviour, Fig. 2.39a.

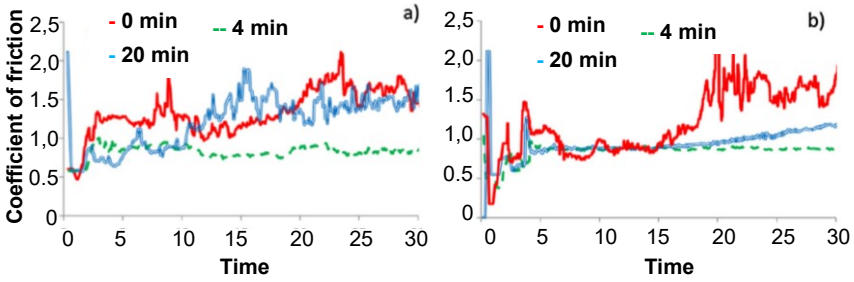


Fig. 2.39 Evolution of the coefficient of friction from tests at (a) 700 °C and (b) 900 °C. Adapted from [83].

Using 4 min soaking time resulted in a lower and more stable coefficient of friction compared to the other soaking times. It was observed that at 900 °C (Fig. 2.39b), the coefficient of friction was unstable and large fluctuations were seen with 0 min soaking time. Once the soaking time was increased from 0 min to 4 min, a stable coefficient of friction was observed. Comparing the coefficient of friction at 900 °C after 4 and 20 min soaking time, a similar behaviour was observed for the two soaking times. With regards to wear, the phases at the surface of the Al-

Si coating significantly affect the tribological response during the interaction with tool steel; galling is reduced when the Fe5Al2 and FeAl2 phases are present at the surface.

M. Merklein in [84], focused on analysing the adhesive wear behaviour of aluminium-silicon pre-coated boron-manganese steel under process relevant conditions by means a wear test rig (Fig. 2.40), which enables investigations on layer build-up on tools (1.2367 steel grade) with respect to contact pressure, blank temperature and austenitization parameters following the time-temperature profile within a hot stamping operation (Fig. 2.41). So, in this way, adhesive wear developing on the tool contact surface is examined in dependency of the used austenitization temperature and dwell time in the furnace by means of topographic measurements of the worn tool.

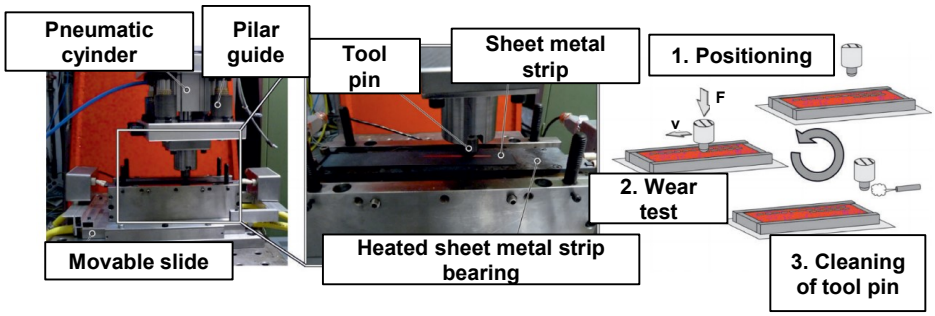


Fig. 2.40 Experimental setup for wear testing regarding hot stamping conditions [84].

| Austenitization temperature $T_\gamma$ (°C) | Austenitization time $t_\gamma$ (s) | Tool temperature $T_{tool}$ (°C) | Contact pressure $p_c$ (*MPa*) | Sliding velocity $v_s$ (mm/s) |
|---|---|---|---|---|
| 930 °C | 120; 180; 240; 300; 360; 420; 480; 540; 600 | 150 | 10 | 10 |
| 880 °C | 120; 180; 240; 300; 360; 420; 480; 540; 600 | 150 | 10 | 10 |

Fig. 2.41 Austenitization and testing parameters. Adapted from [84].

The results show that the development of adhesive wear of the aluminium-silicon coating on hot stamping tools increases by shortening the austenitization time. The longer the austenitization time, the less adhesive wear can be detected on hot stamping tools as a consequence of the development of intermetallic Al-Fe-Si phases in the coating. Moreover, heat treatment parameters impact frictional conditions within hot stamping processes; short austenitization times lead to an increased friction coefficient.

In [85] the Authors presented the comparison of the standard Al-Si coating and a new Zn coating when applied to 22MnB5 metal sheets in hot stamping by means a hot pin on disk test to investigate the tribological conditions during sheet metal working processes. The mechanical cycle is reproduced by pushing cyclically the pin against the rotating sheet metal disk at a temperature of 800 °C, sliding speed of 15 mm/s and a pressure of 7 MPa. Every time the normal pressure is removed, the pin is moved outside the heating chamber and cooled down to room temperature by a forced airflow provided by a nozzle. In addition, the influence that the process thermal parameters exert on the coatings in the ranges typical of the hot stamping processes was analysed by thermal experiments specifically designed and carried out on a Gleeble® 3800 thermo-mechanical simulator; in this type of test, a tensile-type sheet sample was heated by Joule effect and maintained at the target temperature (soaking time) in order to get the full microstructure homogenization and finally quenched by means of compressed air nozzles. Results shown that the heating temperature governs the diffusion

phenomena of both the coatings. In the case of Al-Si coating an Al–Fe–Si ternary alloy was formed, while the Zn coating showed the diffusion of the Zn into the iron; for Al-Si coating, longer holding times allow more homogeneous surface characteristics in terms of chemical elements and topography while no influence of the soaking time was found in case of the Zn coating. Concerning the wear test, it was found that both the coatings show a wear damage ruled by a combination of adhesion- and abrasion-based wear mechanisms. The coatings tend to adhere to the pin surface and scratches are also present due to oxides.

In [86] the frictional behaviour of ZnO coated aluminized 22MnB5 steels under dry condition is investigated and discussed. In order to measure the coefficient of friction at elevated temperature under dry condition, the hot flat drawing machine presented in [62] is used. Aluminized steel and same steels with 0.5 g/m$^2$ ZnO and 1.5 g/m$^2$ ZnO are used as test materials. The thickness of the coating layer of aluminized steel without ZnO is about 30 μm, and that with ZnO is about 20 μm as-delivered conditions. TiN and TiAlN thin hard layers are deposited on the tool surfaces by PVD process and DLC-Si thin hard layer is deposited by CVD process. The drawing tests are carried out over a distance of 70 mm at a constant compression load of 3.5 kN (about 5 MPa) and a constant drawing speed of 10 mm/s under dry condition. The heating duration of the specimen is for 3 min in an infrared image furnace to control the iron content in Al–Fe layer in adequate range. The temperature of the specimen surface reaches in the range between 950 °C and 980 °C. It is estimated that the 22MnB5 steel was austenized and Al–Fe layer formed on the surface of the steels in a furnace. The drawing experiments are carried out at temperatures of around 750 °C.

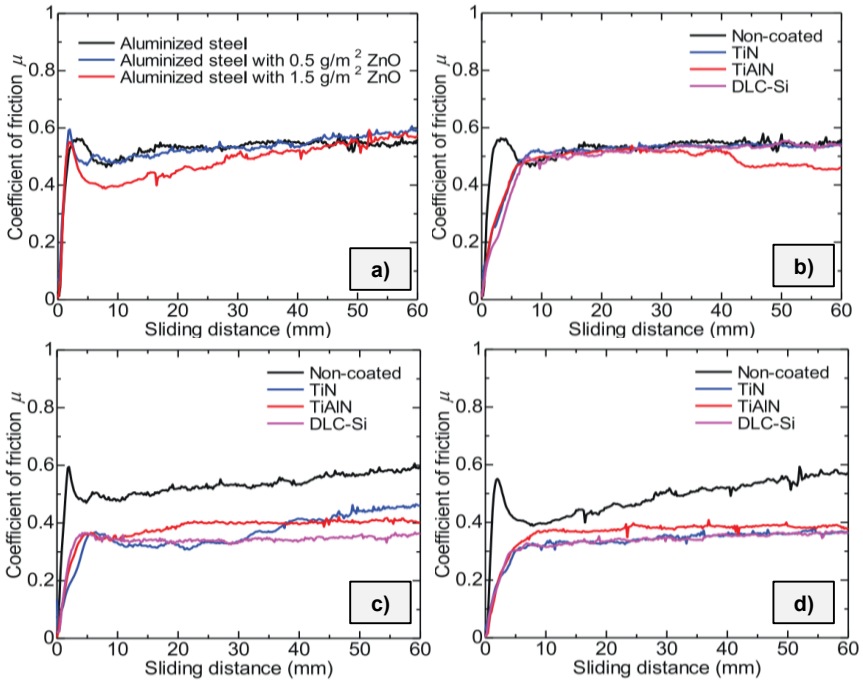


Fig. 2.42 Coefficient of friction vs sliding distance of a)the aluminized steel and same steels with 0.5 g/m2 ZnO and 1.5 g/m2 ZnO under dry condition for the non-coated tool, b) aluminized steel under dry condition for TiN, TiAlN and DLC-Si coated tools, c) aluminized steel with 0.5 g/m2 ZnO under dry condition for TiN, TiAlN and DLC-Si coated tools and d) aluminized steel with 1.5 g/m2 ZnO under dry condition for TiN, TiAlN and DLC-Si coated tools. Adapted from [86].

Results show (Fig. 2.42a) that the coefficient of friction of aluminized steel with 1.5 g/m$^2$ ZnO is lower than those of aluminized steel and aluminized steel with 0.5 g/m$^2$ ZnO. Over a drawing distance of 50 mm the values of three steels are beyond 0.5. When the non-coated tool is used in hot drawing test under dry condition, it can be found that the ZnO coated with 1.5 g/m$^2$ is necessary for decrease in the coefficient of friction. From Fig. 2.42b, Fig. 2.40c and Fig. 2.40d, it is possible to observe that the coefficients of friction for the coated tool do not appear the peak at the starting region. It is estimated that the severe aluminium adhesions do not occur for the coated tools at starting region. Anyway, when the non-coated tool was used, the amounts of the adhered Al–Fe IMC of the 1.5 g/m$^2$ ZnO coated aluminized steels were lower than that of the 0.5 g/m$^2$ ZnO aluminized steel, and the coefficient of friction were lower at short sliding distance. While, for the TiN, TiAlN and DLC-Si coated tools, the coefficient of friction became lower and the adhered Al–Fe IMC became significantly thinner. From these research work, it can be understood that the combination of the ZnO coated aluminized steel and the thin hard coating on the tool surface is effective in hot drawing test under dry condition.

J. Hardell in [87] investigated on the formation of oxide layers and near surface transformed layers during tool steel and boron steel interaction at elevated temperatures and their relation to the friction and wear response; in order to develop this study, three different high temperature tribological contact configurations were employed: unidirectional sliding (levels of pressure 2, 4, 6 MPa, levels of temperature RT, 200, 400 °C and sliding speed 0.2 m/s, with a duration of 900 s) reciprocating sliding (pressure 10 MPa, levels of temperature 40, 200, 400, 600 and 800 °C, stroke 4 mm and frequency 25 Hz, with a duration of 900 s)and three-body abrasive contact (normal load 45 N, sliding distance 600 m and sliding speed 1m/s). The materials used in all three test configuration are: i) 22MnB5 as High Strength Steel and ii) 30CrMo6 as hot work tool steel. For the unidirectional sliding test, results show that friction decreases as the temperature increases and for a given temperature, friction reduces when the load increases. A reduction of about 50% in friction coefficient was observed when the temperature was increased from room temperature to 400 °C. The composition of the oxide layer formed on the boron steel pin was also found to have a strong influence on the frictional response, Fig. 2.43. As regards the wear of the boron steel pin specimen, it was found to decrease by three orders of magnitude as temperature increased from room temperature to 400 °C.

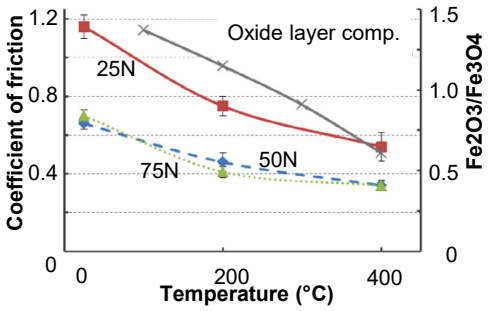


Fig. 2.43 Coefficient of friction as well as the average ratio of Fe2O3/Fe3O4 on the boron steel pin at 50 N and 75 N as function of temperature for boron steel during sliding against tool steel at different loads (v=0.2 m/s; t=900 s). Adapted from [87]

In reciprocating sliding, the friction of the boron steel and tool steel tribopair was also found to decrease but not as significant as in unidirectional sliding, perhaps due to the more severe reciprocating contact with start–stop and varying speed over each stroke. The increase in friction observed at 800 °C was attributed to significant softening of the materials due to phase transformations above the austenitisation temperature. As shown in Fig. 2.44a the wear rate was found to decrease from room temperature up to 400 °C and thereafter increase for both tool steel and boron steel. Lastly, in three body abrasive wear conditions, the tempered martensitic tool steel did not show a large variation in wear rate in the temperature range from room temperature to 300 °C. Above 400 °C an increase in wear was observed due to thermal softening of the tool steel at those temperatures, Fig. 2.44b.

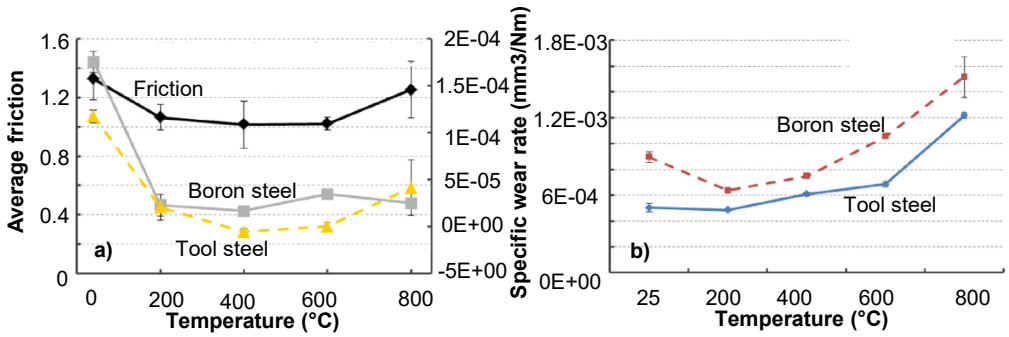


Fig. 2.44 a) Average coefficient of friction and specific wear rate as a function of temperature for boron steel during sliding against tool steel (F=31 N; v=0.2 m/s; t=900s) and b) specific wear rates as a function of temperature for boron steel and tool steel under three body abrasive wear conditions (v=1 m/s; s=600 m). Adapted from [87].

In the research work reported in [88], Authors investigated the friction behaviours of the tool steel H13 in contact with the boron steel 22MnB5 as a function of temperatures, sliding velocities, contact pressures and lubrication conditions by means a ring-on-disc sliding test (SRV reciprocating friction and wear testing machine). The upper specimen is pushed on the lower specimen, a contact pressure was applied and controlled by a servo motor. The lower specimen is fixed on the heater which can heat the specimen up to 900 °C and the temperature is measured precisely by a thermocouple. The friction coefficient is calculated in according with the Coulomb law. For the tool steel (upper specimen), AISI H13 was selected and high strength boron steel 22MnB5 was used to make the lower specimen. A $MoS_2$ spray was chosen as the investigated lubricant, deposited with the spray technique. The main results, from this research work, are: (i) the friction coefficient decreases increasing the temperature (from 0.67 at 650 °C up to 0.52 at 850 °C), resulting from more serious blank oxidation, (ii) the main wear mechanism is a combination of adhesive and abrasive wear and the tool damage at the higher temperature is more serious and (iii) the effect of sliding velocity on the friction coefficient is negligible. (iv) The results regarding the lubricant conditions show that $MoS_2$ lubricant can separate the tool from the blank, which can decrease the friction coefficient, improve the product quality and protect the die from severe wear.

## 2.3. Conclusions

Nowadays, hot stamping is the most important technology for the production of structural parts of the car body-in-white, with the perspective that even more parts of the vehicles will be manufactured using such process. Despite the advantages that the technology offers, in terms of reduced forming loads, enhanced formability and increased mechanical properties of the final part, engineers and process designers have to face quite a few critic drawbacks represented by the intensive energy consumption due to the material heating and the cooling [89], as well as the severe thermal and mechanical conditions at interface between the high temperature metal sheet and the cooled dies, which determine critical issues concerning the service-life of the equipment and tools. On the other hand, being the graphite lubrication conventionally applied to hot forging processes not applicable to sheet components due to paintability and weldability issues, the lack of alternative lubrication systems appeared immediately dramatic in relation to the wear phenomena that may arise at the interfaces between the blank and the dies at elevated temperatures. Consequently, the high shear stress that interests the interfaces in the forming process is accompanied by inefficient heat dissipation in the in-dies quenching due to the absence of the lubricant cooling action, with consequences on the Heat Transfer Coefficient (HTC), surface hardness, wear rate, etc.

The survey of the technical and scientific literature shows a large interest in the development of coatings for the blanks different from the traditional Al-Si up to new Zn-based coating, with improved frictional and wear performances. Other Authors are focused on the analysis of hard PVD and CVD coatings, plasma nitriding, applied on dies, in order to increase the tool life, reducing the wear rate that is established. Among the major fields of research analysed in the literature, another aspect investigated is the heat transfer between the HSS sheets and the common steel grades for dies, during the quenching phase in closed die in order to improve the microstructure of the final piece, further increasing the mechanical properties.

Fewer investigations have been focused on the development and test of new tools steels grades capable to improve the wear resistance and the thermal properties that are required for the in-die quenching during forming. Unfortunately, common materials actually used to manufacture dies and tools are not designed for such purposes yet, and start to be a critical limit to speed up the processes [36]. In hot stamping process, simultaneous forming and high rate quenching is the key to obtaining high strength steel components, but conventional hot work tool steels used in the process have lower thermal conductivity properties of 28 W/m K; the need to decrease the cycle time of the process, and to ensure the obtaining of a fully martensitic structure of the component requires the development of new steels for die and analysis of their tribological performance under real process conditions. Furthermore, the research works reported using approaches that individually analyse the influence of the test parameters on friction, wear and thermal aspects, when instead, the latter are mutually coupled.

# Chapter 3

# **Approach**

The reference industrial process is the direct hot stamping of High Strength Steels to produce automotive components. The objective of the proposed project has both high scientific and industrial relevance. The scientific relevance comes from the lack of knowledge envisaged in the current state-of-the-art; at the same time, the automotive sector is an added value industrial field.

On the basis of the lack of knowledge in the scientific literature, the objectives of this research work consist in developing an approach able to offer accurate evaluations of the tribology in hot stamping field in terms of friction, wear mechanisms and thermal parameters at interface die-metal sheet.

More in detail, the innovative contribution of the work is given by accurate characterization of the tribological behaviour of new steel grades specifically developed for dies in hot stamping applications, with high surface hardness and elevated heat transfer coefficient values to ensure the maximum heat exchange rate in the quenching phase. Therefore, the risk of bainitic or pearlitic transformation is reduced and the hot formed body part can be removed much faster from the tool which increases the number of hot stamped parts per hour. The same procedures, in terms of instrumentation, test parameters, and methodologies are also used to assess a traditional type of steel used to manufacture dies for hot stamping process, in order to provide a proper comparison with the new grades.

To this purpose, a novel testing approach to investigate the friction conditions, the wear and the thermal behaviour has been used, capable of reproducing in a laboratory environment the conditions arising at the interface between the dies and the blank, namely the sliding velocities at the active dies interfaces and the cyclic thermal and mechanical stresses on the dies.

The methodology is based on physical simulation experiments, and integrates the use of scanning electron microscopy and 3D profilometer to evaluate the surface conditions of the steel grades tested.

Physical simulation experiments are carried out by means of a pin on disk testing set up, designed in order to replicate the hot stamping conditions for both, sheet and die. In the case of the blank, a rotation table inside a furnace, where the HSS coated sheet is fixed, is specifically designed to allow controlled testing temperatures up to 1000 °C; while, the mechanical cycle is reproduced by pushing cyclically the pin against the rotating sheet metal disk according to the testing parameters in terms of sliding stroke, sliding speed, temperature and normal pressure. Every time the normal pressure is removed, the pin is moved outside the heating chamber and cooled down to room temperature by a forced airflow provided by a nozzle, with the purpose to reproduce the industrial hot stamping conditions where the dies are kept approximately at room temperature thanks to specifically designed water channels; in this way, once the pin is out of the oven, the mechanical loads are completely removed while surface thermal stresses are induced since it is cooled down by a forced air flow just outside the hot chamber. The final temperature of the pin and the cooling rate can be adjusted through a manometer in a range of pressure from 0.0 to 8.0($\pm$0.1) bar.

This simulative approach to reproduce the conditions at the interface between the die and metal sheet was developed with the aim of investigating (i) the influence that the process thermal parameters exert on the dies material in the ranges typical of the hot stamping

processes, (ii) the wear damage at the interface die-sheet and (iii) the friction coefficient in respect of the thermal and mechanical loads that are applied.

Fig. 3.1 shows the flow chart of the main phases of the Ph.D. research activities.

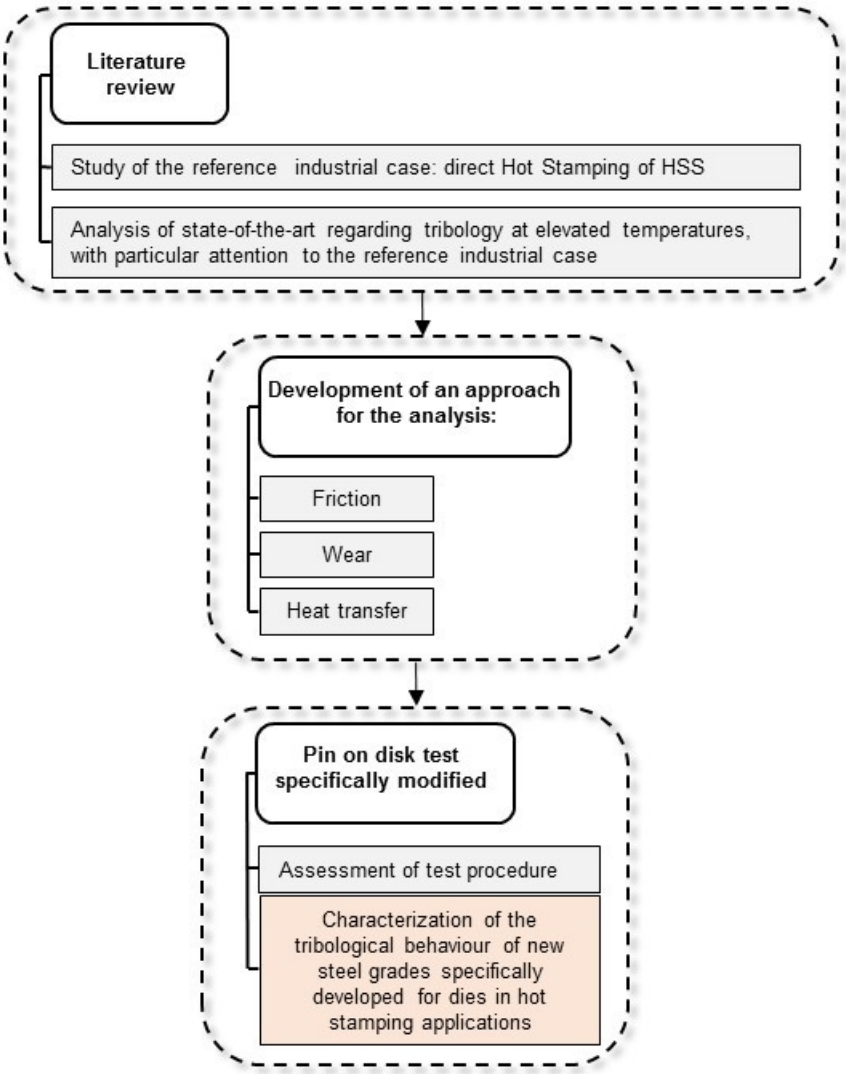


Fig. 3.1 Flux diagram which describes the main phases of the Ph.D. research activities.

# Chapter 4

# **Experimental procedure**

This Chapter is dedicated to the description of the instrumental equipment used, materials involved in the study and the procedures adopted and developed in order to analyse friction, wear and heat transfer in hot stamping process. Firstly, the reference industrial case is discussed, analysing the main process parameters and timing, to get information on thermal and mechanical cycling and on the duration of the forming phase. Subsequently, the test procedures, including the description of the instrumentation and materials used, are described.

## 4.1. The reference industrial case: hot stamping of HSS

The reference industrial process is the direct hot stamping of High Strength Steels sheet coated with Al-Si layer to produce structural parts of the car body-in-white. The thermo-mechanical sequence of the operations that can be realized in hot stamping allows obtaining high mechanical properties for a wide range of parts geometries, with reduced level of stamping loads[90] [91] and improvement of the springback and formability [67]–[96]. During the process, the blank material, which presents a ferritic-pearlitic microstructure in the as-received conditions [97], is heated in a furnace above the austenitization temperature [98][99](approximately above 900-950 °C). After a soaking time of 180-360 s, long enough to assure the fully austenitization, the blank is rapidly transferred to the forming press by a robot in a 5-10 s time, where it is simultaneously formed and quenched, which takes approximately 20 s. Finally, the dies are opened and the formed component is extracted in approximately 15 s. Data about the duration of the different process phases were recorded during industrial trials carried out on a hot stamping plant. On this base, on an average, every 35 s, the forming dies are subjected to a new forming cycle during the hot stamping process, see Fig. 4.1.

Thanks to the high temperatures, the average forming loads are significantly reduced [100], and the normal pressure at the interface between the blank and the dies results in the range between 5 and 15 MPa under the blank holder and with peaks of about 200 MPa in the most critical forming sections [101]. According to the industrial experience, the average normal pressure is in the range of few tens of MPa for large portions of the forming dies. At the end of the cycle, the formed component presents a fully martensitic microstructure, with strength levels above 1500 MPa and still acceptable ductility.

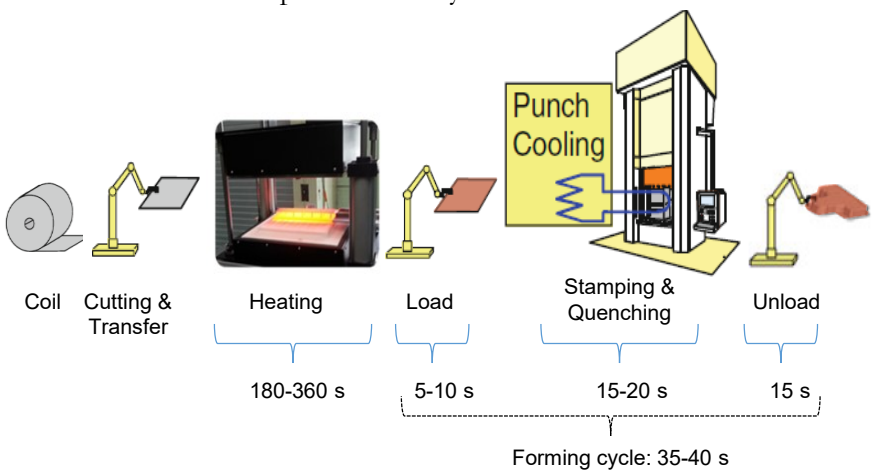


Fig. 4.1 Scheme of hot stamping line for B-pillar with relative timing.

## 4.2. Friction and wear test in hot stamping conditions for HSS

### a. Materials

***Sheet metal and coating***

The sheet steel grade under investigation is the boron steel 22MnB5, typically used in hot stamping and provided in 1.5 mm thick sheets. In the as-received condition, the steel grade has a ferritic-pearlitic microstructure and presents low strength and elevated ductility. The chemical composition and the mechanical properties of the as-delivered material are reported in Table 4.1.

Table 4.1 Chemical composition and mechanical properties of the metal sheet provided with a thickness of 1.5 mm (wt%).

| **Chemical compositions in wt%** | | | | | |
|---|---|---|---|---|---|
| C | Mn | Si | Cr | Ti | B |
| 0.21-0.25 | 1.1-1.4 | 0.15-0.35 | 0.15-0.30 | 0.02-0.05 | 0.03-0.005 |
| **Mechanical properties** | | | | | |
| Yield strength [MPa] | Ultimate tensile strength [MPa] | | Elong. at fracture ($L_0$ =80 mm, th≤3 mm) [%] | | |
| 500 (±75) | 600 (±50) | | >7 | | |

The sheets were provided with Al-Si coating, the most commonly used in direct hot stamping, developed and applied by ArcelorMittal.

*Al-Si coating*

Al-Si coating is the traditional coating used for the commercial USIBOR1500™ that was originally developed to prevent the oxidation at elevated temperatures and deposited by hot-dip galvanizing process [102]. The Scanning Electron Microscope (SEM) analyses and the surface topography measured through a 3D surface profilometer Sensofar Plu Neox show that the coating is characterized by large plateau areas corresponding to the Al matrix, with small cavities representing the Si precipitates, and an average surface roughness Sa equal to 1.292 (±0.006) μm, see Fig. 1.1a, d. According to the Energy Dispersive X-ray spectroscopy (SEM-EDX) analyses, it contains approximately the 13% of silicon. The cross-section shows an average coating thickness of 25 (±10) μm and three different zones can be identified: the coating, where aggregates of silicon are embedded in the aluminium matrix (Zone I), the interface area between the coating and the steel substrate (Zone II), and the steel substrate (Zone III). The interface zone is a ternary system containing iron, aluminium and silicon in

weight percentages of 58.26%, 12.23% and 29.51%, respectively, according to EDX analyses, see Fig. 4.2b. The average Al and Si wt% in the coating are reported in Fig. 4.2c, and they range from are 93.78% and 6.11% in the outer layers and to the 1.37% and 0.26% in the inner layers, according to the EDX.

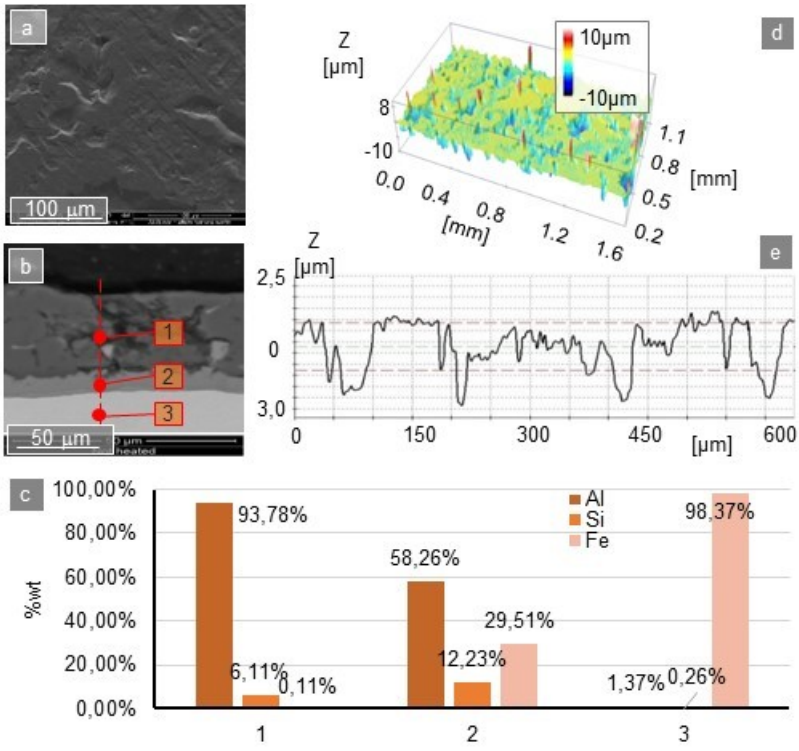


Fig. 4.2 Al-Si coating in the as-delivered condition: (a) SEM surface, (b) coating cross-section, (c) chemical EDX analysis in the cross-section, (d) topography of the surface and (e) metal sheet profile measured along the rolling direction.

## ***Tool steel***

The first tool steel grade used in the research activity is the EN X38CrMoV5-1 alloyed steel, commercially available with the name of Böhler W300. Table 4.2 reports different types of designation of this steel grade.

Table 4.2 Different types of designation of EN X38CrMoV5-1 steel grade.

| **Standards** | | | |
|---|---|---|---|
| **EN/DIN** | **AISI** | **JIS** | **UNI** |
| (1.2343) EN X38CrMoV5-1 | H11 | SDK6 | EN X37CrMoV5-1 |

To improve its wear resistance at the hot stamping temperatures, the tool steel is heat treated to the hardening temperature of 1040 °C, oil quenched, and subsequently tempered at a temperature of 350 °C for about 30 min to obtain a surface hardness of 51 (±1) HRC. Table 4.3 reports the chemical compositions in wt% provided by the supplier, mechanical properties of the tool steel measured by means of laboratory tests and the thermal conductivity. The pins used in the pin-on-disk experiments are machined to obtain a final surface roughness Sa of

2.412 (±0.041) μm. Fig. 4.3 shows the pin surface topography in the as-delivered conditions observed with the SEM and 3D profiler. The values of the roughness in the sliding direction and perpendicular to the sliding direction are, respectively, Ra// =2.922(±0.036) μm, Ra⊥=2.491(±0.033) μm.

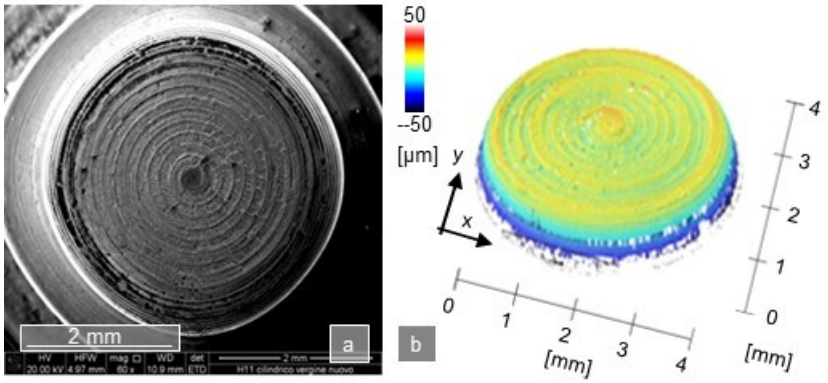


Fig. 4.3 Surface topography of the pins after machining observed with the (a) SEM and (b) 3D profiler.

Table 4.3 Chemical composition and material properties of the tool grade.

| **Chemical compositions in wt%** | | | | | | | | |
|---|---|---|---|---|---|---|---|---|
| C | Si | Mn | P | S | Cr | Mo | Ni | V |
| 0.39 | 0.97 | 0,43 | 0.015 | 0.006 | 5.01 | 1.14 | 0.21 | 0.35 |
| **Material properties** | | | | | | | | |
| Hardness after annealing [HRB] | | | Hardness at room temperature [HRC] | | | Thermal conductivity at 700°C [W/mK] | | |
| max 205 | | | 51(±1) | | | 29.2(±0.1) | | |

The other two steel grades tested are patented formulation produced by Rovalma™. This typology of tool steel is commercially available with the name of High Thermal Conductivity Steels (HTCS®), provided in two grades named HTCS1 and HTCS3 [103]. Such steels, specifically designed for hot stamping processes, present a thermal conductivity up to 60 W/mK, which is more than twice of the thermal conductivity of conventional hot stamping steels, such as the EN X38CrMoV5-1 alloyed steel. After the machining operations to obtain the pins for the tribological tests, both the steel grades were heat treated in order to increase their wear resistance and obtain a final surface hardness of 56(±1.5) HRC. Table 4.4 reports the values of the pin surface roughness, where Ra⊥ and Ra// are the linear roughness values perpendicular and parallel to the sliding direction, respectively.

Table 4.4 Surface roughness of the as-delivered pins.

| **Grade** | **$S_a$ [μm]** | **$R_{a\perp}$ [μm]** | **$R_{a//}$ [μm]** |
|---|---|---|---|
| HTCS1 | 0.264± 0.008 | 0.358± 0.025 | 0.256± 0.032 |
| HTCS3 | 0.896± 0.045 | 1.079± 0.098 | 1.035± 0.103 |

Also in this case, the machining parameters used to realize the testing samples were chosen according to the industrial practice for the manufacturing of stamping dies. Fig. 4.4 shows the pin surfaces for both the HTCS1 and HTCS3 steel grades observed through the SEM Electron Back Scattered (EBS) and the 3D profiler. The difference in the topography between the two materials (see Fig. 4.4) is due to their machinability and, for both the materials, it was verified that the values are in agreement with the industrial practice.

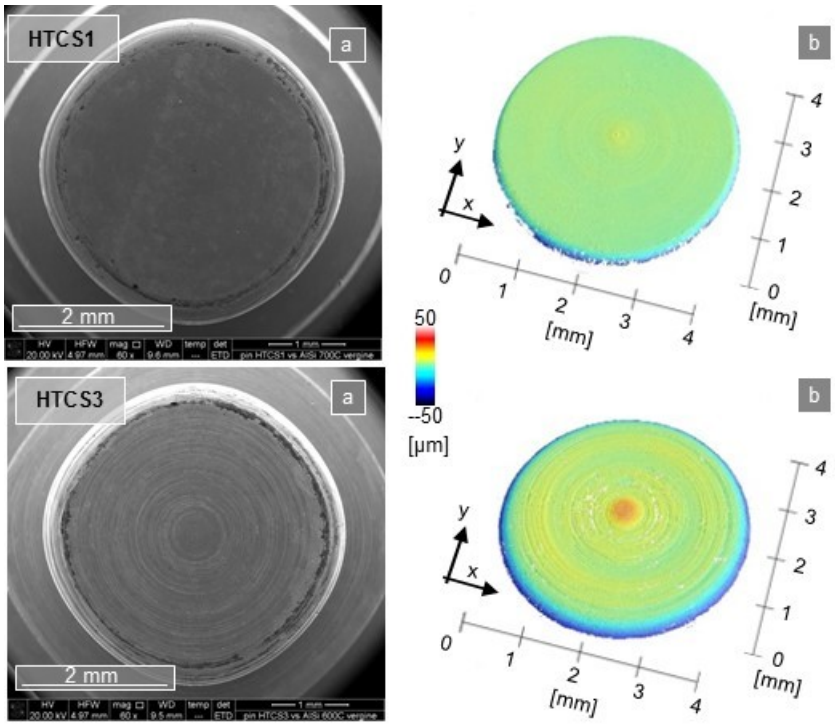


Fig. 4.4 (a) Surface topography of the pins after machining observed with the SEM and 3D profiler (b).

Fig. 4.5a and Fig. 4.5b show a map of the elements of the two materials and their chemical concentration measured through the Energy Dispersive X-ray (EDX) detector of the SEM. Although the two steel grades have similar composition in terms of chemical elements, the solubility of the elements themselves appears totally different. In the case of the HTCS3 grade, small agglomerates of molybdenum can be observed, which could help to increase the corrosion resistance as well as the strength at elevated temperatures, while the HTCS1 grade presents finer elements with a uniform distribution in the matrix.

The HTCSs were manufactured using powder press technique that uses nanomaterial technology composed of processes such as mixing, binding, compressing and sintering. This methodology can realize near net shape steel alloys with high quality grade, composition and different properties at various zones. This method is used to realize the HTCSs due to the presence of tungsten; in conventional casting method, tungsten is not possible to be melted and can cause defects such as high segregation and porosity [104].

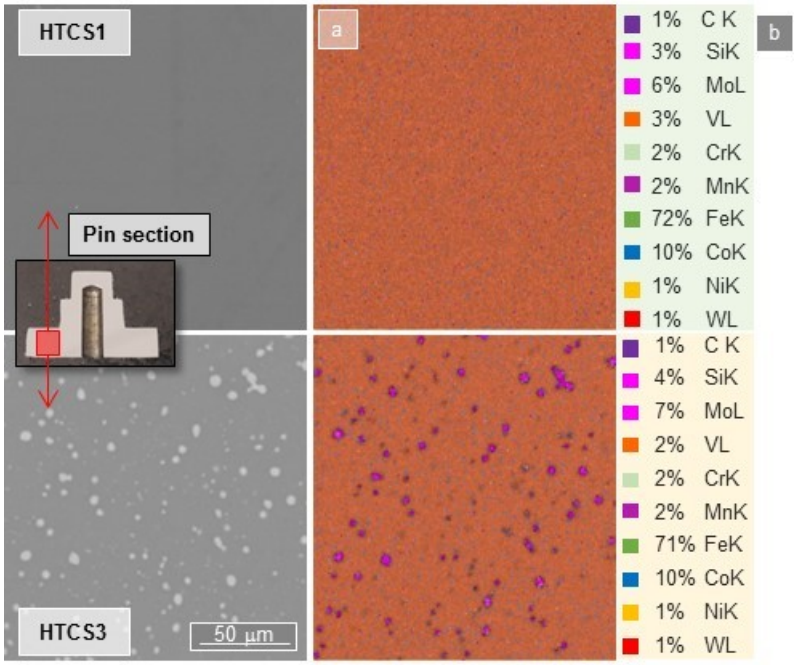


Fig. 4.5 (a) Maps of the elements of the steel grades measured with the SEM-BSE and (b) percentages of the elements measured with the SEM-EDX.

## b. Hot Friction Tests (HFTs)

The frictional behaviour of the tool steels during sliding against the 22MnB5 coated is investigated by means of pin-on-disk tests carried out at elevated temperatures on the Bruker® UMT-3 tribometer equipped with a furnace, as shown in Fig. 4.6a. The pins (see Fig. 4.6b), manufactured with the tool steels described in Section 4.2.a, are mounted on a controlled head, movable into both the vertical and the lateral direction thanks to electric motors, while the disk, cut from the blank material with a diameter of 45.0(±0.1) mm, is fixed to a rotary drive. A load-control mode is adopted to apply a constant pressure at the interface between the pin and the disk during the test. To perform the pin-on-disk experiments at elevated temperatures, the tribometer is equipped with a furnace (see Fig. 4.6c), specifically designed to allow controlled testing temperatures up to 1000 (±0.1%) °C. The furnace temperature is monitored by a thermocouple located inside the chamber that provides the control feedback to the temperature controller.

During the experimental tests, the 22MnB5 disks positioned in the furnace are heated above the austenitization temperature to obtain the full material austenitization by adopting a heating rate of 0.43 °C/s and a soaking time of 180.0 (±0.1) s to assure the fully austenitization, in agreement with the industrial practice; subsequently the sheets sample are cooled down to the target test temperature with a constant cooling rate equal to 0.33 °C/s, (see the thermal cycle reported in Fig. 4.6d). Even if the applied cooling rate is lower than the industrial one, it was shown in [75] that the adopted heating and cooling rates do not influence the coating structure. To reproduce the industrial hot stamping conditions where the dies are kept approximately at room temperature thanks to specifically designed water channels, the pin is

kept outside the furnace during the sheet heating; once the sheet disk has reached the target temperature, the pin is moved inside the chamber and brought into contact with the specimen.

Table 4.5 shows the experimental plan of the hot friction tests, where the ranges of the investigated parameters, namely sliding speed, metal disk temperature and normal pressure, are reported. The experiments were carried out under dry sliding conditions, without additional lubricants, and using air as testing atmosphere in accordance with the industrial process.

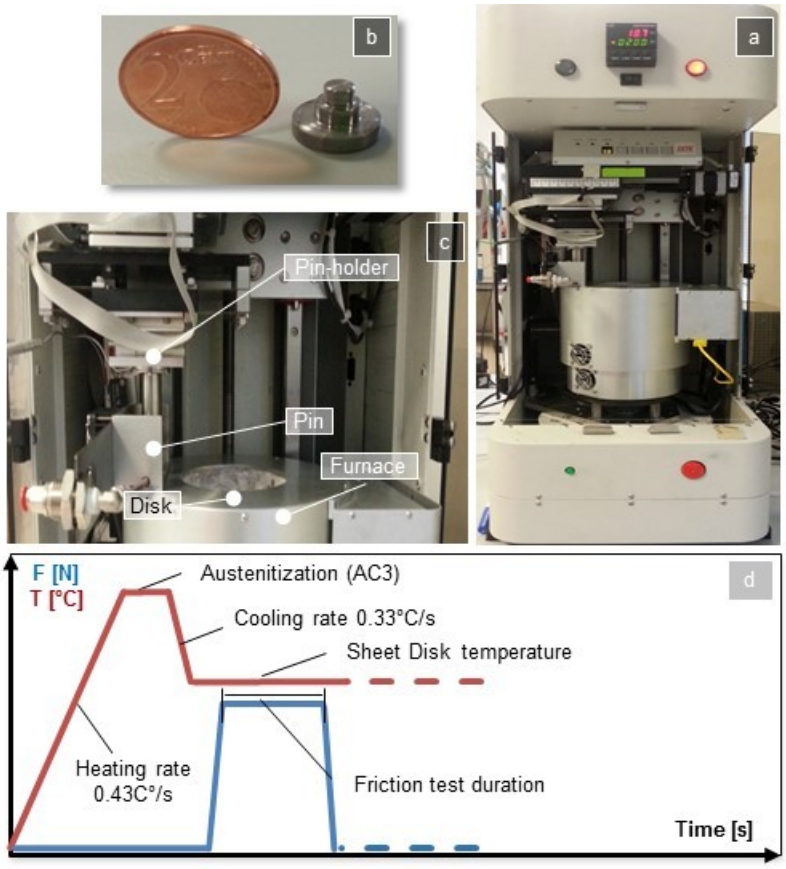


Fig. 4.6 HFTs: (a) apparatus with detail of the pin (b) and of the furnace to heat up the specimen to 1000°C (c); (d) thermo-mechanical conditions of the test.

Table 4.5 Plan of the HFTs.

| | |
|---|---|
| **Sheet material** | 22MnB5 |
| **Coating** | Al-Si |
| **Pin steel grade** | EN X38CrMoV5-1, HTCS1, HTCS3 |
| **Sheet temperature [°C]** | 600, 700, 800 (±1%) |
| **Pin temperature** | Room temperature |
| **Normal pressure [MPa]** | 10 (±0.1) |
| **Sliding speed [mm/s]** | 15 (±1) |
| **Sliding distance per test [mm]** | 75 |

| | |
|---|---|
| **Humidity conditions** | Dry |
| **Repeatability** | 5 |

## c. Hot Wear Tests (HWTs) and Heat Transfer Evaluation (HTE)

Hot Wear Tests (HWTs) based on a pin-on-disk configuration are used to investigate the wear mechanisms at high temperatures for EN X38CrMoV5-1, HTCS1 and HTCS3 alloyed steels against 22MnB5 steel coated with Al-Si coating. To this aim, the Bruker® UMT-3 tribometer equipped with the furnace described in Section 4.2.b was modified with a specifically designed cooling apparatus to replicate the thermo-mechanical cycles of the hot stamping dies, Fig. 4.7a. Compared to the HFTs, the diameter of the disks cut from the metal sheet is increased to 54.0 (±0.1) mm, Fig. 4.7b, to allow more wear tacks on the same disk. The pin temperature is monitored by a type K thermocouple spot-welded at the bottom of an axial hole inside the pin, with a diameter of 2 mm and a depth of 7.5 mm, Fig. 4.7c.

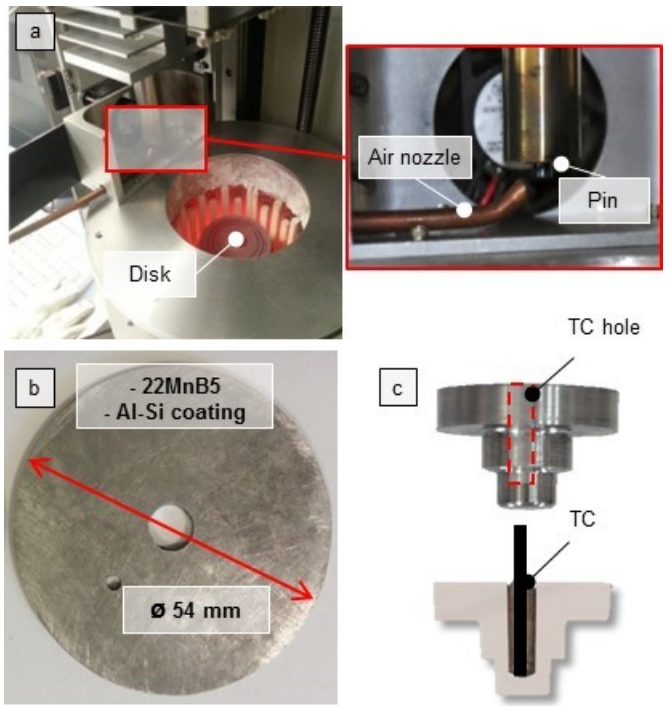


Fig. 4.7 HWTs: (a) testing set-up, (b) metal sheet disk sample and (c) detail of thermocouple hole.

Also in this case, in accordance with the industrial process, before starting the Hot Wear Test, the sheet disks positioned in the furnace are heated above the austenitization temperature by adopting a heating rate of 0.43 °C/s and a soaking time of 180.0 (±0.1) s and then are cooled down to the target test temperature with a constant cooling rate equal to 0.33 °C/s. At this point, with the sheet disk maintained at the target constant temperature, at the beginning of each cycle, the cold pin is moved into the furnace and then is pushed against the rotating hot disk for a fixed time, which was evaluated to be representative of the actual contact-time between the blank and the dies in typical hot stamping processes (Section 4.1). At that time, both thermal and mechanical loads are simultaneously applied to the pin surface, and the pin

temperature rises up as the dies in the industrial process. When the pin is moved away from the hot disk, the mechanical loads are completely removed while surface thermal stresses are induced since it is cooled down by a forced air flow just outside the hot chamber. The above-described cycle can be repeated several times and Fig. 4.8a shows a schematic representation of the cyclic thermal-mechanical loads applied to the pins and metal disk.

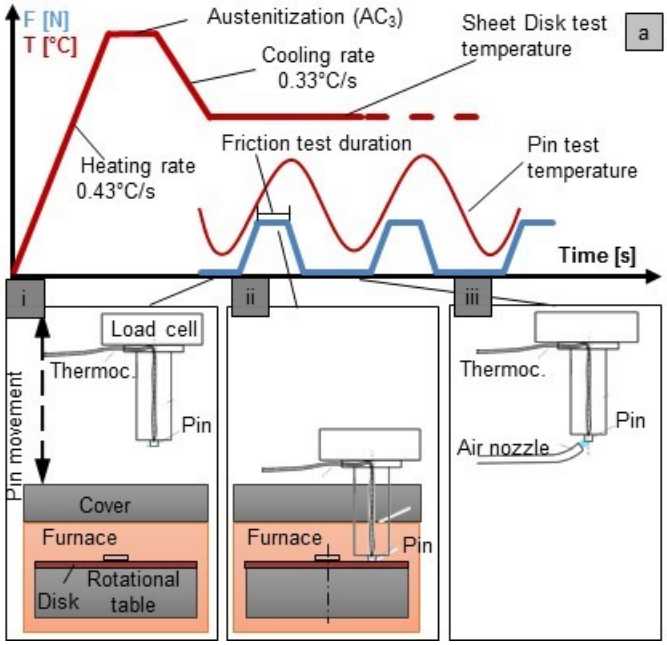


Fig. 4.8 (a) Thermal and mechanical conditions during the test and (i-iii) schematic representation of the main test phases.

The final temperature of the pin and the cooling rate are adjusted through a manometer in a range of pressure from 0 to 8 (±0.1) bar.

The characteristics of the Al-Si coating of the blank in the wear track were preliminary checked, and after every 100 cycles a new wear track was selected to continue the test, although the coating was almost undamaged on the disk surface. An acquisition frequency of 10 Hz was assumed during the tests. The wear test parameters are given in Table 4.6. According to the procedure presented in [79], the tests were stopped at 200, 600, 1200 and 2000 cycles to analyse the pin and metal sheet surfaces, and evaluate the wear mechanisms.

Table 4.6 Plan of the HWTs.

| | |
|---|---|
| **Sheet material** | 22MnB5 |
| **Coating** | Al-Si |
| **Pin steel grade** | EN X38CrMoV5-1, HTCS1, HTCS3 |
| **Sheet temperature [°C]** | 600, 700, 800 (±1%) |
| **Sheet heating rate [°C/s]** | 0.43 |
| **Sheet cooling rate [°C/s]** | 0.33 |
| **Normal pressure [MPa]** | 10 (±0.1) |

| | |
|---|---|
| **Sliding speed [mm/s]** | 15 (±1) |
| **Sliding distance per cycle [mm]** | 75 |
| **Pin cooling time [s]** | 15 |
| **Test duration [cycles]** | 2000 |
| **Humidity conditions** | Dry |
| **Repeatability** | 3 |

The decision to end the Hot Wear Test, for the three testing conditions, at 2000 cycles test was decided on the basis of industrial practice; in the industrial environment, for what concerns the reference process, the dies are usually substituted after 200.000 cycles, but after the production of 2000–3000 parts they are reground [78].

This wear experimental procedure comprises two main objectives: the former has the purpose to identify the main wear mechanisms that are established at the interface die-sheet under real process condition; the latter is to analyse the heat transfer between sheet and die in the whole process temperature range.

## d. Hot Hardness Tests (HHTs)

With the purpose of analysing the evolution of the hardness of the steels used to vary the operating temperature, in order to explain the wear mechanisms that are established, Rockwell hardness tests were carried out using a Wilson Rockwell 2000 hot hardness tester, equipped with an electrical furnace that allows performing tests up to the nominal testing temperature of 650 °C, Fig. 4.9.

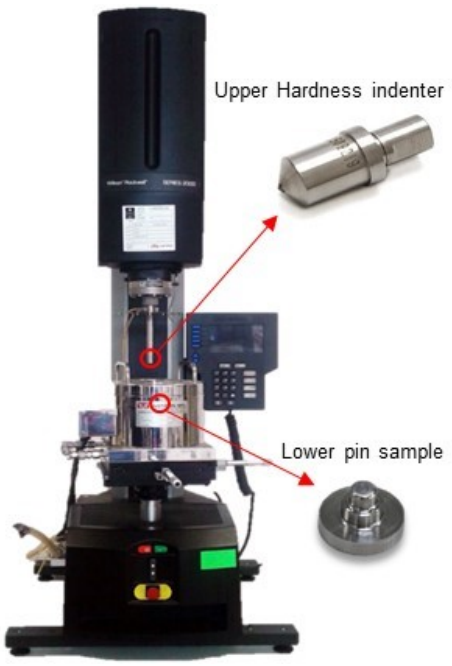


Fig. 4.9 Wilson Rockwell 2000 hot hardness tester.

The pin samples, were placed in the hot plate and then heated up to the target temperature for the tests. Six temperatures were tested, namely Room Temperature (RT), 200, 300, 400, 500, 600(±1) °C and a soaking time of 180 s was assumed to permit the temperature homogenization in the specimen. The loading cycle consists in the application of an initial load $F_0$ for 5 s, to recover the elastic deformation of the indenter, followed by the application on an additional load $F_1$ for 10 s. After every test, the indenter was cleaned using diethyl ether. Table 4.7 shows the details of the testing parameters.

Table 4.7 Experimental plan for the Hot Hardness Tests.

| | |
|---|---|
| **Hardness test** | Rockwell |
| **Type** | C |
| **Indenter material** | Diamond |
| **Indenter shape** | Right circular cone with summit angle of 120° |
| **Loads [N]** | $F_0$ = 98.0 (±0.1) / $F_1$= 1372.0 (±0.1) |
| **Time for pre-load [s]** | 5 ($F_0$), 10 ($F_1$) |
| **Load time [s]** | 30 ($F_1$) |
| **Temperature [°C]** | RT; 200; 300; 400; 500; 600 (±1) |
| **Pin steel grade** | EN X38CrMoV5-1, HTCS1, HTCS3 |

# Chapter 5

# **Results and discussions**

In the present Chapter the experimental results concerning the tribological performance of the three steel grades of interest are presented. In the first paragraph, the friction behaviour is discussed; then, in the second paragraph, a careful analysis on the main wear mechanisms present is developed. The third paragraph gives conclusions emphasizing the results in terms of heat transfer. Lastly, the conclusion summarizes the results obtained.

# 5.1. Tribological behaviour of new die steel grades as a function of the main process parameters

## 5.1.1 Hot Friction Test results

The friction coefficient was evaluated according to the Coulomb model (Eqn. 4)

$$\mu = \frac{F}{N} = \frac{\tau A_r}{\sigma A_r} = \frac{\tau}{\sigma} \qquad \text{(Eqn. 4)}$$

where $F$ is the tangential load, $N$ the normal load applied by the pin to the disk surface while $\tau$ the shear stress of the junctions, $\sigma$ is the normal stress while $A_r$ is the real area of contact between the surfaces.

Fig. 5.1 shows the results of the HFTs according to the experimental plan described in Section 4.2.b. Friction test above 800 °C were not carried out because, on the basis of the industrial practice, an approximate temperature drop of 100 °C during the blank transfer from the furnace to the dies takes generally place.

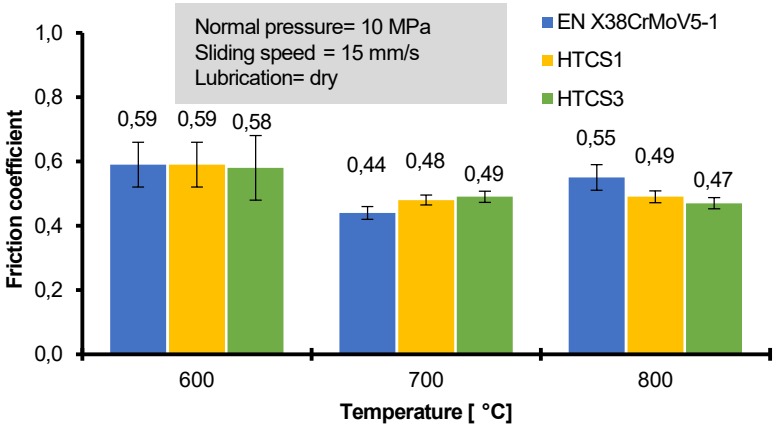


Fig. 5.1 Friction coefficients measured in HFTs for the three die steel grades by applying typical hot stamping process parameters.

The steel grades present similar values of the coefficients of friction at the tested temperatures, with high stability as proved by the low scattering of the data. The highest values are observed at the lowest temperature, while a decrease is detected increasing the testing temperature. At the lowest tested temperature equal to 600 °C, the Al-Si coating shows a slight increase of friction coefficient, probably due to the higher shear strength of the coating with,

lowering the temperature. The friction coefficients measured at 700 °C present almost the same values, but lower than 600 °C; at this temperature, EN X38CrMoV5-1 steel presents a lower friction than HTCSs (about 10% less). Further raising the test temperature up to 800 °C, an increase of the COF for the steel EN X38CrMoV5-1 is observed, reaching values greater than about 15% compared to HTCSs. Such behaviour, higher temperature lower COF, already observed and explained in [79], is due to the decrease of the coating shear strength and the activation of an intra-film lubrication mechanism so to accommodate the relative displacements of the two surfaces. As a consequence, when the pin slides over the coated surface, the asperities are more easily deformed provoking a decrease of the friction coefficient. This observation is also supported by the equation (4), for which, while decreasing the shear stress and therefore, increasing the temperature of the test, there is a reduction of the friction coefficient. Observing the error uncertainty bands, it is possible to note that they are greater for the temperature of 600 °C; a possible explanation is that, at lower testing temperatures, the coating shear strength increases [75], by preventing the pin to slide homogeneously on the sheet, encountering more difficult deformable asperity compared to higher temperatures. It is possible to observe this behaviour from Fig. 5.2, which contains the 5 friction test for HTCS3 grade steel at a temperature of 600 and 800 °C; at the lower test temperature the curves appear serrated while at 800 °C they have an almost linear profile. APPENDIX A reports all friction curves for the different steel grades and test parameters.

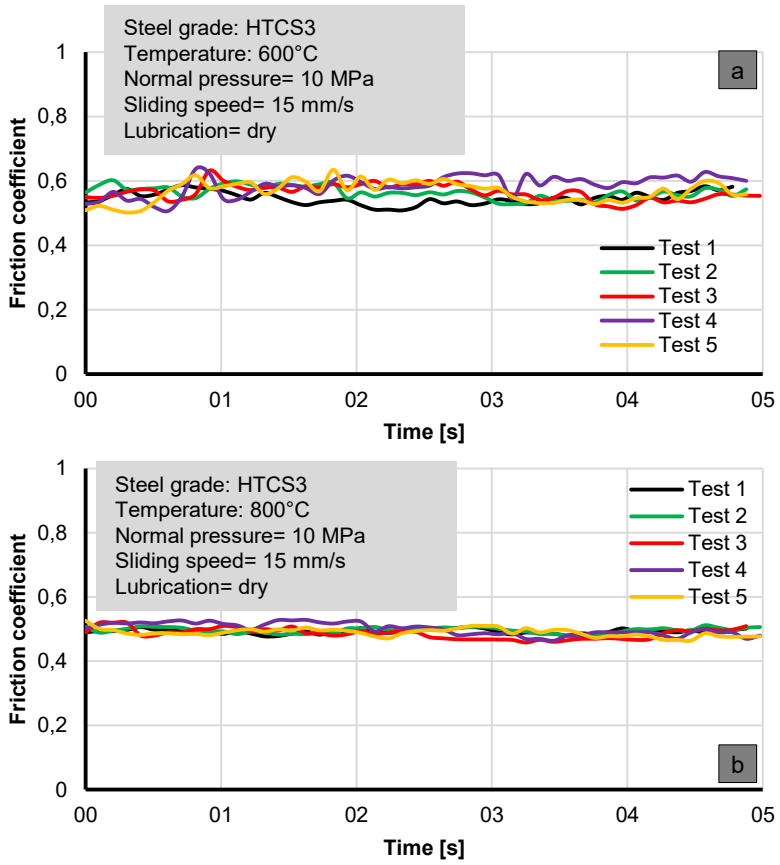


Fig. 5.2 Friction coefficient curves registered in the case of HTCS3 at (a) 600 °C and (b) 800 °C.

Compared to standard steel grade EN X38CrMoV5-1 implemented in high temperature processes, both the HTCS grades present lower coefficient of friction with consequent lower

resistance to the sliding. This is mainly due to the different initial surface roughness Sa and thermal treatments that are typically realized in the stamping tools and were reproduced on the pins used in the experiments: all the pins manufactured with the EN X38CrMoV5-1 steel present higher values of Sa than the HTCS1 and HTCS3 steels. Furthermore, the new grades present less tendency of breaking the oxides as showed by the stable tangential loads that were measured during the tests. The friction values measured are comparable, as an order of magnitude, to others values reported in studies devoted to the evaluation of tribological performance of Al–Si-coated 22MnB5 steel in hot stamping conditions, see Fig. 5.3 (A. Azushima [64], P. F. Bariani [85], A. Ghiotti [79], A. Yanagida [63], F. Borsetto [105]).

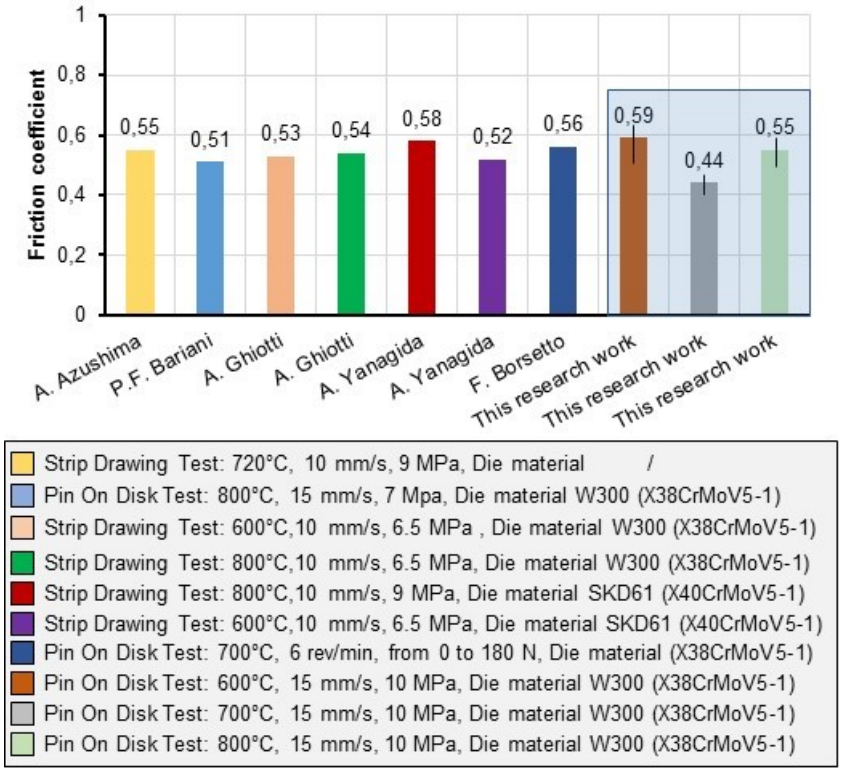


Fig. 5.3 Summary researches of the tribological behaviours in hot stamping. (22MnB5, Al-Si coating, and dry conditions).

## 5.1.2 Hot Wear Test results

The wear of the tool steels at varying number of cycles was evaluated by means of: (i) measurement of the pins weight variation at different number of cycles, (ii) SEM-EDX analysis to understand the material transferred from the metal sheet to the pin or vice-versa, if present, (iii) optical observations and measurements of the pins sliding surface through the SEM and 3D optical profilometer.

For all three steel grades, the wear track was investigated after each batch of 100 cycles in order to assess the limit stroke after which the coating layers start to be removed from the pin track on the disk. Fig. 5.4 shows the chemical element maps of the wear track on the disk surfaces after being tested for 100 cycles at the highest test temperature. Al-Si coating appears overall undamaged and it shows only small areas with relevant percentages of Fe, Mn and Cr,

thus proving acceptable the choice of the number of cycles on the same wear track. Observing the tracks, for all three steels tested, some material transfer from the pin to the metal sheet was observed, due to the abrasive wear mechanism that was detected, as supported by the measurements of the pin weight and SEM-BSE observations.

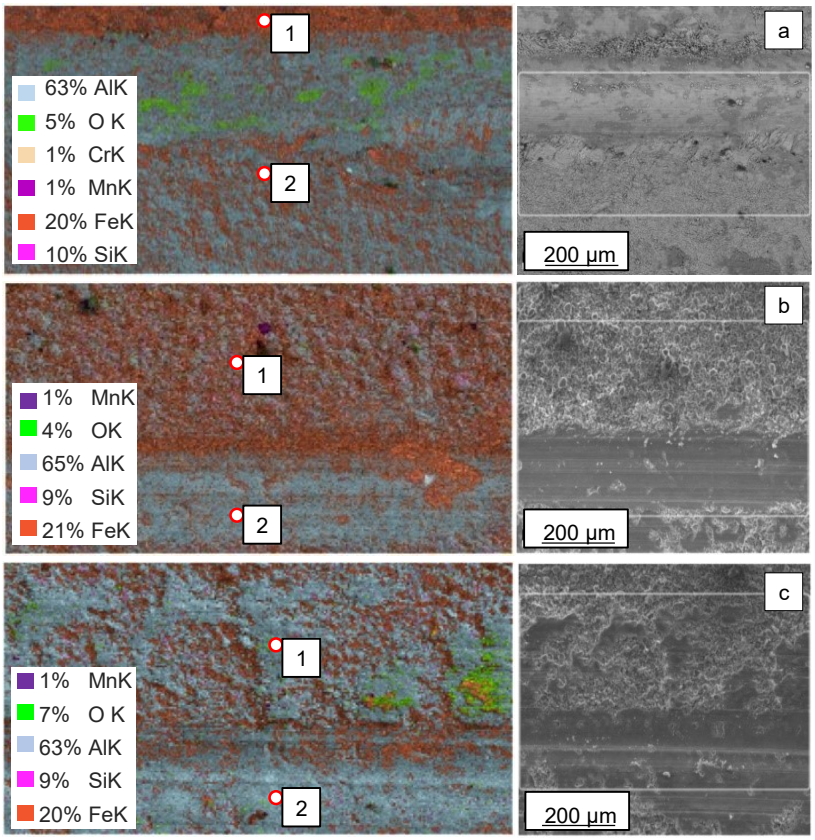


Fig. 5.4 Wear track integrity at 800 °C at 100 cycles in the case of Al-Si coated disks for a) EN X38CrMoV5-1 b) HTCS1 and c) HTCS3. Point 1 indicates the original coating while point 2 the wear track area.

All the three grades were interested by abrasive and adhesive wear mechanisms, albeit to differing degrees, as shown in Fig. 5.5 where the variations in weight of the pins are plotted versus the number of cycles.

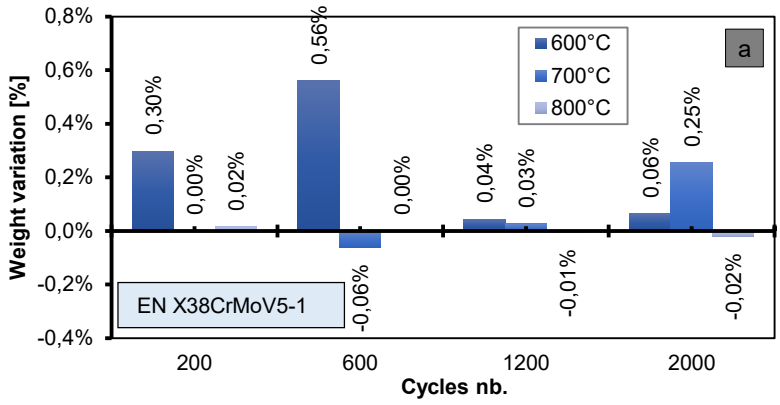

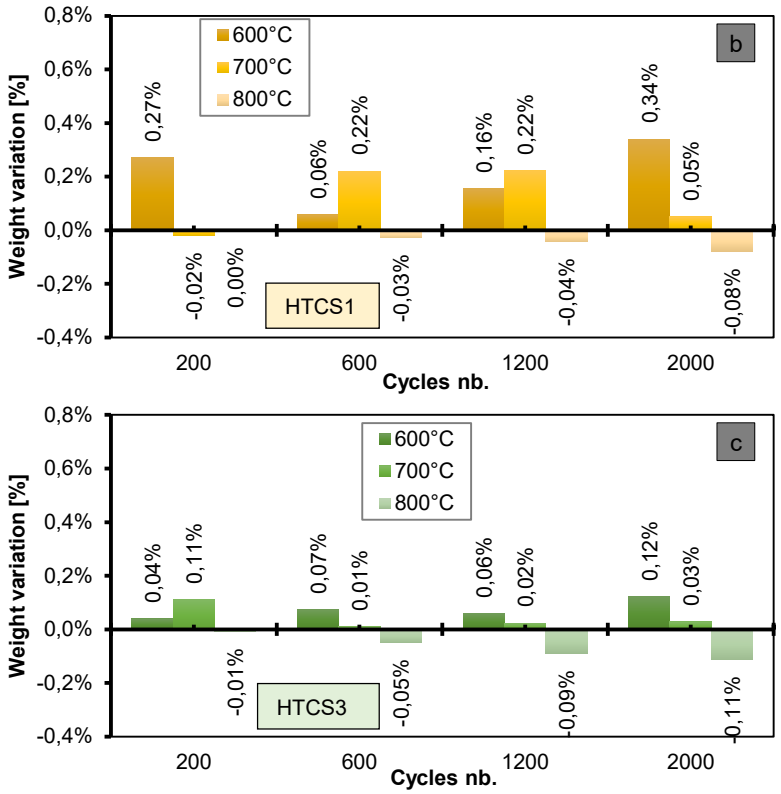


Fig. 5.5 Pin weight variation at different temperatures measured after 200, 600, 1200, 2000 cycles in the case of a) EN X38CrMoV5-1, b) HTCS1 and c) HTCS3 steel grade.

The HTCS3 steel grade appears to be less interested by adhesion phenomena than the other two grades, with a maximum weight increase of 0.12% compared to the 0.34% of the HTCS1 and the 0.25% of the EN X38CrMoV5-1 after 2000 cycles.

For all the steel grades tested, the temperature appears having the major influence on the phenomena: at 800 °C, which corresponds to the first contact between the blank and the dies at the beginning of the deformation in the industrial process, an average weight loss of about 0.07% was detected after 2000 cycles, while the lowest temperatures are interested mainly by adhesion. The change of wear mechanism from adhesion to abrasion can be explained with the fall of surface hardness that the steel grades present as the temperature increases. Fig. 5.6 shows the HRC hardness of the three steel grades measured before the Hot Wear Tests by means the Hot Hardness Tests explained in Section 4.2.d. In the case of the wear tests carried out at 700 °C, the temperature measured by the thermocouple embedded in the pin rises up to 180 °C (with an estimated temperature on the outer surface above 500 °C) with a consequent fall of the surface hardness that determines the abrasive mechanism. Moreover, from Fig. 5.6, it is possible to observe that the steel EN X38CrMoV5-1 maintains a higher hardness than the HTCSs, whose gap becomes significant from a temperature of 400 °C; this may explain the lower abrasive wear of the EN X38CrMoV5-1 steel, resulting in less weight loss reported in Fig. 5.5 than the other two steels.

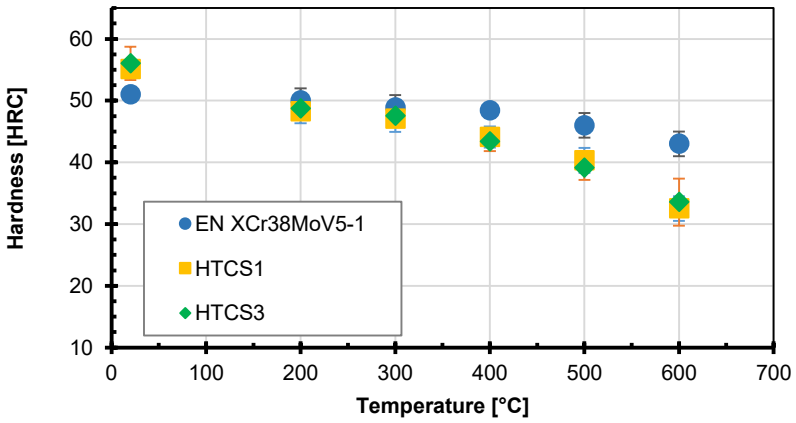


Fig. 5.6 Pin surface HRC hardness measured at different temperatures.

Furthermore, the abrasion at the highest testing temperature can be related to the abrasive particle generated on the surface by oxidation or coating dusts: the oxide particles can be larger than the carbides distributed in the matrix and determine the abrasion of the pins. The same mechanisms are those described by F. Stott [106][107]; (i) the debris act as freely-moving particles, causing abrasion damage to both the surfaces, (ii) at the higher test temperatures, further oxidation can cause the development of hard oxide 'glaze' surfaces on these layers, leading to very low rates of wear adhesion.

Fig. 5.7 and Fig. 5.8 show the SEM-BSE and EDX of the pin surfaces and the weight percentage of the chemical components after 2000 cycles, in the case of HTCS1 and 3 steel grade, measured at the different test temperatures, respectively.

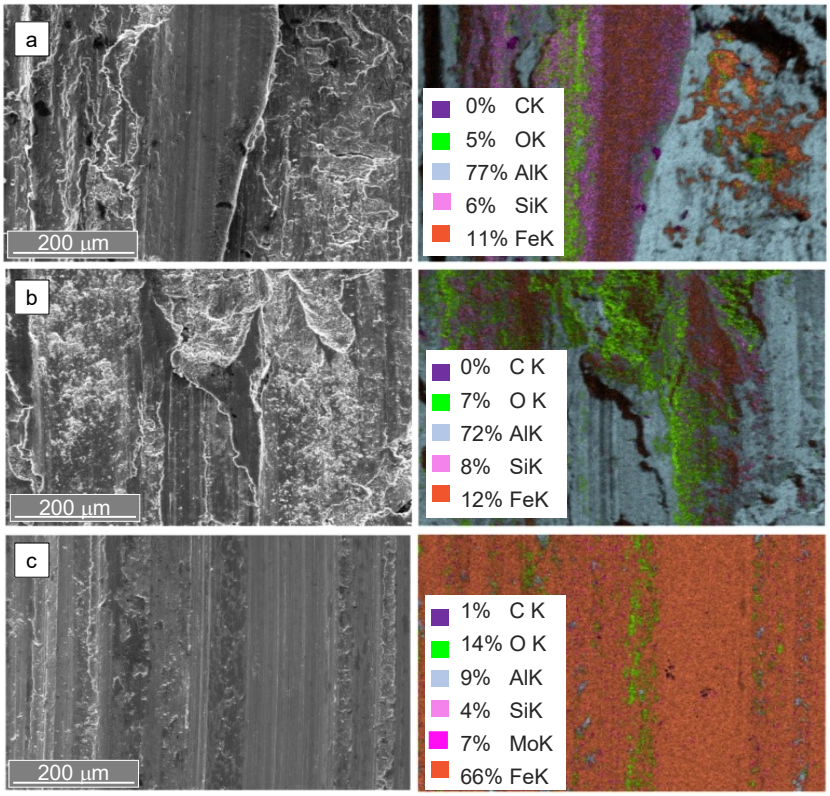


Fig. 5.7 SEM-BSE and EDX analysis of the HTCS1 pins surface at (a) 600 °C (b) 700 °C (c) 800 °C.

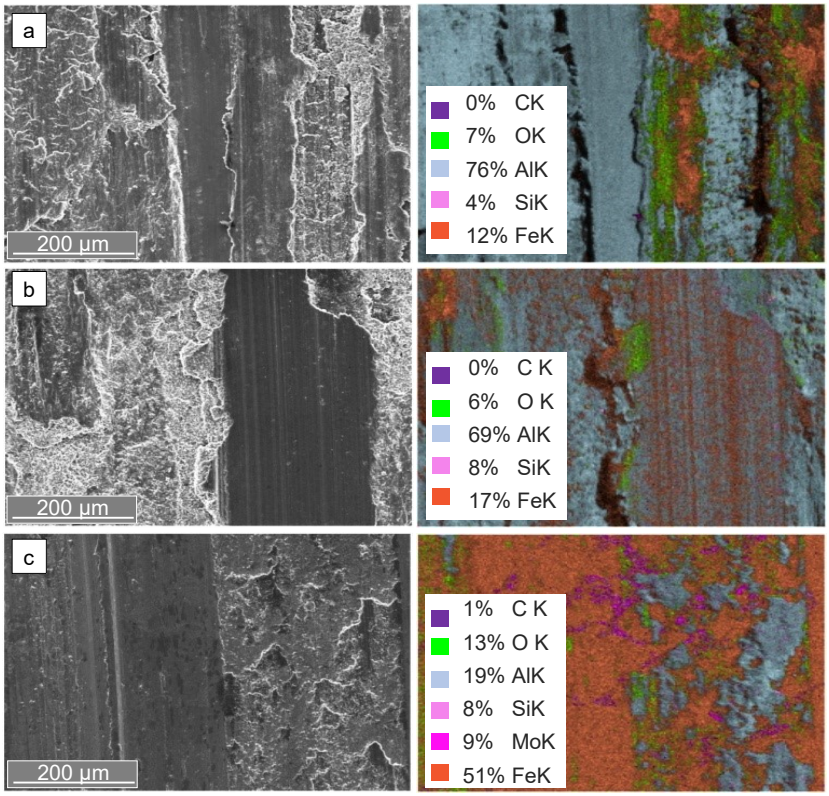


Fig. 5.8 SEM-BSE and EDX analysis of the HTCS3 pins surface at (a) 600 °C (b) 700 °C (c) 800 °C.

The SEM images, carried on the pin surfaces, confirm the indications of the weight measurements, with large material transfer from the metal sheet to the pin surface at the lower temperatures, while abrasion takes place mainly at 800 °C. Such behaviour is supported also by the quantity of Al detected with the chemical analysis, which is part of the 22MnB5 coating to prevent the oxidation of the blank at elevated temperatures. The weight comparison with the standard EN X38CrMoV5-1 reveals larger abrasion in the HTCS grades especially at the highest temperatures, so as to assume a more significant impact of the wear in the dies service-life.

Fig. 5.9 shows a larger magnification of the pin surfaces after 2000 cycles tested with a furnace temperature of 800 °C. It is possible to see that the Mo agglomerates are still visible on the pin surface manufactured with the HTCS3 grade as well as the Al-Si coating that was transferred from the 22MnB5 disk.

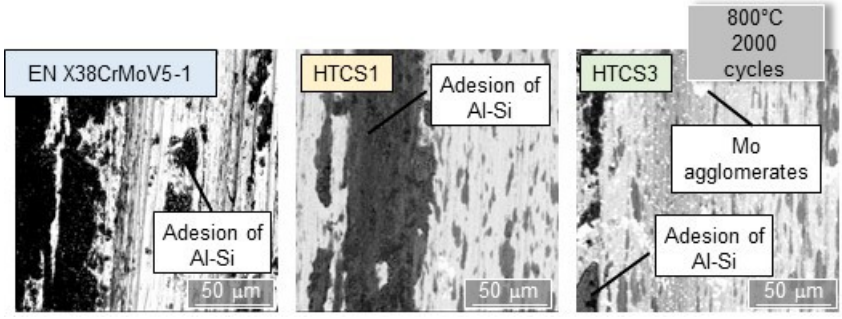


Fig. 5.9 SEM-BSE images of the EN X38CrMoV5-1, HTCS1 and HTCS3 pins surface tested at a furnace temperature of 800 °C.

Below the pin sliding surface for the three steel grades at 800, 700, 600 °C at different number of cycles, as reported in Section 4.2.c, are discussed and analysed. Fig. 5.10 shows the pin wear at 800 °C in the case of EN X38CrMoV5-1 steel grade.

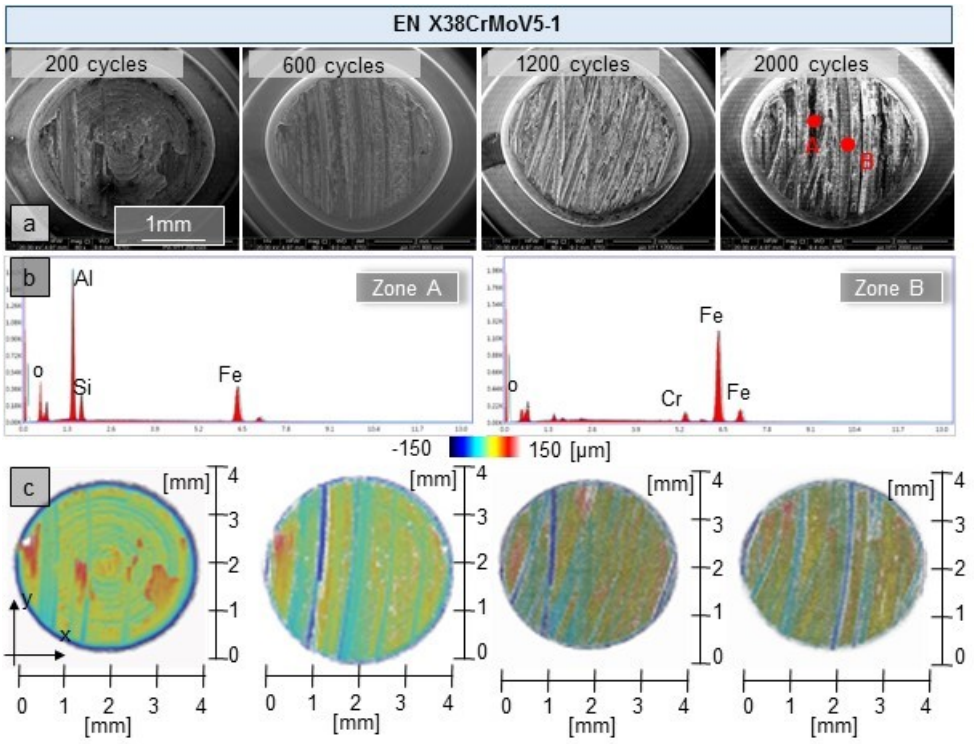


Fig. 5.10 Pin wear of EN X38CrMoV5-1 steel grade when sliding on the AlSi-coated disks at 800 °C: (a) pin surface at different cycles number, with detail of the EDX analyses (b), and (c) Sa measurements of the pin surface.

At the test temperature of 800 °C, which corresponds to the first contact temperature between die-sheet at the beginning of the simultaneous forming and quenching phase in closed die in the industrial process, the wear is mainly abrasive, see Fig. 5.10. A slight adhesion can be verified in the case of the Al-Si coating, as shown by the SEM-Back Scattered (SEM-BSE) in Fig. 5.10a, where at 2000 cycles the Al and Si elements are detected onto the pin surface. The SEM-EDX analyses of Fig. 5.10b show the presence of the Al (corresponding to the darkest areas) in small portions of the pin surface and large parts characterized only by abrasive wear (the lighter zones) in which only the elements of the EN X38CrMoV5-1 steel grade can be found. The pin surface roughness changes accordingly, with local peaks that were measured up to 50 µm, see Fig. 5.10c.

Fig. 5.11 and Fig. 5.12 show the pin wear at 800 °C in the case of HTCS1 and HTCS3 steel grades. Since the first measurement carried out after 200 cycles, large plastic deformation of the surface is detected, with removal of large portions of the contact surface. For both steels, as a consequence of the harder debris that remains between the sliding surfaces, some scratches can also appear on the pin surface with Al that is ploughed from the disk surface as proved by the point chemical analysis performed and plotted in the spectra Fig. 5.11b and Fig. 5.12b. The 3D profiler images show that the wear remains almost uniform, apart for the zones where the scratches are detected.

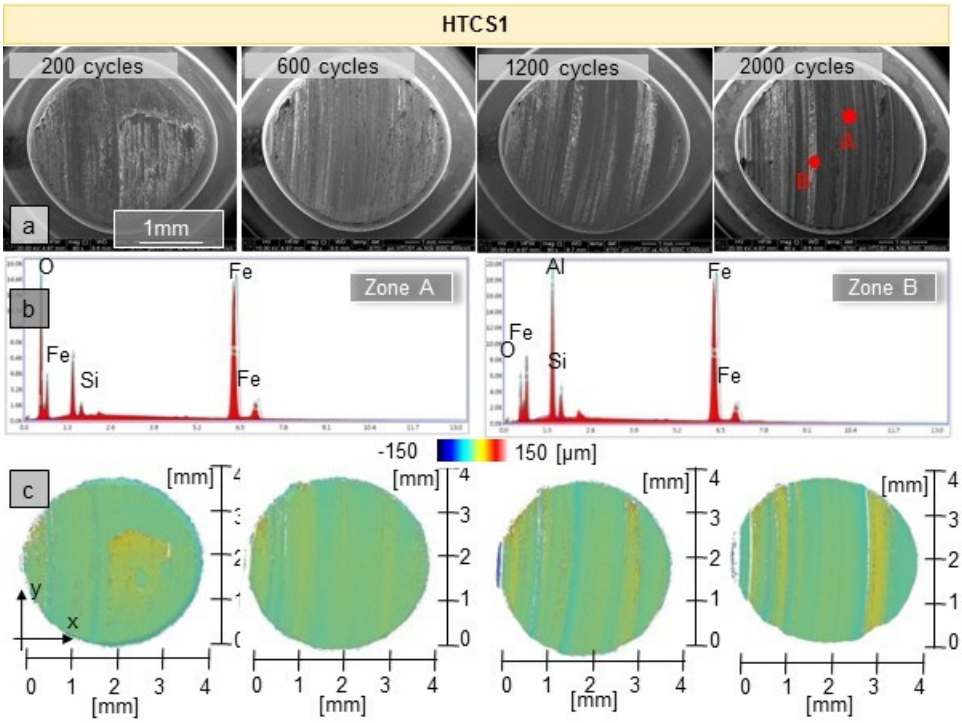


Fig. 5.11 Pin wear of HTCS1 steel grade when sliding on the AlSi-coated disks at 800 °C: (a) pin surface at different cycles number, with detail of the EDX analyses (b), and (c) Sa measurements of the pin surface.

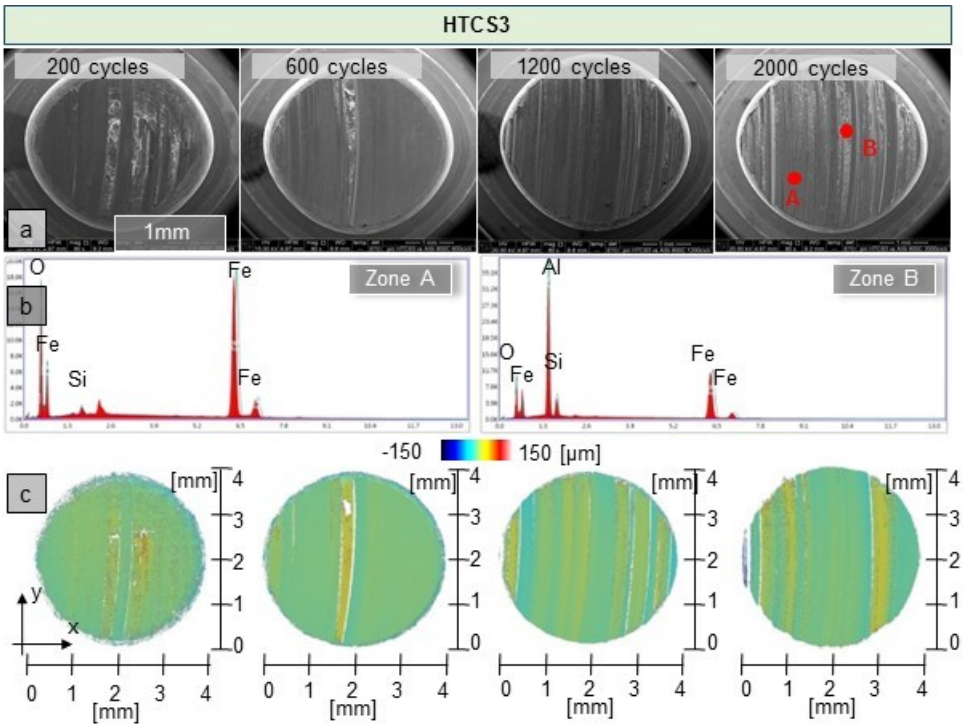


Fig. 5.12 Pin wear of HTCS3 steel grade when sliding on the AlSi-coated disks at 800 °C: (a) pin surface at different cycles number, with detail of the EDX analyses (b), and (c) Sa measurements of the pin surface.

Fig. 5.13, Fig. 5.14 and Fig. 5.15 show the results of the HWTs at 700 °C, where a different behaviour of the three steel grades was detected in the SEM-BSE and EDX analysis. Analysing

the EN X38CrMoV5-1 steel grade, Fig. 5.13, it is possible to observe that the coating adheres to the pin surface starting from 1200 cycles, with large material transfer that was measured also as weight increase of 0.03% and a surface roughness $S_a$ of 10.51(±2.72) μm. At 2000 cycles, greater adhesion can be observed, also in agreement with the weight increase up to 0.25% and a surface roughness $S_a$ of 17.63(±1.63) μm. Some material transfer can be detected also at lower number of cycles, but it is limited to small portions of the surface. At 700 °C, adhesion appears to be more significant than abrasion, see Fig. 5.13c.

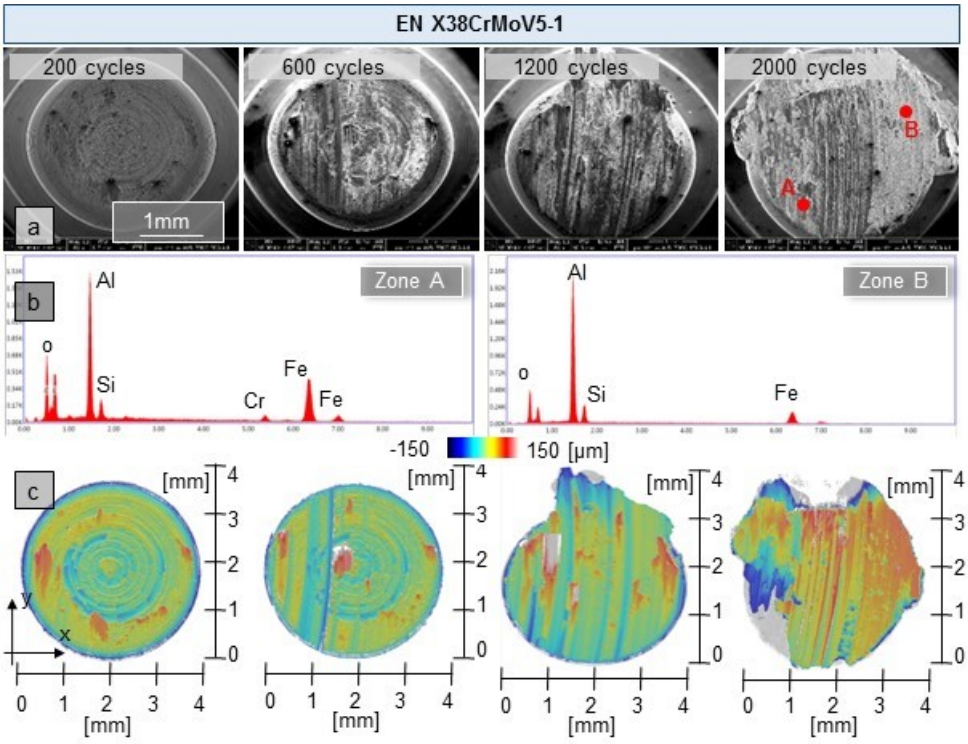


Fig. 5.13 Pin wear of EN X38CrMoV5-1 steel grade when sliding on the AlSi-coated disks at 700 °C: (a) pin surface at different cycles number, with detail of the EDX analyses (b), and (c) Sa measurements of the pin surface.

In the case of HTCS1, Fig. 5.14, large material transfer from the disk to the pin surface is detected since the first 600 cycles: large plateaus are welded onto the pin surface and can be suddenly torn away, as it happens after 1200 cycles. Also in this case, the images are in agreement with the weight variation reported in Fig. 5.5; at 600 and 1200 cycles, the pin maintains a weight increase equal to 0.22%, while at 2000 cycles it stabilizes at 0.05%.

The HTCS3 steel grade, Fig. 5.15, appears more interested by adhesion since the first measurement carried out at 200 cycles, reflecting the increase in weight amounted to 0.11%; the following measurements show a more stable situation with small portions of material adhered to the pin surface, resulting in a stationary weight change around 0.02%.

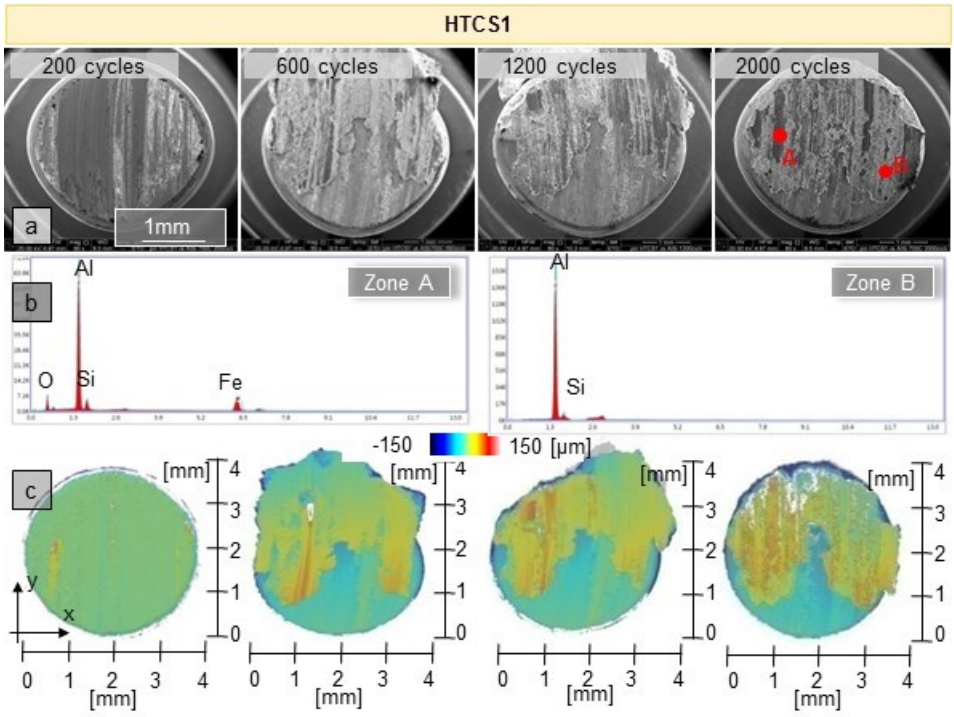


Fig. 5.14 Pin wear of HTCS1 steel grade when sliding on the AlSi-coated disks at 700 °C: (a) pin surface at different cycles number, with detail of the EDX analyses (b), and (c) Sa measurements of the pin surface.

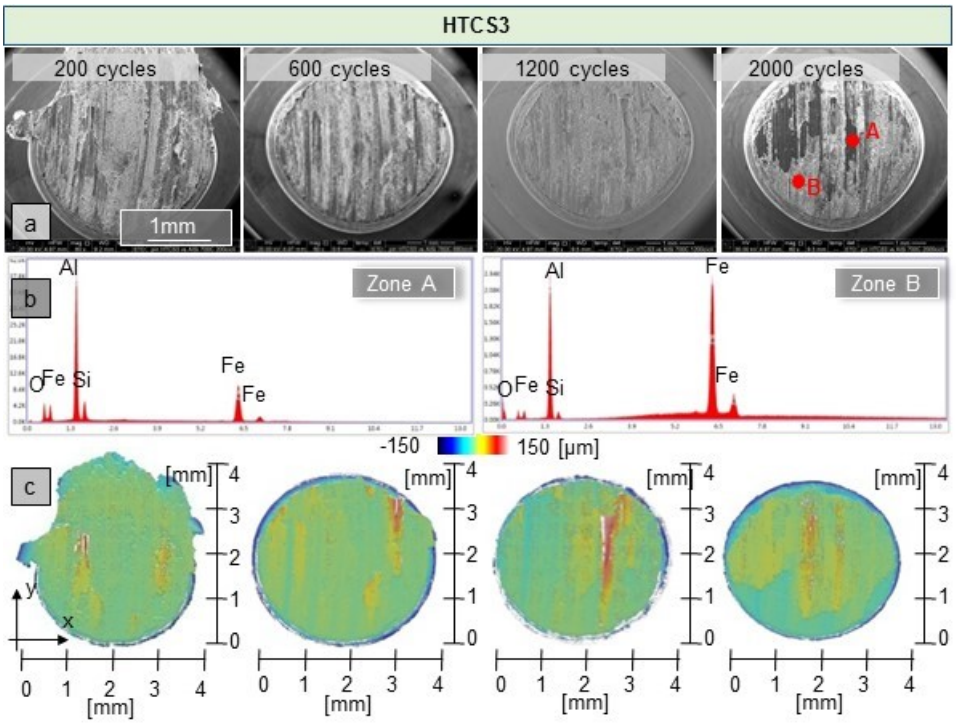


Fig. 5.15 Pin wear of HTCS3 steel grade when sliding on the AlSi-coated disks at 700 °C: (a) pin surface at different cycles number, with detail of the EDX analyses (b), and (c) Sa measurements of the pin surface.

Fig. 5.16, Fig. 5.17 and Fig. 5.18 show the test results at 600 °C that is the lowest temperature at which the metal sheet deformation typically takes place in hot stamping. From

Fig. 5.16 and Fig. 5.17, according to the changes of weight showed in Fig. 5.5, at such test temperature, the heavy adhesion of the sheet metal coating on the pin surface appears since the first cycles for both EN X38CrMoV5-1 and HTCS1, while it seems lower for HTCS3 steel, Fig. 5.18. Anyway, at 600°C, for all the three steel grades, the surface analysis revealed that after only 200 cycles, the machining marks produced by turning the tool on pin surface were almost completely cancelled by scratches and adhering material that filled the valley. In fact, as explained by L. Pelcastre in [70], [80], [81], surface roughness highly influenced the adhesive phenomena. Surface defects, such as machining marks, are the privileged place for the accumulation of wear debris and the incoming of adhesive galling. For the EN X38CrMoV5-1, the transferred material is less evident in the measurements carried out at 1200 and 2000 cycle, since the quantity of adhered material was too large and, consequently, it was torn away in the form of debris when removing the pin for the measurements.

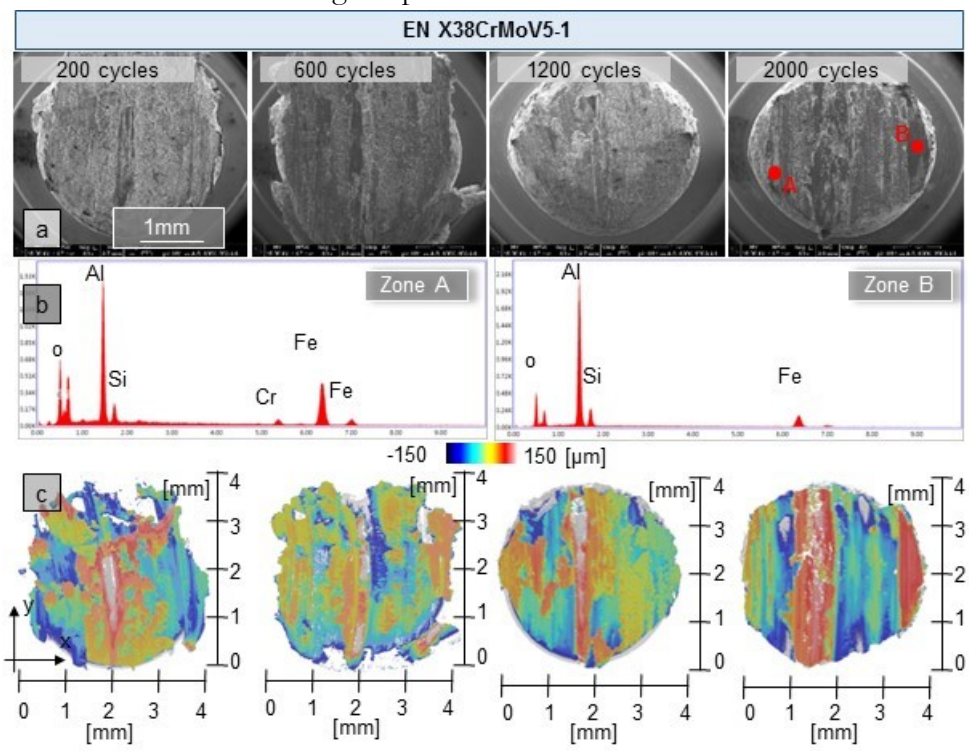


Fig. 5.16 Pin wear of EN X38CrMoV5-1 steel grade when sliding on the AlSi-coated disks at 600 °C: (a) pin surface at different cycles number, with detail of the EDX analyses (b), and (c) Sa measurements of the pin surface.

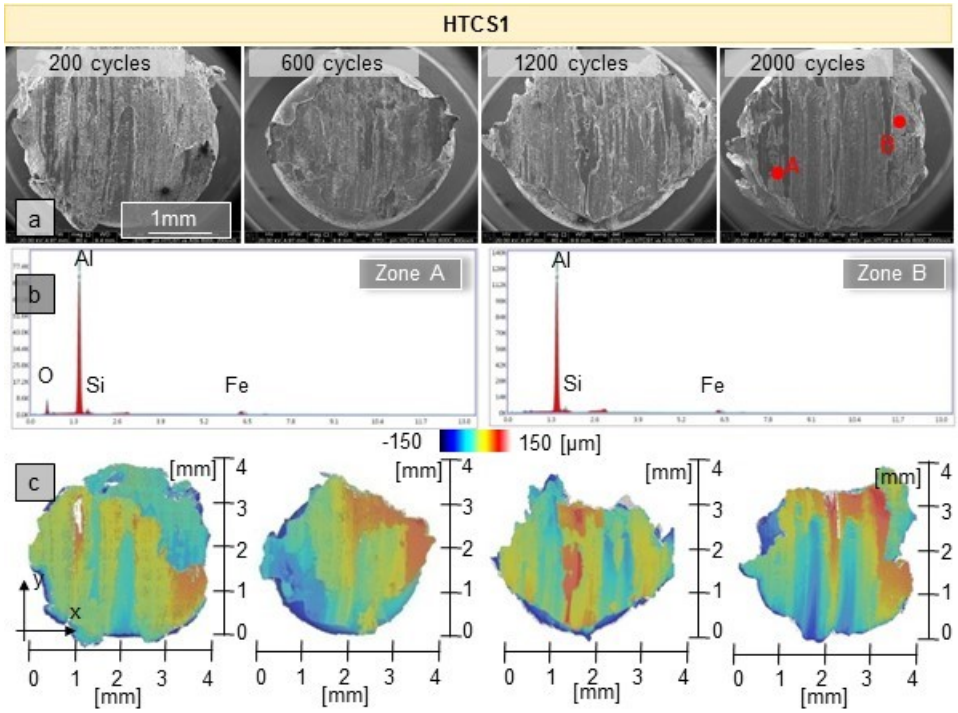


Fig. 5.17 Pin wear of HTCS1 steel grade when sliding on the AlSi-coated disks at 600 °C: (a) pin surface at different cycles number, with detail of the EDX analyses (b), and (c) Sa measurements of the pin surface.

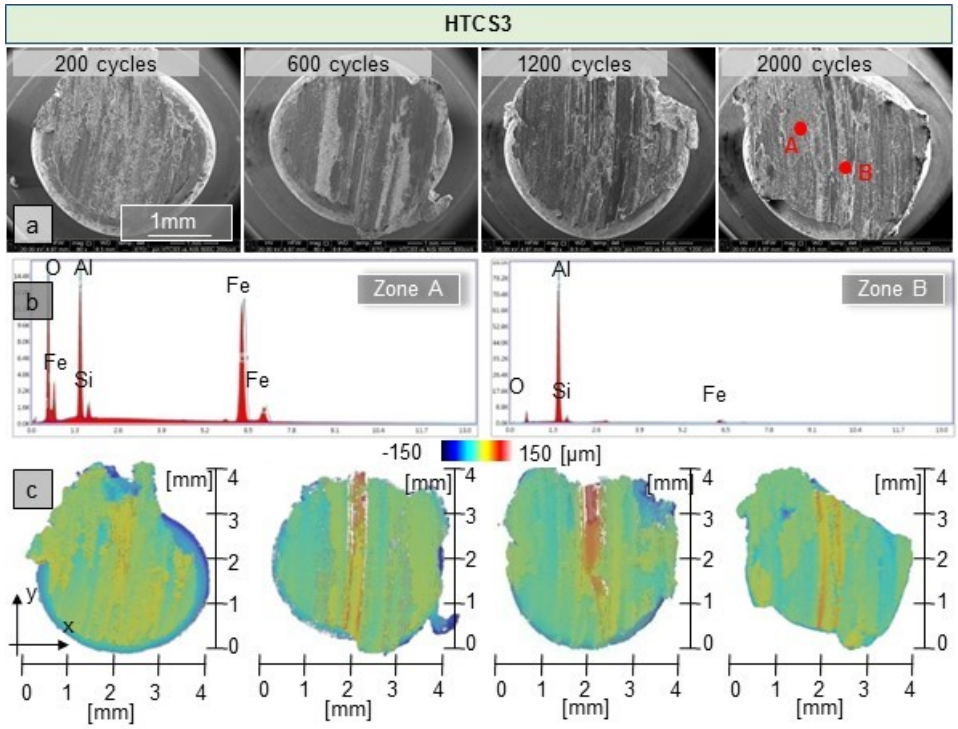


Fig. 5.18 Pin wear of HTCS3 steel grade when sliding on the AlSi-coated disks at 600 °C: (a) pin surface at different cycles number, with detail of the EDX analyses (b), and (c) Sa measurements of the pin surface.

At each test stop, large portions of the Al-Si coating were detected on the pin surface, as shown in the SEM-BSE and 3D profiler measurements. At such temperature the worst surface conditions in terms of surface roughness were detected.

For all the tested conditions, the SEM-EDX analysis does not show elements of the original boron steel transferred to the pin.

Fig. 5.19 reports the values of the surface roughness $S_a$ as it was measured for different number of cycles at the tested temperatures. The measurements of the pins roughness reflect the evolution of the wear mechanisms described above; lower roughness values are detected at the temperature of 800 °C for all the grades, where the abrasive wear is predominant and the surface appears more uniform and smoother. Conversely, the surface roughness values increase by decreasing the temperature of the test, as the strong adhesion on pin generates an indented surface.

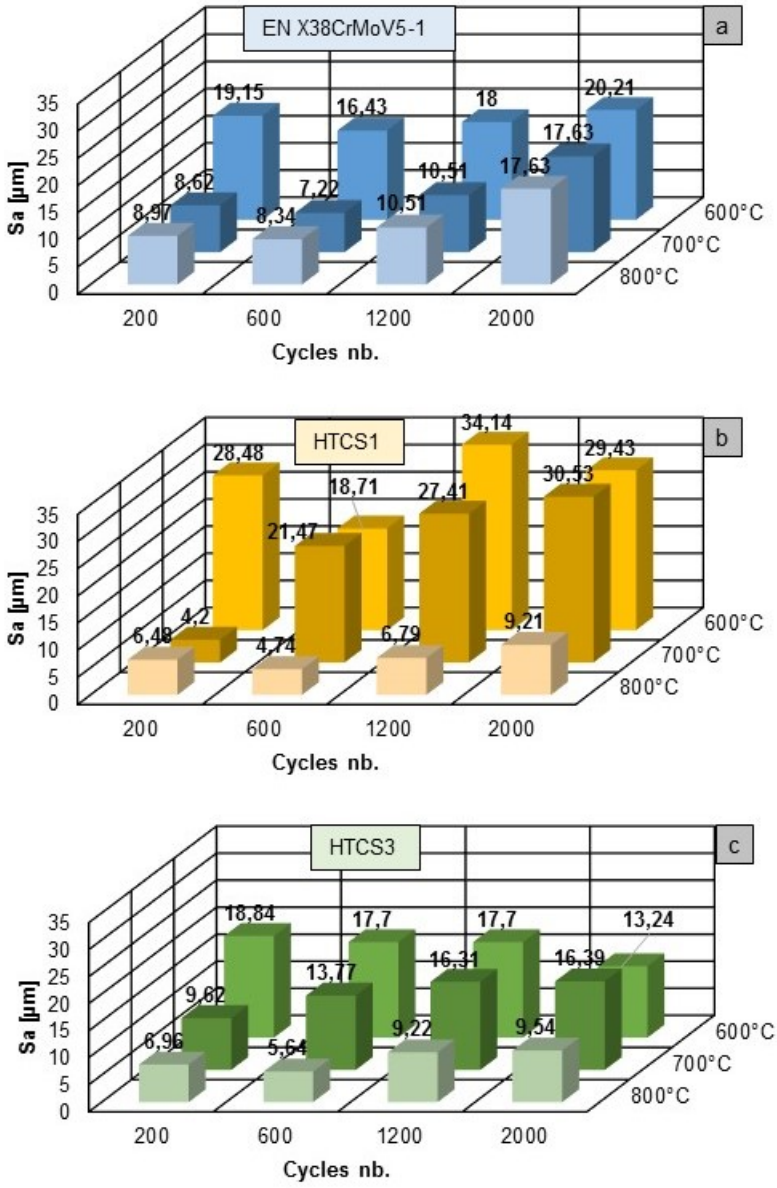


Fig. 5.19 Pin surface roughness $S_a$ at the different temperatures measured after 200, 600, 1200, 2000 cycles: a) EN X38CrMoV5-1, b) HTCS1 and c) HTCS3.

In order to ensure the stability of the mechanical conditions during the long Hot Wear Tests, the forces at the interface between the pin and the dies were controlled by monitoring the friction coefficient during the tests. Fig. 5.20 shows, for example, the average of the coefficient of friction calculated for each stop test to change the sliding track, during the 2000 cycles for EN X38CrMoV5-1 steel grade at 800 °C. The results extrapolated in terms of friction are compatible with those obtained for single strokes carried out in the Hot Friction Test reported in Fig. 5.1 and are almost stable during all the cycles of the wear tests. APPENDIX B reports all friction diagrams used to monitor the mechanical stability during the Hot Wear Tests for different steel grades and test parameters.

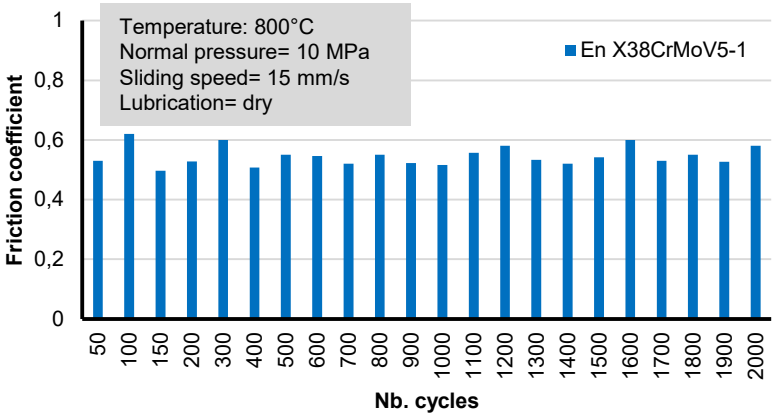


Fig. 5.20 Average of the coefficient of friction calculated for each stop test to change the sliding track, during the 2000 cycles for EN X38CrMoV5-1 steel grade at 800 °C.

### 5.1.3 Heat Transfer results

The thermal parameters - namely the minimum, the average and the maximum temperatures, the heating and the cooling rates - were monitored during the HWTs thanks to the thermocouples embedded in the pins, explained in Section 4.2.c. The summary of all the measured values is reported in Table 5.1 for all the steel grades.

Being all the experimental parameters constant, namely the contact time, the air-cooling time, the sliding speed and the pressure at the interface, the steels' conductivity shows a large influence on the heat transfer between the disk and the pin.

Table 5.1 Pin temperatures acquired during the HWTs with an uncertainty (±2) °C.

| | | **EN X38CrMoV5-1** | | | **HTCS1** | | | **HTCS3** | | |
|---|---|---|---|---|---|---|---|---|---|---|
| Disk | T. [°C] | 600 | 700 | 800 | 600 | 700 | 800 | 600 | 700 | 800 |
| Pin | Min T. [°C] | 70.3 | 104.0 | 138.9 | 78.3 | 97.3 | 113.0 | 83.3 | 98.8 | 114.6 |
| | Avg. T. [°C] | 88.7 | 124.7 | 161.8 | 95.3 | 121.8 | 137.8 | 98.2 | 116.7 | 141.3 |
| | Max T. [°C] | 115.7 | 152.8 | 192.8 | 117.7 | 147.1 | 168.3 | 123.7 | 140.3 | 177.0 |
| | ΔT [°C] | 45.4 | 48.8 | 53.9 | 39.4 | 49.7 | 55.3 | 40.4 | 41.5 | 62.4 |

A general overview shows that the HTCS3 allows higher heat dissipation for fixed cooling time: at the highest test temperature of 800 °C the heat exchanged between the hot disk and the pin is higher (difference between the maximum and the minimum measured temperature $\Delta T$ equal to 62.4 °C for the HTCS3 vs a $\Delta T$ equal to 53.9 °C for the EN X38CrMoV5-1), while at the lower furnace temperature of 700 °C the HTCS1 grade offers better performances in terms of heat dissipation. Such behaviour can be ascribed to a change in the materials conductivity that presents a discontinuity between 700 °C and 800 °C. Further decreasing the test temperature at 600 °C, it is possible to observe that steel grade EN X38CrMoV5-1 presents the largest heat dissipation; this means that the HTCSs perform the function, for which they were developed, at elevated service temperatures. It is possible to notice the same behaviour even observing the average pin temperatures recorded during testing, Fig. 5.21. The steel EN X38CrMoV5-1 presents a lower average working temperature lower than HTCS grades only in the tests carried out at 600 °C while, increasing the temperature up to 700 and 800 °C, the HTCS grades present much lower operating temperatures than EN X38CrMoV5-1 steel, with a decrease up to 15% in the case of HTCS1 at 800 °C.

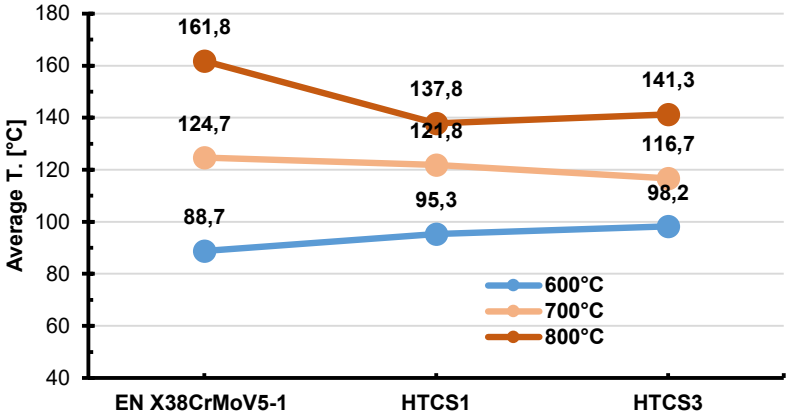


Fig. 5.21 Pin average temperatures recorded HWTs.

On the base of test parameters listed in Table 4.6, recorded during the HWTs, Fig. 5.22 shows a schematic representation of the pin temperature evolution during each cycle of the wear test as recorded by the embedded K-type thermocouple, with the indication of the testing steps and their duration. It is possible to note that the total cycle time is 36.8 s, close to the one the forming dies are subjected to during the hot stamping process, as indicated in Section 4.1. Observing the temperature trend reported in Fig. 5.22a, it is possible to note that the maximum and minimum peak of temperature of the cycle were not reached when the pin moved out from the oven and at the end of the cooling phase, but subsequently. This was due to the delay in the response of the thermocouple being placed at a distance of 2 mm from the pin sliding surface, Fig. 5.22b, and to the pin thermal inertia.

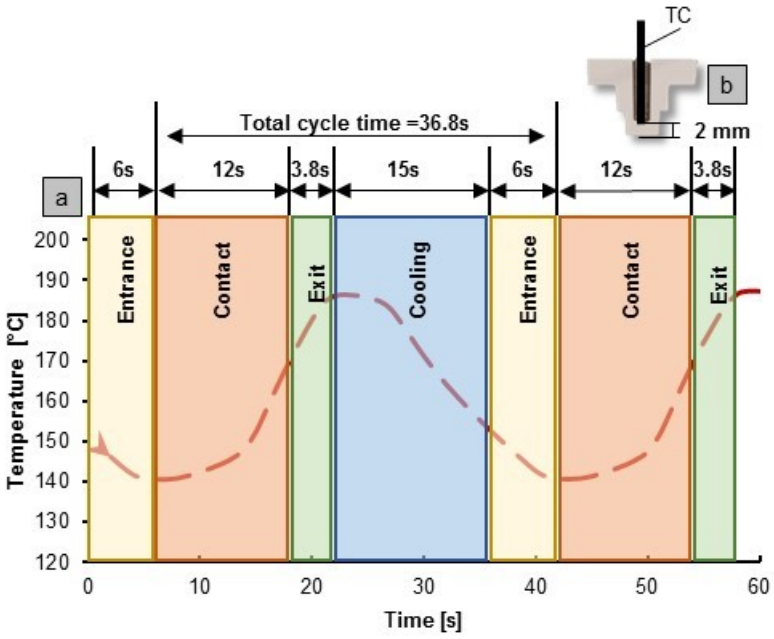


Fig. 5.22 a) Schematic representation of the pin temperature evolution during each cycle of the wear test and b) detail of thermocouple hole.

Fig. 5.23 shows the details of the temperatures measured during the tests for the three steel grades at different test temperatures.

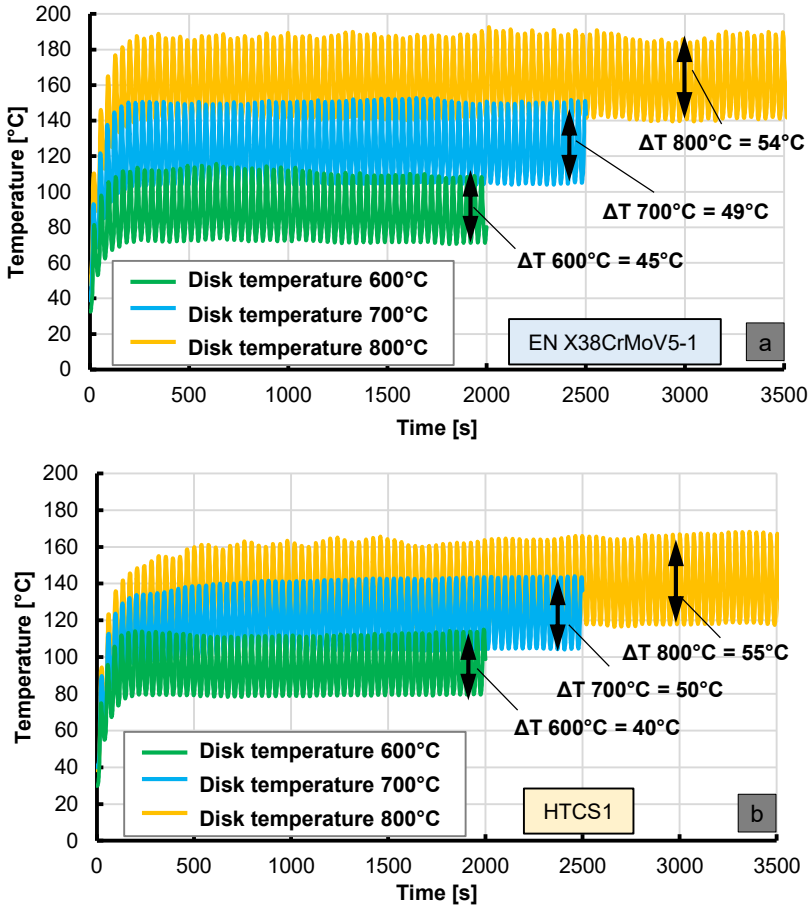

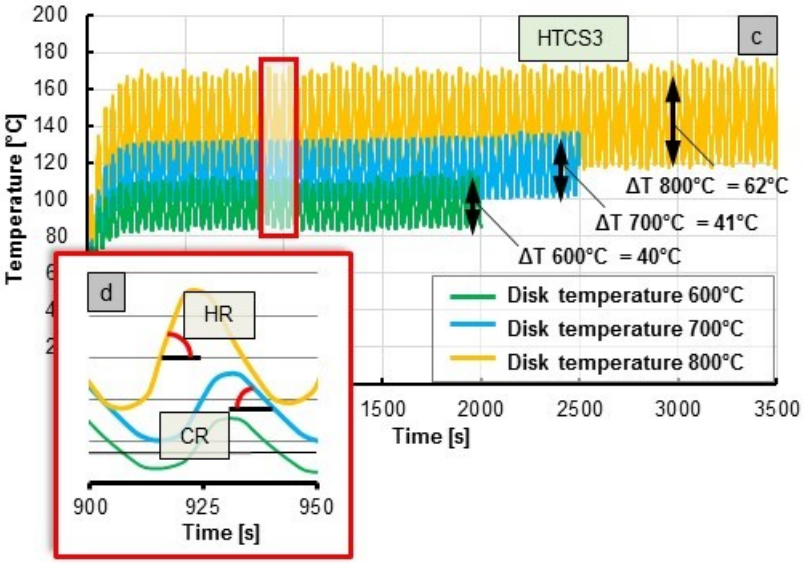


Fig. 5.23 Temperature evolution measured by the thermocouple embedded in the pin with a furnace temperature of 600 °C, 700 °C and 800 °C in the case of a) EN X38CrMoV5-1, b) HTCS1 and c) HTCS3 grade (*The temperature is recorded for the duration of 100 cycles per track, also at 600 and 700 °C; the profiles 600 and 700 °C are interrupted to make the image clearer).

The zoom area, Fig. 5.23d, indicates a detail concerning the heating and cooling rate (HR and CR); results showed that the Heating Rate (HR) - since all parameters tested are maintained constant in terms of normal pressure, sheet temperature, sliding velocity, stroke, heating, cooling and sliding timeframes - mainly depends on the material and varies from a value of 3.4 °C/s for the steel EN X38CrMoV5-1 at the test temperature of 800 ° C up to 3.9 °C/s in the case of steel HTCS3 at the same test temperature (greater than 13%). By contrast, regarding the Cooling Rate, which, also in this case, depends only on the type of steel as the parameters used for the test are the same, it undergoes variations from a value of 2.5 °C/s in the case of the EN X38CrMoV5-1 up to a value of 3.0 °C/s for the steel HTCS3 at the test temperature of 800 °C (increased by nearly 17%). This was mainly due to the greater thermal conductivity values of the HTCSs, which permitted a higher thermal exchange both inside the heating chamber, when pin slid on hot metal sheet, and outside, when pin was cooled down with the air nozzle.

The behaviour of HTCSs, which maintained a lower operating temperature, present a greater Heating/Cooling Rate and a higher heat exchange than the more commonly used EN X38CrMoV5-1 steel, can be explained due to greater fraction of non-metallic inclusions and precipitated primary carbides, together additional alloying elements such as cobalt, tungsten resulted in a higher thermal conductivity steel. These elements have high melting temperature, which formed carbide network in the alloy. The interfacial carbide in alloys increased the heat transmission in it, being interfacial layer an important factor for improving the thermal conductivity [108]–[111].

## 5.2. Conclusions

This paragraph summarizes the main results regarding the friction, wear and thermal evaluation of three die steel grades into contact with sheets in HSS, Al-Si coated, in hot stamping conditions. These targets were achieved by using an approach which replicates thermo-mechanical stress comparable with the hot stamping process.

The frictional behaviour has been studied as function of the main critical process parameters namely normal pressure, sliding speed and sheet metal temperature, using the Hot Friction Test reported in Section 4.2.b. It was found that at constant testing temperatures, the tribological systems analysed, present a similar coefficient of friction, with greater stability with increasing temperature. Moreover, a reduction in friction was observed by increasing the test temperature, due to the decrease of the coating shear strength and the relative lubrication mechanism that is established.

The wear behaviour in hot stamping conditions was carried out by the Hot Wear Test described in Section 4.2.c, while the wear analysis of the tool steels at varying number of cycles was evaluated by means of measurement of: (i) the weight variation, (ii) SEM-EDX analysis of the sliding track and pin surface to understand the material transferred from the metal sheet to the pin or vice-versa and optical observations together with (iii) roughness measurements of the pins sliding surface through the 3D optical profilometer. For all the testing condition, the wear track was investigated in order to assess the limit stroke after which the coating layers start to be removed from the pin track on the disk, in order to replicate the real production process to each wear cycle. Using the variations in terms of pin weight, a combination of abrasion and adhesion phenomena was observed albeit with different influence. The temperature appears having the major influence on the phenomena for all the steel grades tested: at the greatest testing temperature of 800 °C, a weight loss was highlighted after 2000 cycles, while the lowest temperatures are interested mainly by adhesion. The change of wear mechanism from adhesion to abrasion can be explained with the fall of surface hardness that the steel grades present as the temperature increases. Furthermore, the increase in temperature facilitates the formation of oxide layers at the sliding interface sheet-pin, which preserve the pin from the adhesion of the Al-Si coating but rather facilitate abrasion phenomenon. The SEM-EDX analysis, carried on the pin surfaces, confirm the indications of the weight measurements, with large Al-Si coating transfer from the metal sheet to the pin surface at the lower temperatures, while abrasion takes place prevalently at 800 °C. The measurements of the pins roughness by using 3D profilometer reflect the evolution of the wear mechanisms described by weight and SEM analysis; at the temperature of 800 °C lower roughness values are detected for all the grades, where the abrasive wear is predominant and the surface appears more uniform smoother. Vice versa, the surface roughness values increase by decreasing the temperature of the test, as the strong adhesion on pin generates an indented surface. The assessment of the mechanical testing conditions was performed by verifying the reproducibility of the friction characteristics between the metal sheet and the pin during testing; along the 2000 cycles, the friction coefficients recorded were comparable with those extrapolated during the HFTs. Moreover, the SEM-EDX analysis did not show elements of the original boron steel transferred to the pin for all the tested condition.

During the HWTs, by means of a thermocouple embedded inside the pins, the main thermal parameters in terms of the minimum, the average and the maximum temperatures, the Heating and the Cooling rates were monitored. The recorded temperature profiles have demonstrated the reproducibility of the thermal cycle imposed on the pin during testing and its closeness to the one the forming dies are subjected to. Compared with the commonly used EN X38CrMoV5-1, HTCSs presented a higher thermal exchange both during the heating phase, when pin slid against hot metal sheet, and outside, during the cooling phase by means of the air nozzle. This behaviour is evidenced because the HTCSs have shown, compared to EN X38CrMoV5-1, (i) a lower working temperatures with increasing of testing temperature, (ii) greater Heating/Cooling Rate and (iii) a higher heat dissipation. This was mainly due to the greater thermal conductivity values of the HTCSs, which permitted a higher thermal exchange. Moreover, comparing the two HTCSs, the results show that the internal structure of the material characterizes the heat exchange; HTCS1, characterized finer elements of Mo homogeneously distributed in the metal matrix, presented a better heat dissipation at 700 °C than HTCS3 with small agglomerates of Mo; vice versa, at 800 °C, small agglomerates of HTCS3 presented a better performance.

# Chapter 6

# **Conclusions**

The aim of this study is to gain new knowledge that will be useful from the viewpoints of tribology of hot metal forming of HSS sheets and to improve the process efficiency or to reach an improved performance.

Starting from this point of view, the tribological behaviour of High Thermal Conductivity Steel grades for hot stamping tools has been investigated and compared with a commonly used tool steel. In particular, steel grades with different aggregations of Molybdenum in the metal matrix were compared and the effects on friction, wear damage and heat exchange were analysed. The approach followed in the research is based on physical-simulation techniques to reproduce cyclic thermo-mechanical loads that are typical of the industrial conditions. A novel High Temperature Tribological testing procedure, as well as an experimental apparatus, were used to investigate the tribological conditions of the dies material reproducing the thermo-mechanical cyclic loads in the temperature range from 600 °C up to 800 °C and pressures in the range of few tens of MPa.

It was found that both the grades present an almost similar friction coefficient with high stability in the investigated process window. The higher the temperature, the lower the friction coefficients that were measured in the tests according to the Coulomb model; if the temperature is increased, the coating shear strength decreases, by sliding the pin on a more easily deformable surface.

In terms of wear damage, all the grades are interested by a combination of adhesion and abrasion phenomena, with the latter that becomes more relevant at the highest test temperature. At the greatest testing temperature, the formation of an oxide layer may cause a stable separation between workpiece and tool surface providing satisfactory lowering of friction and avoiding material pick-up. At the lowest test temperature HTCS1 grade appears more heavily interested by adhesion, while at the temperature of 800 °C all the grades are mainly interested by abrasion, whereas the formation of oxide particles acting as wear debris can provoke the occurrence of abrasive wear.

Concerning the thermal parameters analysis, the HTCSs have presented the characteristics expected as steels with a High Thermal Conductivity; compared with the common EN X38CrMoV5-1 die steel grade, increasing the testing temperature, HTCSs have a lower average working temperature, with a decrease up to 15% in the case of HTCS1 at 800 °C. Moreover, by analysing the maximum and minimum temperatures of the steels ($\Delta T$), during the Hot Wear Tests, results showed that the HTCS3 allows higher heat dissipation: at the greatest testing temperature of 800 °C the heat exchanged is higher, while at the lower furnace temperature of 700 °C the HTCS1 grade offers better performances in terms of heat dissipation. At the lowest testing temperature of 600 °C, EN X38CrMoV5-1 offers the greatest heat exchange, synonym that the High Thermal Conductivity of HTCSs, has a greater effect at high test temperatures. Such behaviour has been verified by analysing gradients of the temperature profiles, in both the heating phase, inside the furnace, and in the cooling phase thanks to the air nozzle; at the highest test temperature of 800 °C, HTCS3 steel grade presents a greater CR and HR while, at 700 °C, HTCS1 offers the best performance in terms of heat exchange rate. Even in this case, as for discussions made about the results concerning to $\Delta T$, at 600 °C, EN X38CrMoV5-1 steel offers the highest Heating and Cooling rate.

Concerning the approach and methodology used in the research work, it is possible to state that:

- the friction values recorded in the tests are in agreement with similar works presented by other Authors;
- the stability of thermal and mechanical cycles during the Hot Wear Tests has proved the suitability of the testing set up used in the investigation,
- the combination of weight analysis, SEM-EDS microscopy and 3D topographic investigations are essential to understand the combination of mechanisms at the interface between the dies and the metal sheet.

# A.1. Hot Friction Test diagrams

- **EN X38CrMoV5-1 grade steel**

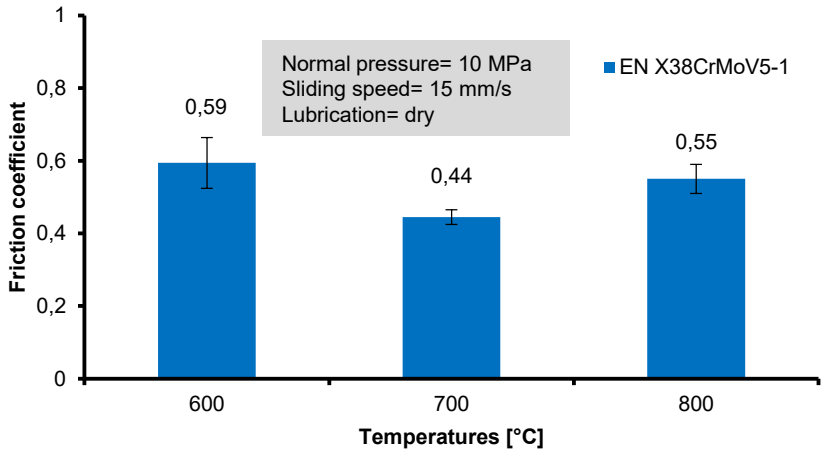


Fig. A.1. 1 Average of the coefficient of friction calculated during the 2000 cycles for EN X38CrMoV5-1 steel grade.

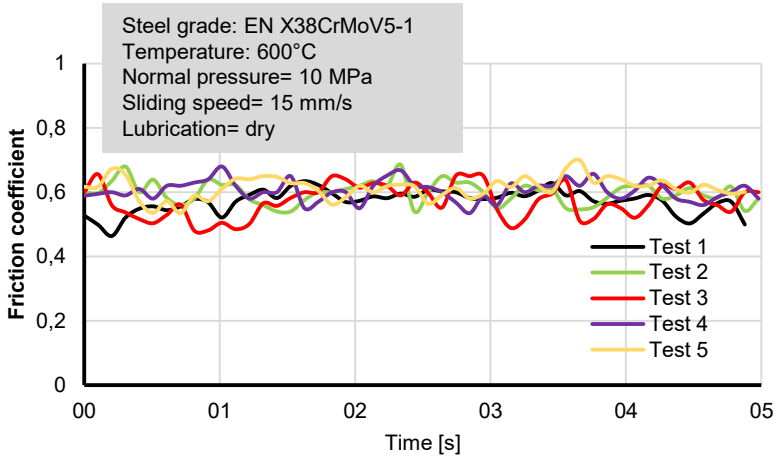


Fig. A.1. 2 Friction coefficient curves registered in the case of EN X38CrMoV5-1 at 600°C.

.

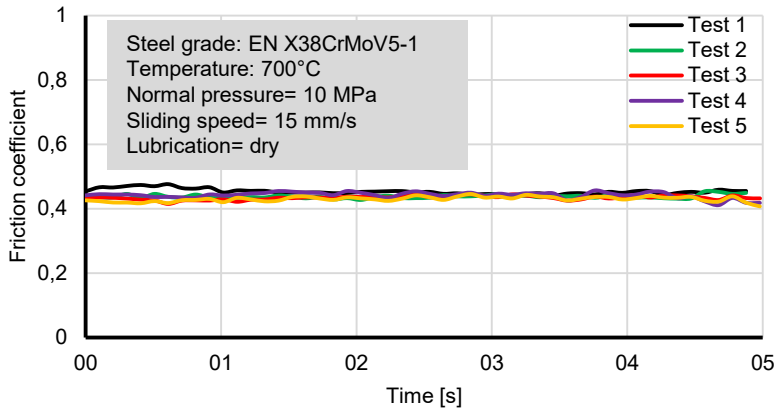


Fig. A.1. 3 Friction coefficient curves registered in the case of EN X38CrMoV5-1 at 700°C

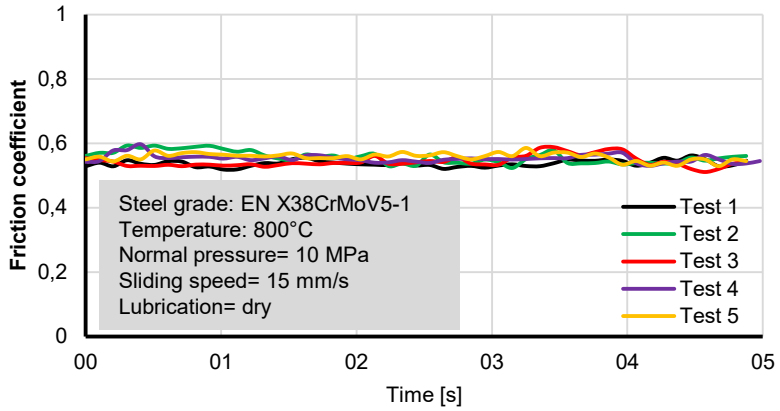


Fig. A.1. 4 Friction coefficient curves registered in the case of EN X38CrMoV5-1 at 800

- **HTCS1 grade steel**

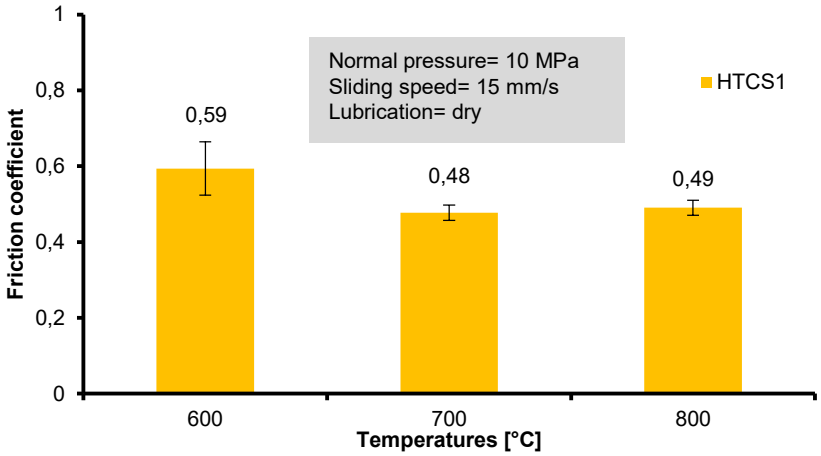


Fig. A.1. 5 Average of the coefficient of friction calculated during the 2000 cycles for HTCS1 steel grade.

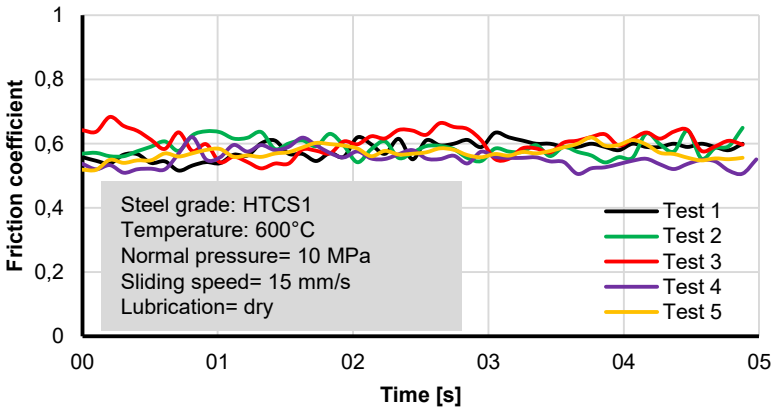


Fig. A.1. 6 Friction coefficient curves registered in the case of HTCS1 at 600°C

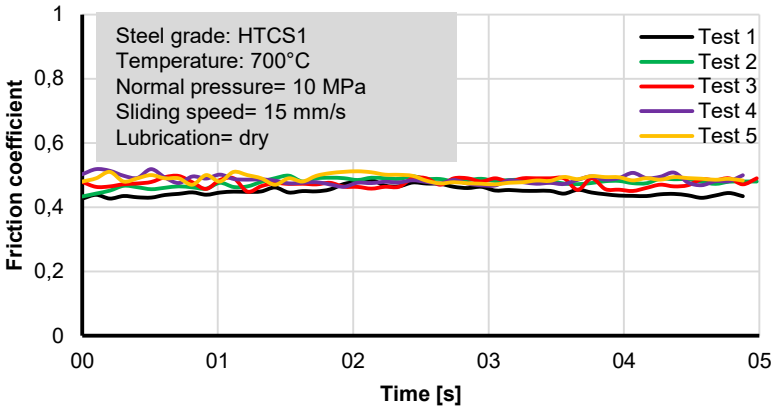


Fig. A.1. 7 Friction coefficient curves registered in the case of HTCS1 at 700°C.

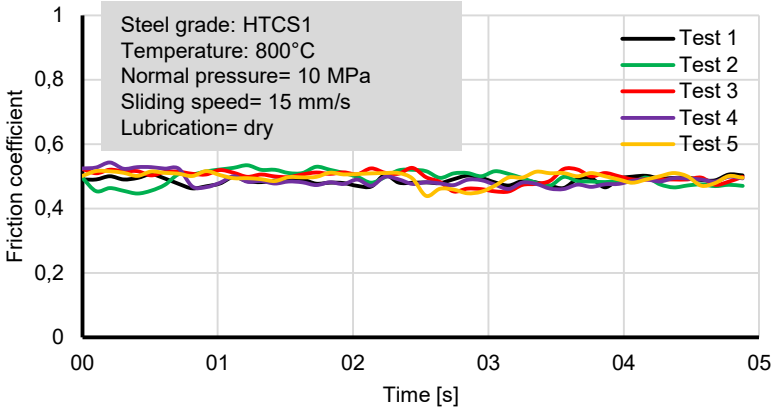


Fig. A.1. 8 Friction coefficient curves registered in the case of HTCS1 at 800°C

- **HTCS3 steel grade**

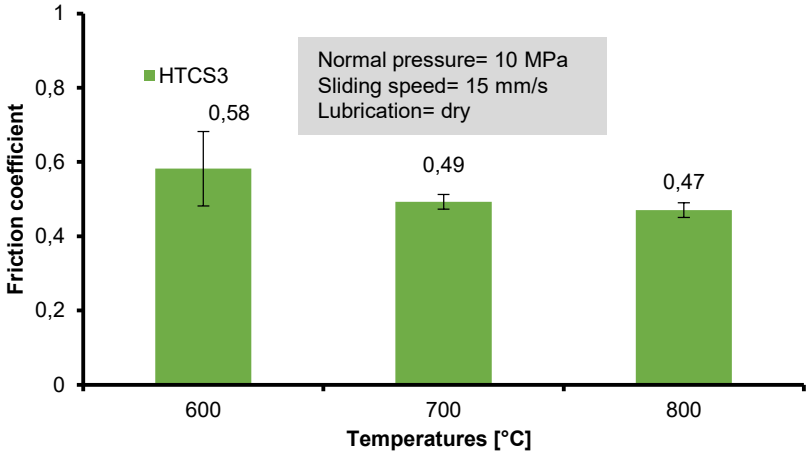


Fig. A.1. 9 Average of the coefficient of friction calculated during the 2000 cycles for HTCS3 steel grade.

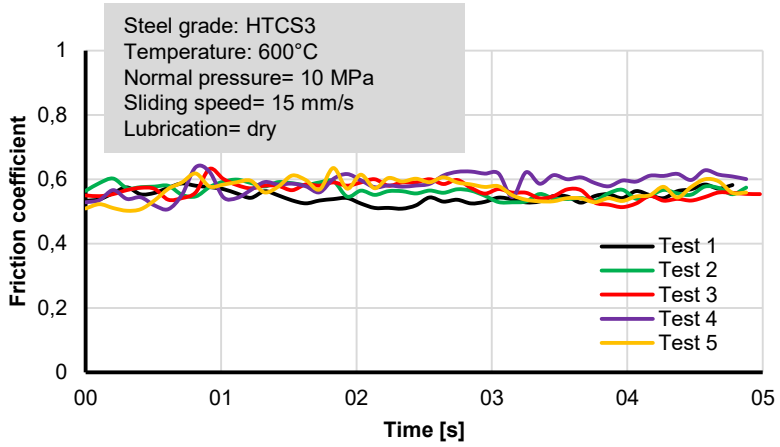


Fig. A.1. 10 Friction coefficient curves registered in the case of HTCS3 at 600°C.

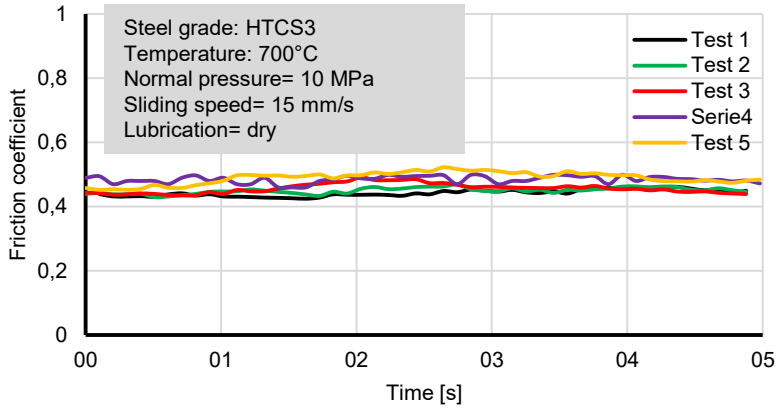


Fig. A.1. 11 Friction coefficient curves registered in the case of HTCS3 at 700°C.

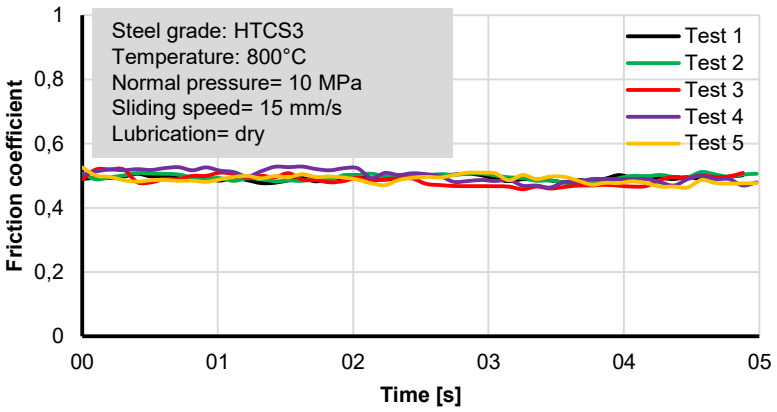


Fig. A.1. 12 Friction coefficient curves registered in the case of HTCS3 at 800°C.

# A.2. Monitoring the friction coefficient during the Hot Wear Test

- **EN X38CrMoV5-1 grade steel**

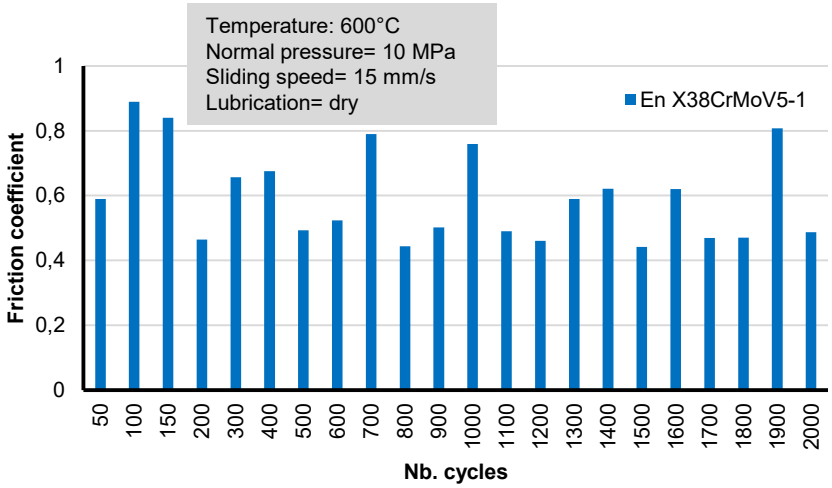


Fig. A.2. 1 Average of the coefficient of friction calculated for each stop test to change the sliding track, during the 2000 cycles for EN X38CrMoV5-1 steel grade at 600°C.

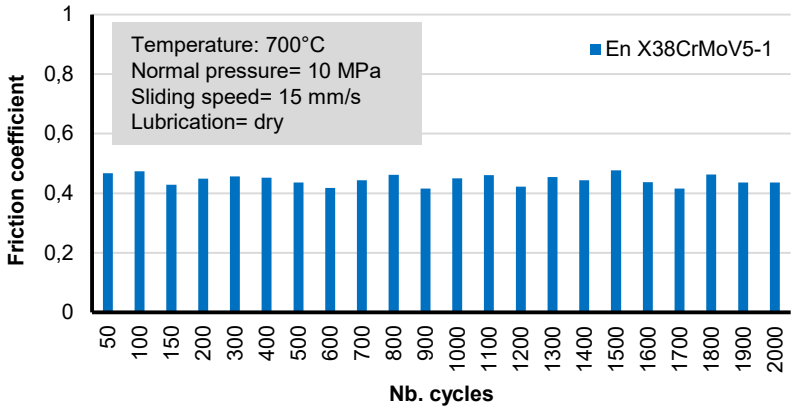


Fig. A.2. 2 Average of the coefficient of friction calculated for each stop test to change the sliding track, during the 2000 cycles for EN X38CrMoV5-1 steel grade at 700°C.

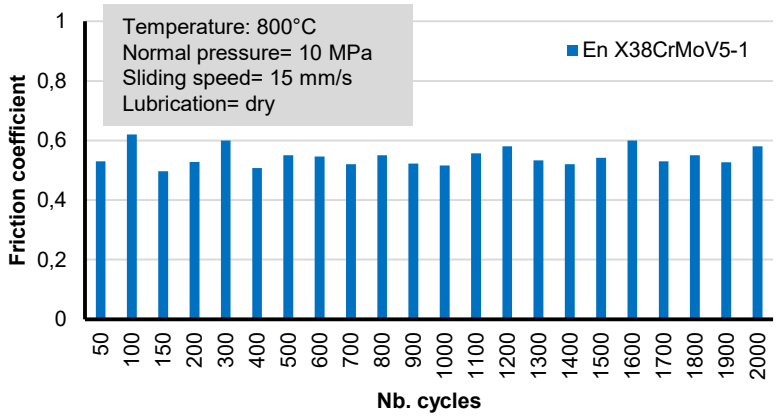


Fig. A.2. 3 Average of the coefficient of friction calculated for each stop test to change the sliding track, during the 2000 cycles for EN X38CrMoV5-1 steel grade at 800°C.

- **HTCS1 grade steel**

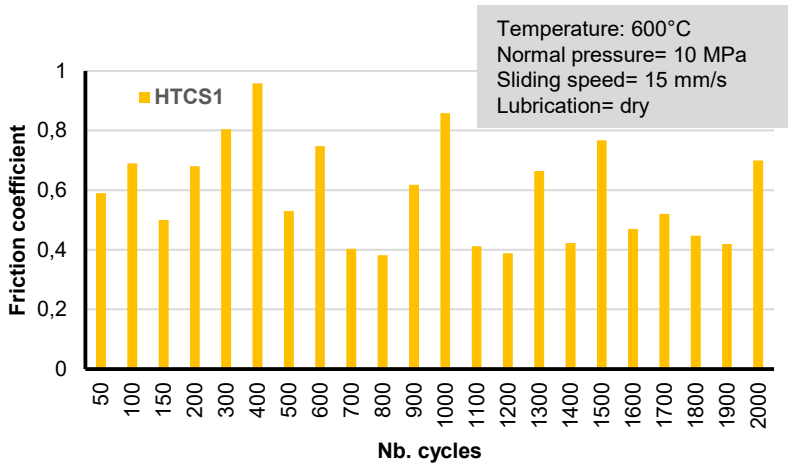


Fig. A.2. 4 Average of the coefficient of friction calculated for each stop test to change the sliding track, during the 2000 cycles for HTCS1 steel grade at 600°C.

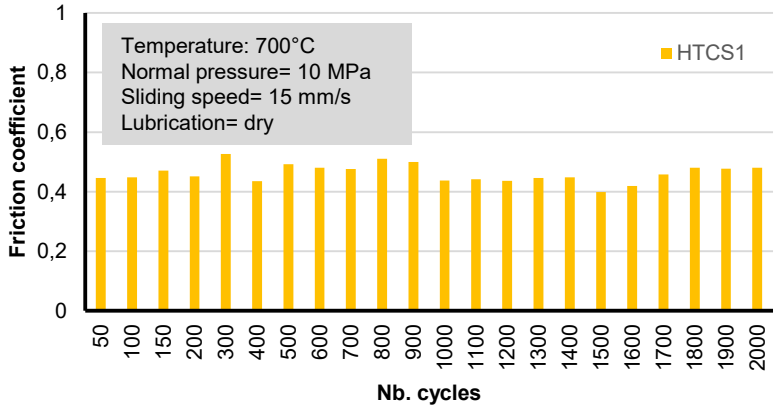


Fig. A.2. 5 Average of the coefficient of friction calculated for each stop test to change the sliding track, during the 2000 cycles for HTCS1 steel grade at 700°C.

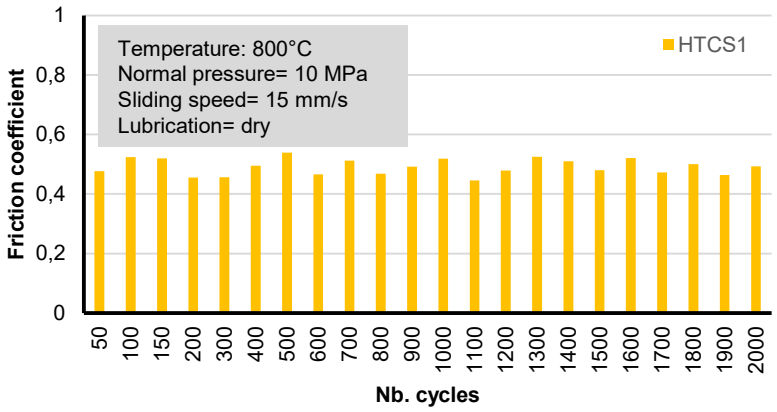


Fig. A.2. 6 Average of the coefficient of friction calculated for each stop test to change the sliding track, during the 2000 cycles for HTCS1 steel grade at 800°C.

- **HTCS3 steel grade**

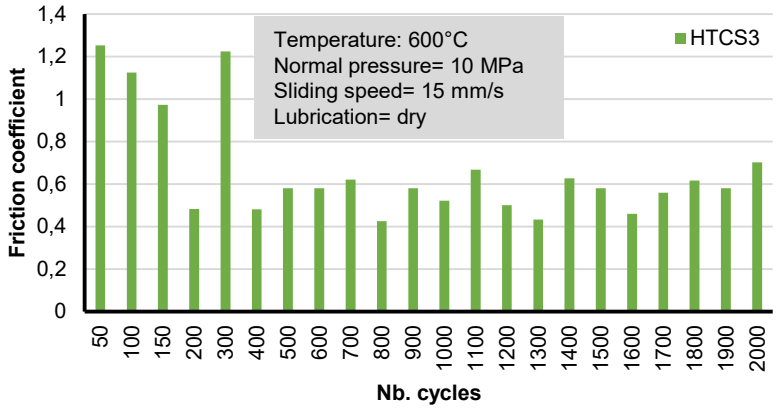


Fig. A.2. 7 Average of the coefficient of friction calculated for each stop test to change the sliding track, during the 2000 cycles for HTCS3 steel grade at 600°C.

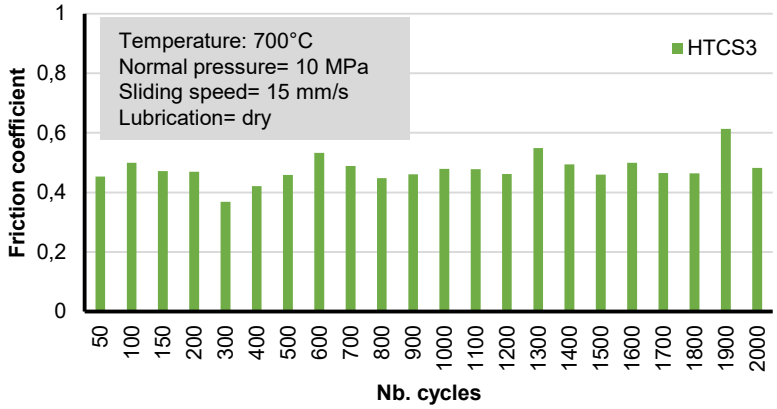


Fig. A.2. 8 Average of the coefficient of friction calculated for each stop test to change the sliding track, during the 2000 cycles for HTCS3 steel grade at 700°C.

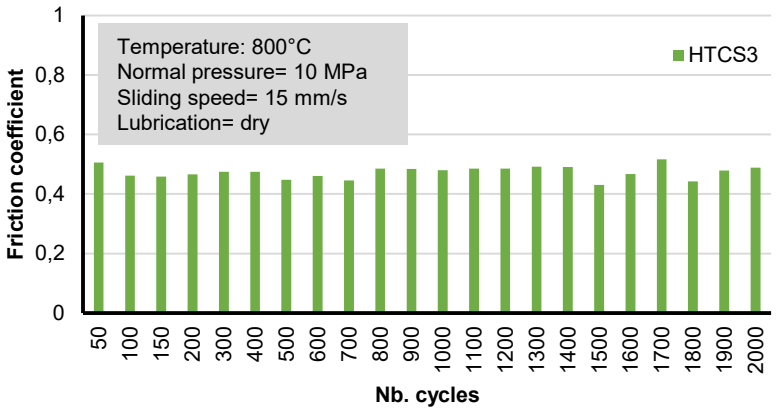


Fig. A.2. 9 Average of the coefficient of friction calculated for each stop test to change the sliding track, during the 2000 cycles for HTCS3 steel grade at 800°C.

# List of figures

# List of tables

# References


[1] A. T. Beyene, E. G. Koricho, G. Belingardi, and B. Martorana, "Design and manufacturing issues in the development of lightweight solution for a vehicle frontal bumper," *Procedia Eng.*, vol. 88, pp. 77–84, 2014.

[2] G. Belingardi, A. T. Beyene, E. G. Koricho, and B. Martorana, "Alternative lightweight materials and component manufacturing technologies for vehicle frontal bumper beam," *Compos. Struct.*, vol. 120, pp. 483–495, 2015.

[3] C. Wang, Y. Zhang, X. Tian, B. Zhu, and J. Li, "Thermal contact conductance estimation and experimental validation in hot stamping process," *Sci. China Technol. Sci.*, vol. 55, no. 7, pp. 1852–1857, 2012.

[4] P. Hu, B. He, and L. Ying, "Numerical investigation on cooling performance of hot stamping tool with various channel designs," *Appl. Therm. Eng.*, vol. 96, pp. 338–351, 2016.

[5] S. Wang and P. Lee, "Investigation of Die Quench Properties of Hot Stamping," vol. 2, no. 26, pp. 22–31, 2013.

[6] M. Takahashi, "Development of high strength steels for automobiles," *Nippon Steel Tech. Rep. No. 88*, no. 88, pp. 2–6, 2003.

[7] K. ichiro Mori, "Smart hot stamping for ultra-high strength steel parts," *60 Excell. Invent. Met. Form.*, vol. 22, no. October, pp. 403–408, 2015.

[8] F. Bruschi, "Comprehensive Materials Processing Hot Stamping," *Compr. Mater. Process.*, vol. 3, pp. 27–54, 2014.

[9] C. Löbbe, O. Hering, L. Hiegemann, and A. E. Tekkaya, "Setting Mechanical Properties of High Strength Steels for Rapid Hot Forming Processes," *Materials (Basel).*, 2016.

[10] T. Altan, "Hot-stamping boron-alloyed steels for automotive parts Part II : Microstructure , material strength changes during hot stamping," *Microstruct. Mater. strength Chang. Dur. hot Stamp.*, 2007.

[11] T. Stöhr, J. Lechler, and M. Merklein, "Investigations on different strategies for influencing the microstructural properties with respect to partial hot stamping," in *2nd International Conference on Hot Sheet Metal Forming of High- Performance Steel*, 2009, vol. 1, pp. 273–281.

[12] R. Autengruber, G. Luckeneder, and A. W. Hassel, "Corrosion of press-hardened galvanized steel," *Corros. Sci.*, vol. 63, pp. 12–19, 2012.

[13] X. Han, Y. Zhong, K. Yang, Z. Cui, and J. Chen, "Application of hot stamping process by integrating quenching & partitioning heat treatment to improve mechanical properties," *Procedia Eng.*, vol. 81, no. October, pp. 1737–1743, 2014.

[14] a. E. Tekkaya, H. Karbasian, W. Homberg, and M. Kleiner, "Thermo-mechanical coupled simulation of hot stamping components for process design," *Prod. Eng.*, vol. 1, pp. 85–89, 2007.

[15] M. Merklein, J. Lechler, and M. Geiger, "Characterisation of the flow properties of the quenchenable ultra high strength steel 22MnB5," *CIRP Ann. - Manuf. Technol.*, vol. 55, no. 1, pp. 229–232, 2006.

[16] M. Merklein and J. Lechler, "Investigation of the thermo-mechanical properties of hot stamping steels," *J. Mater. Process. Technol.*, vol. 177, no. 1–3, pp. 452–455, 2006.

[17] H. Steinbeiss, H. So, T. Michelitsch, and H. Hoffmann, "Method for optimizing the cooling design of hot stamping tools," *Prod. Eng.*, vol. 1, no. 2, pp. 149–155, 2007.

[18] G. Zhong-Xiang, W. Kai, Z. Yi-Sheng, and Z. Bin, "Cracking and interfacial debonding

of the Al-Si coating in hot stamping of pre-coated boron steel," *Appl. Surf. Sci.*, vol. 316, no. 1, pp. 595–603, 2014.

[19] M. Naderi, L. Durrenberger, A. Molinari, and W. Bleck, "Constitutive relationships for 22MnB5 boron steel deformed isothermally at high temperatures," *Mater. Sci. Eng. A*, vol. 478, no. 1–2, pp. 130–139, 2008.

[20] Y. Dahan, Y. Chastel, P. Duroux, P. Hein, E. Massoni, and J. Wilsius, "Formability investigations for the hot stamping process," *Iddrg 2006*, p. 8, 2006.

[21] S. Zhong-de, Z. Mi-lan, J. Chao, X. Ying, and R. Wea-juan, "Basic study on die cooling system of hot stamping proces," in *Advanced Design Technology*, 2010, vol. Section 1, pp. 1–4.

[22] M. Merklein, M. Wieland, M. Lechner, S. Bruschi, and A. Ghiotti, "Hot stamping of boron steel sheets with tailored properties: A review," *J. Mater. Process. Technol.*, vol. 228, pp. 11–24, 2016.

[23] P. F. Bariani, S. Bruschi, A. Ghiotti, and F. Michieletto, "Hot stamping of AA5083 aluminium alloy sheets," *CIRP Ann. - Manuf. Technol.*, vol. 62, no. 1, pp. 251–254, 2013.

[24] P. Hu, L. Ying, Y. Li, and Z. Liao, "Effect of oxide scale on temperature-dependent interfacial heat transfer in hot stamping process," *J. Mater. Process. Technol.*, vol. 213, no. 9, pp. 1475–1483, 2013.

[25] Z. X. Gui, W. K. Liang, and Y. S. Zhang, "Formability of aluminum-silicon coated boron steel in hot stamping process," *Trans. Nonferrous Met. Soc. China (English Ed.*, vol. 24, no. 6, pp. 1750–1757, 2014.

[26] M. Suehiro, K. Kusumi, T. Miyakoshi, J. Maki, and M. Ohgami, "Properties of aluminum-coated steels for hot-forming," *Nippon Steel Tech. Rep.*, no. 88, pp. 16–21, 2003.

[27] J. Kondratiuk, P. Kuhn, E. Labrenz, and C. Bischoff, "Zinc coatings for hot sheet metal forming: Comparison of phase evolution and microstructure during heat treatment," *Surf. Coatings Technol.*, vol. 205, no. 17–18, pp. 4141–4153, 2011.

[28] R. Veit, H. Hofmann, R. Kolleck, P. Brugger, I. Thomas, and S. Sikora, "Phase Formation of Al / Si-Coatings during Induction Heating of Boron Alloyed Steel Sheets."

[29] H. Fukuchi, "Automotive Solution ( 1 ): Development of Hot Stamping of Improved Productivity," no. 112, pp. 71–73, 2016.

[30] A. Bardelcik, M. J. Worswick, S. Winkler, and M. A. Wells, "A strain rate sensitive constitutive model for quenched boron steel with tailored properties," *Int. J. Impact Eng.*, vol. 50, pp. 49–62, 2012.

[31] R. George, "Hot Forming of Boron Steels with Tailored Mechanical Properties Experiments and Numerical Simulations," 2011.

[32] P. Hein and J. Wilsius, "Status and Innovation Trends in Hot Stamping of USIBOR 1500 P," *Steel Res. Int.*, vol. 2, pp. 85–91, 2008.

[33] T. Stöhr, J. Lechler, and M. Merklein, "Investigations on different strategies for influencing the microstructural properties with respect to partial hot stamping," in *2nd International Conference on Hot Sheet Metal Forming of High- Performance Steel*, 2009, pp. 273–281.

[34] T. Labudde and W. Bleck, "Formability characterization of press hardened steels," *Proc. Hot Sheet Met. Form. High Perform. Steel*, pp. 127–135, 2009.

[35] A. Bardelcik, "High Strain Rate Behaviour of Hot Formed Boron Steel with Tailored Properties by," 2010.

[36] T. Maeno, K. Mori, and T. Nagai, "CIRP Annals - Manufacturing Technology Improvements in productivity and formability by water and die quenching in hot stamping of ultra-high strength steel parts," vol. 2, pp. 5–8, 2014.

[37] R. Kolleck and R. Veit, "Current and Future Trends in the field of Hot Stamping of Car Body Parts."
[38] B. Bharat, *Introduction to Tribology P-328*. 2013.
[39] "www2.warwick.ac.uk." [Online]. Available: http://www2.warwick.ac.uk/services/ris/impactinnovation/impact/analyticalguide/tribology/.
[40] "faculty2.ucmerced.edu." [Online]. Available: http://faculty2.ucmerced.edu/amartini/tribology.shtml.
[41] P. J. Blau, *Friction, Lubrication and Wear Technology*, vol. 18. 1992.
[42] "Tribology_Applications @ www.stle.org." [Online]. Available: http://www.stle.org/files/What_is_tribology/Tribology_Applications.aspx.
[43] F. P. Bowden and D. Tabor, *The Friction and Lubrication of Solids, Volume 1*. New York: Oxford Univ., 2001.
[44] S. Kalpakjian and S. R. Schmid, "Manufacturing Engineering & Technology," 2013, p. Seventh edition.
[45] K. G. Budinski, *Guide to Friction, Wear, and Erosion Testing*. 2007.
[46] G. Strafellini, *Attrito e usura*, Tecniche n. Milano, 2005.
[47] G. X. Chen and Z. R. Zhou, "Study on transition between fretting and reciprocating sliding wear," *Wear*, vol. 250–251, no. PART 1, pp. 665–672, 2001.
[48] O. Vingsbo, "On fretting maps," *Wear*, pp. 131–147, 1998.
[49] M. O. Alam and A. S. M. A. Haseeb, "Response of Ti-6Al-4V and Ti-24Al-11Nb alloys to dry sliding wear against hardened steel," *Tribol. Int.*, vol. 35, no. 6, pp. 357–362, 2002.
[50] M. A. Schmidt and R. D. Compton, *ASM Handbook, Volume 18, Friction, Lubrication, and Wear Technology*, vol. 18. 1992.
[51] R. Haar, *Friction in sheet metal forming, the influence of (local) contact conditions and deformation*. 1996.
[52] B. Bharat, *Modern Tribology Handbook*. .
[53] K. Holmberg, "Coatings Tribology," *Igarss 2014*, vol. 28, no. 1, pp. 1–5, 2014.
[54] B. Abdulhay, B. Bourouga, and C. Dessain, "Experimental and theoretical study of thermal aspects of the hot stamping process," *Appl. Therm. Eng.*, vol. 31, no. 5, pp. 674–685, 2011.
[55] M. Merklein, J. Lechler, and T. Stoehr, "Characterization of tribological and thermal properties of metallic coatings for hot stamping boron manganese steels," … *Conf. Coatings* …, no. October, pp. 1–3, 2008.
[56] W. Liu, H. S. Liu, Z. W. Xing, G. Liu, and J. Bao, "Effect of tool temperature and punch speed on hot stamping of ultra high strength steel," *Trans. Nonferrous Met. Soc. China (English Ed.*, vol. 22, no. SUPPL.2, pp. 534–541, 2012.
[57] Y. Chang, X. Tang, K. Zhao, P. Hu, and Y. Wu, "Investigation of the factors influencing the interfacial heat transfer coefficient in hot stamping," *J. Mater. Process. Technol.*, vol. 228, pp. 25–33, 2016.
[58] C. Fuh-Kuo, H. Tzu-Hao, T. Pei-Wu, L. Cheng-Kuo, H. Tying-Bin, and L. Ping-Kun, "Characterization of the interface heat transfer properties in the hot stamping process," *Proc. Hot Sheet Met. High-Performance Steel*, pp. 559–567, 2015.
[59] T.-H. Hung, P.-W. Tsai, F.-K. Chen, T.-B. Huang, and W.-L. Liu, "Measurement of Heat Transfer Coefficient of Boron Steel in Hot Stamping," *Procedia Eng.*, vol. 81, no. October, pp. 1750–1755, 2014.
[60] H. Hoffmann, H. So, and H. Steinbeiss, "Design of hot stamping tools with cooling system," *CIRP Ann. - Manuf. Technol.*, vol. 56, no. 1, pp. 269–272, 2007.
[61] F. Schieck, C. Hochmuth, S. Polster, and A. Mosel, "Modern tool design for component grading incorporating simulation models, efficient tool cooling concepts and tool

coating systems," *CIRP J. Manuf. Sci. Technol.*, vol. 4, no. 2, pp. 189–199, 2011.
[62] A. Yanagida, T. Kurihara, and A. Azushima, "Development of tribo-simulator for hot stamping," *J. Mater. Process. Technol.*, vol. 210, no. 3, pp. 456–460, 2010.
[63] A. Yanagida and A. Azushima, "Evaluation of coefficients of friction in hot stamping by hot flat drawing test," *CIRP Ann. - Manuf. Technol.*, vol. 58, no. 1, pp. 247–250, 2009.
[64] A. Azushima, K. Uda, and A. Yanagida, "Friction behaviour of aluminum-coated 22MnB5 in hot stamping under dry and lubricated conditions," *J. Mater. Process. Technol.*, vol. 212, no. 5, pp. 1014–1021, 2012.
[65] A. Ghiotti, S. Bruschi, F. Sgarabotto, and F. Medea, *Novel wear testing apparatus to investigate the reciprocating sliding wear in sheet metal forming at elevated temperatures*, vol. 622–623. 2014.
[66] J. Ã. Hardell and B. Prakash, "High-temperature friction and wear behaviour of different tool steels during sliding against Al – Si-coated high-strength steel," *Tribol. Int.*, vol. 41, no. 7, pp. 663–671, 2008.
[67] J. Hardell, E. Kassfeldt, and B. Prakash, "Friction and wear behaviour of high strength boron steel at elevated temperatures of up to 800 °C," *Wear*, vol. 264, no. 9–10, pp. 788–799, 2008.
[68] M. Geiger, M. Merklein, and J. Lechler, "Determination of tribological conditions within hot stamping," *Prod. Eng.*, vol. 2, no. 3, pp. 269–276, 2008.
[69] L. Pelcastre, J. Hardell, C. Courbon, and B. Prakash, "Tribological behaviour of Al-Si-coated ultra-high-strength steel during interaction with tool steel at elevated temperatures: Influence of tool steel surface topography parameters on galling," *Proc. Inst. Mech. Eng. Part B J. Eng. Manuf.*, vol. 229, no. 8, pp. 1373–1384, 2015.
[70] L. Pelcastre, J. Hardell, and B. Prakash, "Investigations into the occurrence of galling during hot forming of Al-Si-coated high-strength steel," *Proc. Inst. Mech. Eng. Part J J. Eng. Tribol.*, vol. 225, no. 6, pp. 487–498, 2011.
[71] X. Tian, Y. Zhang, and J. Li, "Investigation on tribological behaviour of advanced high strength steels: Influence of hot stamping process parameters," *Tribol. Lett.*, vol. 45, no. 3, pp. 489–495, 2012.
[72] J. Kondratiuk and P. Kuhn, "Tribological investigation on friction and wear behaviour of coatings for hot sheet metal forming," *Wear*, vol. 270, no. 11–12, pp. 839–849, 2011.
[73] C. Boher, S. Le Roux, L. Penazzi, and C. Dessain, "Experimental investigation of the tribological behaviour and wear mechanisms of tool steel grades in hot stamping of a high-strength boron steel," *Wear*, vol. 294–295, pp. 286–295, 2012.
[74] S. Le Roux, C. Boher, L. Penazzi, C. Dessain, and B. Tavernier, "A methodology and new criteria to quantify the adhesive and abrasive wear damage on a die radius using white light profilometry," *Tribol. Int.*, vol. 52, pp. 40–49, 2012.
[75] A. Ghiotti, S. Bruschi, and F. Borsetto, "Tribological characteristics of high strength steel sheets under hot stamping conditions," *J. Mater. Process. Technol.*, vol. 211, no. 11, pp. 1694–1700, 2011.
[76] J. Hardell, H. Le Quang, and B. Prakash, "Tribological Performance of Surface Coated Tool Steel At Elevated Temperatures," pp. 1–19.
[77] M. Vilaseca, J. Pujante, G. Ramírez, and D. Casellas, "Investigation into adhesive wear of PVD coated and uncoated hot stamping production tools," *Wear*, vol. 308, no. 1–2, pp. 148–154, 2013.
[78] A. Ghiotti, F. Sgarabotto, and S. Bruschi, "A novel approach to wear testing in hot stamping of high strength boron steel sheets," *Wear*, vol. 302, no. 1–2, pp. 1319–1326, 2013.
[79] A. Ghiotti, S. Bruschi, F. Sgarabotto, and P. F. Bariani, "Tribological performances of Zn-based coating in direct hot stamping," *Tribol. Int.*, vol. 78, pp. 142–151, 2014.
[80] L. Pelcastre, J. Hardell, and B. Prakash, "Galling mechanisms during interaction of tool

steel and Al-Si coated ultra-high strength steel at elevated temperature," *Tribol. Int.*, vol. 67, pp. 263–271, 2013.

[81] L. Pelcastre, J. Hardell, N. Herrera, and B. Prakash, "Investigations into the damage mechanisms of form fixture hardening tools," *Eng. Fail. Anal.*, vol. 25, pp. 219–226, 2012.

[82] A. Tomala, S. Hernandez, M. Rodriguez Ripoll, E. Badisch, and B. Prakash, "Tribological performance of some solid lubricants for hot forming through laboratory simulative tests," *Tribol. Int.*, vol. 74, pp. 164–173, 2014.

[83] L. Pelcastre, J. Hardell, A. Rolland, and B. Prakash, "Influence of microstructural evolution of Al-Si coated UHSS on its tribological behaviour against tool steel at elevated temperatures," *J. Mater. Process. Technol.*, vol. 228, pp. 117–124, 2016.

[84] M. Merklein and M. Wieland, "Investigations on austenitization parameters influencing wear behaviour within hot stamping," *Procedia Eng.*, vol. 81, no. October, pp. 1695–1700, 2014.

[85] F. Bariani, Paolo F; Bruschi, Stefania; Ghiotti, Andrea; Medea, "Wear Behaviour of Al-Si and Zn Coated 22MnB5 in Hot Stamping," *Adv. Mater. Res.*, vol. Chapter 4:, pp. 209–218, 2014.

[86] A. Azushima, K. Uda, J. Maki, and N. Nomura, "Frictional behaviour of ZnO coated aluminized steels under hot drawing tests with coated tools," *J. Mater. Process. Technol.*, vol. 228, pp. 106–111, 2016.

[87] J. Hardell, S. Hernandez, S. Mozgovoy, L. Pelcastre, C. Courbon, and B. Prakash, "Effect of oxide layers and near surface transformations on friction and wear during tool steel and boron steel interaction at high temperatures," *Wear*, vol. 330–331, pp. 223–229, 2015.

[88] M. Yanhong, B. Wang, M. Huang, J. Zhou, and X. Li, "Investigation on Tribological Characteristics of Boron Steel 22MnB5-Tool Steel H13 Tribopair at High Temperature," *J. Eng. Tribol.*, 2016.

[89] R. A. Antunes and M. C. L. de Oliveira, "Materials selection for hot stamped automotive body parts: An application of the Ashby approach based on the strain hardening exponent and stacking fault energy of materials," *Mater. Des.*, vol. 63, pp. 247–256, 2014.

[90] M. Naderi, M. Ketabchi, M. Abbasi, and W. Bleck, "Analysis of microstructure and mechanical properties of different high strength carbon steels after hot stamping," *J. Mater. Process. Technol.*, vol. 211, no. 6, pp. 1117–1125, 2011.

[91] K. Mori and D. Ito, "Prevention of oxidation in hot stamping of quenchable steel sheet by oxidation preventive oil," *CIRP Ann. - Manuf. Technol.*, vol. 58, no. 1, pp. 267–270, 2009.

[92] K. Mori, S. Maki, and Y. Tanaka, "Warm and Hot Stamping of Ultra High Tensile Strength Steel Sheets Using Resistance Heating," *CIRP Ann. - Manuf. Technol.*, vol. 54, no. 1, pp. 209–212, 2005.

[93] P. F. Bariani, S. Bruschi, A. Ghiotti, and A. Turetta, "Testing formability in the hot stamping of HSS," *CIRP Ann. - Manuf. Technol.*, vol. 57, no. 1, pp. 265–268, 2008.

[94] R. Neugebauer, T. Altan, M. Geiger, M. Kleiner, and A. Sterzing, "Sheet metal forming at elevated temperatures," *CIRP Ann. - Manuf. Technol.*, vol. 55, no. 2, pp. 793–816, 2006.

[95] J. Yanagimoto, K. Oyamada, and T. Nakagawa, "Springback of High-Strength Steel after Hot and Warm Sheet Formings," *CIRP Ann. - Manuf. Technol.*, vol. 54, no. 1, pp. 213–216, 2005.

[96] A. Turetta, S. Bruschi, and A. Ghiotti, "Investigation of 22MnB5 formability in hot stamping operations," *J. Mater. Process. Technol.*, vol. 177, no. 1–3, pp. 396–400, 2006.

[97] N. Aziz and S. N. Aqida, "Optimization of quenching process in hot press forming of 22MnB5 steel for high strength properties for publication in," *IOP Conf. Ser. Mater. Sci.*

*Eng.*, vol. 50, no. 1, p. 12064, 2013.
[98] H. So, D. Fa??mann, H. Hoffmann, R. Golle, and M. Schaper, "An investigation of the blanking process of the quenchable boron alloyed steel 22MnB5 before and after hot stamping process," *J. Mater. Process. Technol.*, vol. 212, no. 2, pp. 437–449, 2012.
[99] H. Liu, J. Bao, Z. Xing, D. Zhang, B. Song, and C. Lei, "Modeling and FE simulation of quenchable high strength steels sheet metal hot forming process," *J. Mater. Eng. Perform.*, vol. 20, no. 6, pp. 894–902, 2011.
[100] H. S. Liu, Z. W. Xing, J. Bao, and B. Y. Song, "Investigation of the hot-stamping process for advanced high-strength steel sheet by numerical simulation," *J. Mater. Eng. Perform.*, vol. 19, no. 3, pp. 325–334, 2010.
[101] M. Naderi, V. Uthaisangsuk, and U. Prahl, "A numerical and experimental investigation into hot stamping of boron alloyed heat treated steels," *Steel Res.*, no. May, pp. 77–84, 2009.
[102] ArcelorMittal, "Steels for hot stamping -Usibor ®," 2016.
[103] A. Hamasaiid, M. Grausem, and I. Valls, "Recent developments in tool steels for press hardening tools," *Proc. Hot Sheet Met. High-Performance Steel*, pp. 651–658, 2015.
[104] A. R. Zulhishamuddin and S. N. Aqida, "An overview of high thermal conductive hot press forming die material development," *J. Mech. Eng. Sci.*, vol. 9, p. 1686–, 2015.
[105] F. Borsetto, A. Ghiotti, and S. Bruschi, "Assesment of friction tests for sheet metal forming at elavated temperatures," *Steel Res. Int.*, vol. 79, pp. 88–93, 2009.
[106] F. H. Stott, "Role of oxidation in the wear of alloys," *Tribol. Int.*, vol. 31, no. 1–3, pp. 61–71, 1998.
[107] F. H. Stott, "High-temperature sliding wear of metals," *Tribol. Int.*, vol. 35, no. 8, pp. 489–495, 2002.
[108] V. Sinha and J. E. Spowart, "Influence of interfacial carbide layer characteristics on thermal properties of copper-diamond composites," *J. Mater. Sci.*, vol. 48, no. 3, pp. 1330–1341, 2013.
[109] X. Y. Shen, X. B. He, S. Bin Ren, H. M. Zhang, and X. H. Qu, "Effect of molybdenum as interfacial element on the thermal conductivity of diamond/Cu composites," *J. Alloys Compd.*, vol. 529, pp. 134–139, 2012.
[110] Y. XIA, Y. qing SONG, C. guang LIN, S. CUI, and Z. zheng FANG, "Effect of carbide formers on microstructure and thermal conductivity of diamond-Cu composites for heat sink materials," *Trans. Nonferrous Met. Soc. China (English Ed.*, vol. 19, no. 5, pp. 1161–1166, 2009.
[111] M. J. Peet, H. S. Hasan, and H. K. D. H. Bhadeshia, "Prediction of thermal conductivity of steel," *Int. J. Heat Mass Transf.*, vol. 54, no. 11–12, pp. 2602–2608, 2011.